Master's thesis

NTNU
Norwegian University of Science and Technology
Faculty of Engineering
Department of Civil and Environmental Engineering

Beyene Feye Fulasa

Investigation on Different Shapes of Broad-crested Weirs by Means of CFD

Master's thesis in Hydropower Development
Supervisor: Nils Ruther
Co-Supervisors: Elena Pummer and Øyvind Pedersen
June 2019

NTNU
Norwegian University of
Science and Technology

Beyene Feye Fulasa

Investigation on Different Shapes of Broad-crested Weirs by Means of CFD

Master's thesis in Hydropower Development
Supervisor: Nils Ruther
Co-Supervisors: Elena Pummer and Øyvind Pedersen
June 2019

Norwegian University of Science and Technology
Faculty of Engineering
Department of Civil and Environmental Engineering

NTNU
Kunnskap for en bedre verden

Abstract

Weirs are a type of hydraulic structure used for flow measurement, to regulate the water level in hydropower plants, and for the diversion of water to a reservoir. In this study, the flow over various shapes of broad-crested weirs was simulated by computational fluid dynamic models (CFD). The 14-extended water surface profiles over a sharp-edged broad-crested weir were measured in a laboratory by Hager and Schwalt (1994) and validated using OpenFOAM. A structured mesh with a high concentration near the wall regions was employed in the numerical model. Reynolds-averaged Navier-Stokes equations with five turbulence models: Standard k-ε, RNG K-ε, Realizable k-ε, Standard k-ω, and KomegaSST were applied to estimate the water surface profiles. The best turbulence model, KomegaSST, was selected based on the least relative errors of the water level. The results of the numerical models were compared with experimental results to evaluate the accuracy of the available data and the ability of the model in describing the behavior of flow parameters over the weirs. There was good agreement between the approach water level and a small variation in the discharge coefficient within the range of 0.55 to 2.85% of the mean error.

In the first case, the weir geometry was modified on the edge of the weir both upstream and downstream with a straight and round cut. The impact of various shapes of weirs on the discharge coefficient and capacity was simulated and analyzed. In total, 40 numerical simulations were done on different weir geometries and the result indicated that the discharge coefficient increases as the weir geometry is modified from sharp-edged to either straight or round edged. By considering the minimum allowable crest length, the broad-crested weir with both sides modified has the maximum percentage of increment in the discharge coefficient (20.211%), compared with the experimental result of square edge. For the selected model, the discharge coefficient equations were developed in terms of weir geometry relative length. A reasonable agreement was noticed between the developed discharge and Sargison and Percy's (2009) equation., with a mean error of less than -1.68%.

The second case of numerical simulation of flow over a broad-crested weir was investigated by modifying the slope of the crest from the upstream to downstream edge of the weir with an inclination angle of 0° to 5°. In this case, 36 simulations over different shapes of weirs were carried out and the effect of both straight cut and round-edged on the formation of the re-circulation zone was investigated. From all modifications, the weir with a rounded edge and crest inclination of 5° was selected as the best model. With this model, the capacity of the weir was increased by 14.91% compared with the square-edged weir, and the equations for the discharge coefficient were developed both in terms of angle of crest inclination angle (α) and relative length.

Acknowledgement

First of all, I would like to thank the 'Almighty God' for giving me the life, patience, audacity, wisdom and who made it possible, to begin and finish this work successfully.

I would gratefully like to acknowledge the Norwegian Agency for Development Cooperation (NORAD) for providing me full a scholarship opportunity and enabling me to pursue my studies at NTNU Norwegian University of Science and Technology, without which I would not have realized my dream to further my studies.

I consider it a profound pleasure to express my deep sense of indebtedness, gratitude, and profound thanks to my main supervisor professor Nils Ruther of the Civil and Environmental Engineering at NTNU University of Science and Technology. Ruther office was always open whenever I ran into a trouble spot or had a question about my research or writing. He consistently allowed this paper to be my work but directed me in the right direction whenever he thought I needed it. His critical comments and helpful guidance on the design hydraulic structure gave me a chance to explore further. I have learned a lot from him during my research time.

I would also like to acknowledge Co-supervisor Professor Elena Pummer for her assisting, recommending, guiding and for her remarkable advice to learn computational fluid dynamics. Working with her gave me a chance to become familiar with the software and simplified the complex tasks in my study. Equally important, I extended my deep gratitude for my co-supervisor Dr. Øyvind Pedersen from Multiconsult company. The idea of this thesis was also partly from the Multiconsult company under the supervision of Pedersen. His kind advice, valuable supervision and critical comments from beginning to the end of my thesis work had helped me to investigate in detail and to carry out my work with more reasonable outcomes.

I would like to take this chance to acknowledge the NTNU Norwegian University of Science and Technology for teaching, offering very essential and useful information. During the study of this master's degree, I got valuable experience from different professors, experts and extinguish guests both in theoretical and practical skills. I would like to say thank you for all NTNU staff who indeed contribute to my studies by supplying me with technical advice and study materials.

Finally, I must express my very profound gratitude to my parents for providing me with unfailing support and continuous encouragement throughout my years of study and through the process of researching and writing this thesis. This accomplishment would not have been possible without them.

Dedication

I dedicate this thesis manuscript to my father FEYE FULASA, and to my mother KIBU BATI, for nursing me with affection, love and for their dedicated partnership in the success of my life.

Table of Contents

List of Figures

List of Tables

List of Abbreviations (or Notation)

a	Vertical height of straight cut [m]
ASTM	American Society Testing of Materials
B	Width of weir [m]
b	Horizontal Length of Straight Cut [m]
Cd	Discharge Coefficient
Cd Simu	Simulated Discharge Coefficient
Cd Exp	Experimental Discharge Coefficient
CFD	Computational Fluid Dynamics
DNS	Direct Numerical Simulation
d/s	Downstream
ε	Rate of dissipation rate
Fo	Froude Number
Ho	Upstream energy head [m]
Ho/Lw	Relative Length of weir or Total Energy Head Divided by Weir Crest Length
ho	Upstream Water Level [m]
h_{exp}	Experimental Approach Water Level [m]
h_{num}	Numerical Approach Water Level [m]
h/t	Relative Thickness of Weir
h/p	Relative of Height Weir
Hmax	Maximum Upstream Energy Head [m]
K	Turbulence Kinetic Energy
Lb	Bottom Length of Weir
LES	Large Eddy Simulation
Lw	Crest length [m]
l/s	Liter Per Second
MAE	Mean Absolute Errors [%]
m	Meter
mm	Millimeter
m^3/s	Cubic Meter Per Second
PDEs	Partial Differential Equations
p	Height of weir [m]
P_rgh	Total pressure [pa]
Pvc	Polyvinylchlorides
RANS	Reynolds-Averaged Navier-Stokes
Re	Reynolds number
RNG	Renormalization Group
RE	Relative Errors Percentage [%]
RMSE	Root Mean Square Errors [m]
SST	Shear Stress Transport

SSIIM2 ..... Sediment Simulation in Intakes with Multiblock

t..... Thickness of Weir [m]

u/s..... Upstream

VOF..... Volume of Fluid

1 Introduction

1.1 Background

In any hydropower project, the diversion structures occupy a key position. Among these, the weir is the most commonly used hydraulic structure, because of its simple design and operation. Weirs are an open- channel flow measurement device that combines hydraulic characteristics of both weirs and channels. As common hydraulic structures, low weirs are widely used to increase the upstream water level in hydropower projects and to measure discharge in irrigation systems.

Rectangular weirs with a finite crest width are often used for the determination discharge capacity. The most commonly used types of weirs in practice are broad-crested weirs, sharp-crested weirs, and ogee-crested weirs. These structures are built for measuring the flow in the open channel systems. Among the types of weirs, ogee crested weirs are characterized by complex geometry and are costly during construction. In addition to this, this type of weir is very difficult to deal with during the rehabilitation of old dams. This challenge occurs due to the topography of the dam site and restrictions on the structures of dams.

The broad-crested weir is characterized with the geometry of a flat structure and a length of crest is large enough compared to the flow thickness over the crest. The crest is labeled broad when the streamline flows are parallel to the crest and the critical depth is present. Along the crest of a broad-crested weir the pressure distribution is hydrostatic Mahtabi and Arvanaghi (2018).

Broad-crested weirs are typically much more robust than the thin plates used for constructing sharp-crested weirs. Their increased durability contributes to their extensive use for flow measurement and water level regulation in small to medium-sized rivers and canals. Typically, they are constructed out of reinforced concrete and span the width of the channel. Their rating curves rely on the flow over the crest of the weir passing through the critical depth. When the weir is constructed to a height large enough to ensure that the critical depth occurs over a crest, a rating curve can be calculated based on the geometry of the critical section. This rating curve allows for a simplified determination of the discharge by only looking at the depth of the water’s surface Julian (2014).

Significant head loss and deposition of sediment will occur upstream of a weir when the shape of the weir is vertical upstream. This will adversely affect the accuracy of the discharge measurement and increase the operating costs. To deal with such problems, the broad-crested weir's structural design can present flexibility to provide better hydraulic characteristics and discharge efficiency. Madadi et al. (2014) investigated whether the weir discharge coefficient will be increased when the weir upstream entrance condition changes from a square-edged to a round-nosed corner.

Sargison and Percy (2009) reported that the upstream and downstream of broad-crested weirs can be sloped to prevent deposition of sediment or solids in the upstream side of the weirs, and cavitation at the downstream corner of the weir and separation zone.

1.2 Weir Functions

Weirs are used to prevent flooding, to measure water discharge, to increase the water level upstream of the reservoir for a power plant, and to help render rivers to be more navigable by boat. A weir is designed to alter the river flow characteristics and can be vary both horizontally and vertically with the smallest being only a few centimeters in height; whilst the largest may be hundreds of meters long. Some of the main functions of weirs are discussed below.

1.2.1 Weirs as Flow Measurement Tools

The weir is a simple method of measuring the volumetric flow rate in small to medium-sized streams or in industrial discharge locations. It allows a simple design and operations for engineers and hydrologists. From the known depth of the flow on the crest of the weir, the amount of flow rate on the weir can be determined; although, this can only be achieved in locations where all the water flows over the top of the weir crest. Where these conditions are not satisfied, it can make flow measurement complicated, inaccurate or even impossible to measure. To improve the accuracy of flow measurement, the design of weirs must be appropriate both numerically and physically, and the accurate value of the discharge coefficient must be applied. The broad-crested weir shown in Figure 1-1 was used for flow measurement and to regulate the upstream water level in a hydropower plant in Thorp, Washington, USA was built in 2008.

Figure 1-1 A broad-crested weir at the Thorp grist mill in Thorp, Washington, USA.

Some advantages of using broad-crested weirs for flow measurement and regulation: -

- Broad-crested weirs can be computer calibrated;
- Structural stability up to a 2 to the 3m head may easily be accomplished;
- Concrete may be used as a material with the steel upstream corner for abrasion protection;
- Low cost and extremely low sensitivity to tailwater submergence;
- Cost effective installation due to the ease of design and construction;
- Relatively small head loss across the structure;

- Sturdy and capable of measuring discharge in small to medium channels;
- Theoretical calibration possible based on post-construction dimensions; and
- Capable of passing floating debris.

Some disadvantages of using broad-crested weirs for flow measurement and regulation: -

- It may interfere with fish passage and disrupt the ecological equilibrium;
- Sediment deposition occurs on the upstream side of the structure, leading to lower sediment flow downstream and higher water levels upstream of the weir;
- The channel immediately upstream of the weir is susceptible to sediment deposition, which in turn can compromise the accuracy of the rating curve.

1.2.2 Weirs for Control of Invasive Species

As weirs are a physical barrier, they can impede the longitudinal movement of fish and other animals up and downstream of a river. As we can see from the from (b)

Figure **1-2** (b)below, a broad-crested weir will have a negative impact on fish species that migrate as part of their breeding cycle. However, it is also useful as a method of preventing invasive species from moving upstream.

(a) (b)

Figure 1-2 A broad-crested weir in Warkworth, New Zealand (a); and a weir on the Humber River near Raymore Park in Toronto, Ontario, Canada (b)

1.2.3 Weirs for Flood Control and Altering River Conditions

Weirs are normally used to control the flow rates of rivers during periods of high discharge. Sluice gates can be altered to increase or decrease the volume of water flowing downstream. Weirs for this purpose are commonly found upstream of towns or villages and can either be mechanically or manually operated.

During the rehabilitation of old dams, it is very difficult to provide a realistically shaped hydraulic structure on the dam to measure water flow and for the determination of capacity. Most of engineers were interested in the broad-crested weir due to its simple geometry and accurate discharge measurement tools. Broad-crested weirs are often used

in spillways for the rehabilitation of old dams, especially in dam structures which do not allow more ideal shapes such as an ogee-crested weir.

In this study, an investigation of the various shapes of broad-crested weirs will be taken into consideration. When the upstream edge of a broad-crested weir is sharp it will create a separation zone which leads to a wrong reading of the water depth above the crest; this will cause an underestimate or an overestimate of the discharge capacity. Broad-crested weirs with a large formation of a recirculation zone were not recommended in the designing of hydraulic structures, especially for flow measurement. In order to prevent these problems and increase the capacity, the upstream side of the weir is often rounded or cut, and the downstream surface is also often inclined. Finding the capacity for such customized weir shapes can be challenging. At the same time, the recent research into numerical modeling and computational fluid dynamics (CFD) shows that, when properly set up, a 2D width-averaged Reynolds-averaged Navier-Stokes (RANS) model can give a very accurate capacity estimate for the flow over the broad-crested weir.

1.3 Objective

1.3.1 General Objective

The main objective of this thesis is to investigate the flow parameters over various shapes of broad-crested weirs by using computational fluid dynamics (CFD) software with OpenFOAM toolbox and to discover the capacity of the most practical shapes of a broad-crested weir.

1.3.2 Specific objective

- To set up a 2D width averaged Reynolds-average Navier-Stokes (RANS) model and run simulations for the selected literature studied on the sharp edge broad-crested weir and validated it with experimental data.
- To find the most significant and cost-effective shape of broad crested weir using the CFD OpenFOAM toolbox.
- To examine the effects of the upstream and downstream face inclination on the discharge coefficient and on the behavior of the broad-crested weir.
- To develop equations of the discharge coefficient as a function of the inclined angle, the round radius and the ratio of crest length to bottom length of weirs.

1.4 Structure of Thesis

This thesis is presented in five chapters and appendices. Each of the chapters comprises the contents listed as follows:

Chapter 1 includes general information about broad-crested weirs and explains the idea behind this thesis. It also presented the general and specific objectives of the thesis.

Chapter 2 highlights the literature review on both experimental and numerical investigations of broad-crested weirs.

Chapter 3 discuss the materials and methodology used throughout the thesis. The validation of the experimental data with the relevant turbulence and calibration of the input parameters' model was carried out.

Chapter 4 analyzes the detailed investigation of flow over different shapes of broad-crested weirs based on the basic design.

- The discharge equations for the best model were discovered both in terms of weir geometry and relative length of weir.
- The numerical result from all modification methods is discussed and the comparison of the new and existing equations of the discharge coefficient are analyzed.

Chapter 5: presents the conclusion of the work and the associated limitations and recommendations for future work.

Some important tables, figures, and result of numerical simulations such as convergency, separation zone, pressure distribution and velocity will be presented in the appendices.

2 Literature Review

2.1 Review of an Experimental Investigation of Flow over a Broad-crested Weir.

The characteristics of the flow over a broad-crested weir with different upstream cross sections have been of interest to many investigators. Broad-crested weirs are among the major types of measuring structures which, because of their low cost, easy installation and high accuracy, have attracted significant attention. For better capacity and hydraulic efficiency, many researchers have carried out both experimental and numerical investigations on square-edged broad-crested weirs. Most of the analysis on various shapes of weirs has been done by modification of up and downstream faces to the inclined, and around the edge.

M.G. Bos et al. (1975.) described a broad-crested weir as an overflow structure with a horizontal crest, in which the deviation from hydrostatic pressure distribution because of centripetal acceleration may be neglected. In other words, the streamlines are practically straight and parallel as shown in Figure 2-1 below. To obtain this situation, the length of the weir crest in the direction of flow should related to the total energy head over the weir crest as $0.08 < Ho/Lw < 0.5$. He also summarized that for Ho/Lw $\geq$ 0.08, the energy losses above the weir crest cannot be neglected, and undulations may occur on the crest; Ho/Lw $\leq$ 0.5, so that only slight curvature of streamlines occurs above the crest and the hydrostatic pressure distribution may be assumed.

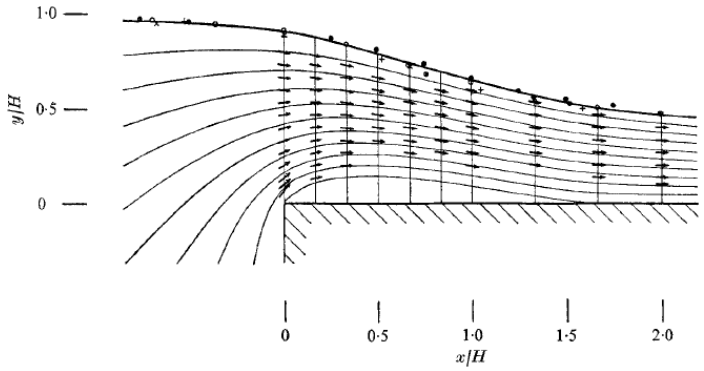

Figure 2-1 Computed profile and streamlines with observation superimposed Moss (1972)

Rectangular broad-crested weirs with square or round-nosed upstream corners are widely used in the field and laboratory channels for flow measurement. These weirs have an advantage over other flow metering structures because of their good ranges of discharge and high modular limit. Nevertheless, rounding the upstream corner of square-edged weirs increases the discharge coefficient, Cd, and renders the weir less sensitive to sediment deposition at the upstream face, especially when the weir height is small.

Ramamurthy et al. (1988) did an experimental investigation on an upstream round-nosed weir shown in Figure 2-2 below with ranges of radiuses and analyzed the impact on discharge coefficient, Cd. Ramamurthy et al. (1988) derived an expression for the free-flow characteristics of square-edged broad-crested weirs using the boundary layer and

verified their expression by using experimental data. They also derived an expression for the coefficient of discharge for a streamlined broad-crested weir based on critical flow theory, allowing boundary layer development. They highlight that the main influential factor to increase the capacity was the reduction or avoiding of the separation zone, as R/H_{max} is increased up to 0.11.

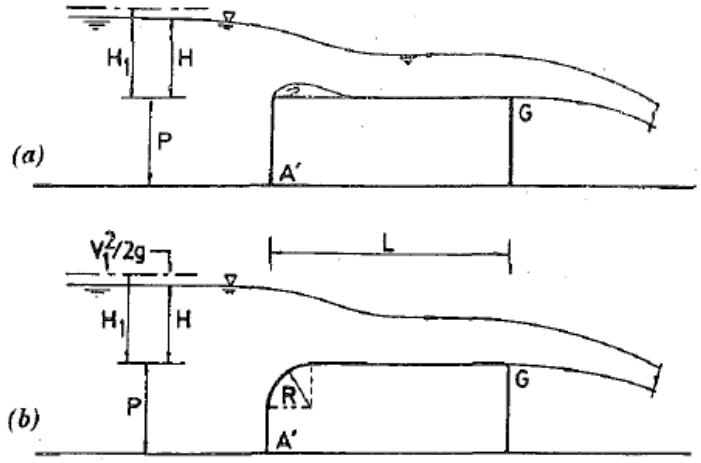

Figure 2-2 Flow over broad-crested weirs (a) Definition Sketch of Free flow over Square-Edge weir; (b) Definition Sketch of free flow over Round-Nosed Weir (Ramamurthy et al. 1988)

GOodarzi et al. (2012) carried out an experimental investigation of the effect of the upstream slope of a broad-crested weir on the flow parameters and discharge coefficient. The experimental analysis was carried out in a flume with dimension of L=12 m, width = 0.25 m, height = 0.5 m. The cross-section of broad-crested weirs used in this investigation have a length of 0.6 m, a width of 0.25 m and a height of 025 m as shown in Figure 2-3 below. The ranges of discharge from 0.015 to 0.035 m^3/s were considered. They analyzed the upstream inclination angle of the broad crested weir from 10° to 90°. The result of a numerical model of the same dimensions as the weir was used to validate flow parameters like water surface, velocity distribution and pressure distribution for each case and Figure 2-3 below plotted water surface profiles for square edged broad crested weir. From their analysis, the upstream inclination of between 22° to 23.5° was found as the most efficient dimension in the estimation of flow over the broad-rested weir.

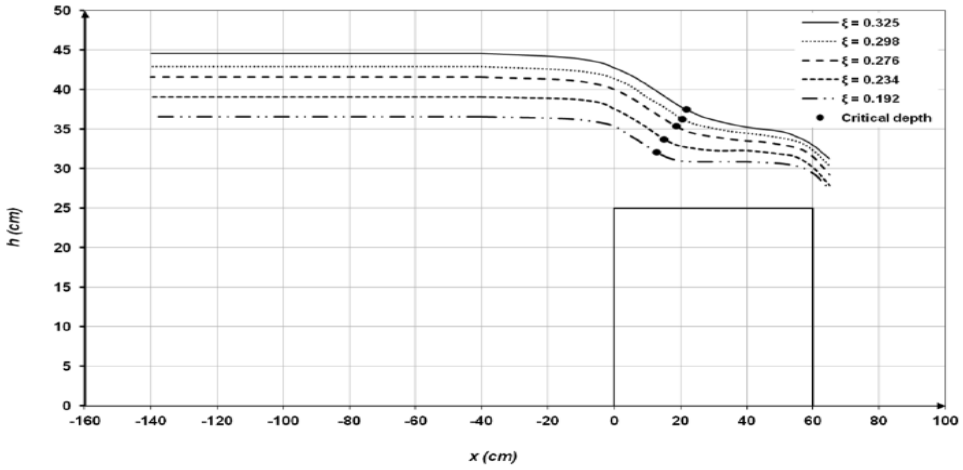

Figure 2-3 Water surface profiles with standard square-edged broad-crested weir GOodarzi et al. (2012)

Felder and Chanson (2012) carried out an examination on a large, broad-crested weir with an upstream round corner. They used the flume with a length of 7 m, a width of 0.52 m and height 1 m. The upstream round-edge broad-crested weir with a dimension of 1.01 m long, 0.52 m wide and height of 0.5 m was used. Their main experimental investigation analyzed the pressure and velocity distribution on the broad crested weir with an upstream round edge. The location of the critical depth with respect to ranges of discharge was also identified and analyzed. They found a good agreement between their experimental results and different literature studies investigated by different researchers. The water surface, velocity distribution and pressure distribution of the upstream round corner of broad-crested weirs were tested with a range of discharge (Q) from 2.5 l/s to 142 l/s. They presented that the dimensions' discharge coefficient Cd was close to the former results with a rounded broad-crested weir. Although, the value of the Cd for the square-edged broad crested was less than round edged broad crested weir.

The flow futures over the broad-crested weir with vertical upstream walls and sharp-crested corners were analyzed experimentally by Hager and Schwalt (1994). In their study, 14 extended series of observations were conducted and the water's surface profile, the bottom pressure profile and the discharge coefficient were measured. They only considered a long-crested weir for which the discharge coefficient remains practically constant. Based on the earlier literature and their analysis, the broad-crested weir was identified as an accurate discharge measurement structure. They proposed broad-crested weirs as standard discharge measurement structures provided that a few certain conditions are satisfied.

Fritz and Hager (1998) study showed that the broad-crested weir with a 90º upstream face slope is more accurate than with a round-edge upstream face. The inclined embankment of the broad-crested weir has a higher discharge coefficient, which increases the discharge capacity related to a traditionally upstream squared edge of a broad-crested weir.

Azimi and Rajaratnam (2009) suggested a classification of the flow over weirs of a finite crest length based on $\mathrm{Ho/L}$. For $\frac{\mathrm{Ho}}{\mathrm{Lw}}$ <0.08, the appearance of standing waves on the weir suggested and the effects of surface tension and viscosity may have to be considered. Azimi et al. (2013) recommended that Cd depends exclusively on the ratio of the upstream head to the weir length $\mathrm{Ho/Lw}$ and that the effects of viscosity and surface tension may be neglected for an energy head (H_o) value higher than 30 mm.

Sargison and Percy (2009) investigated the flow over a trapezoidal broad-crested weir with varying upstream and downstream slopes. In their research, the effect of 1V:1H and 1V:2H slopes, as well as the slope in various combinations on the upstream and downstream faces of the weir, was examined. They found that increasing the upstream slope in the vertical direction reduced the discharge coefficient and the effect of downstream slopes on the water surface and pressure profiles over the broad crested weir could be ignored.

Zachoval et al. (2014) carried out an experimental investigation on the rectangular weir in Brno University of Technology. Their main investigation objective was to study the relationship between the discharge coefficient, Cd, and relative thickness (h/t). They found a new relationship between the discharge coefficient Cd and relative weir height (h/p) for the rectangular sharp-edged broad-crested weir of range between $0.12 \leq \mathrm{h/t} \leq 0.3$ and extended to the new large range of relative weir height $0.2 \leq \mathrm{h/p} \leq 7$.

Table 2-1: Summary of the experimental studies of sharp-edged broad-crested weirs.(Zachoval et al. 2014)

Investigator	Overflow head h [m]	Weir thickness t [m]	Weir height P [m]	Weir width b [m]
Bazin, 1896 (Horton, 1907) (113, 114, 115)	0.055–0.447	0.10–2.00	0.75	2.00
U. S. Geological Survey, 1903 (Horton, 1907) (41, 42, 43, 44, 45, 46, 47)	0.023–1.351	0.28–4.97	3.43	4.87
Woodburn, 1932	0.155–0.429	3.5	0.53	0.61
Prentice, 1935 (Stevens et al., 1941)	0.030–0.183	0.61–0.91	0.20	0.30
Doeringsfeld and Barker, 1941	0.016–0.179	0.34–0.69	0.08–0.16	0.25–0.51
Tison, 1950	0.044–0.165	1.80	0.30	0.50
Berezinskij, 1950 (6a, 8, 9, 9a, 11, 16, 17)	0.045–0.358	0.39–2.50	0.03–0.46	0.51–1.92
Govinda Rao and Muralidhar, 1963	0.031–0.277	0.10–3.05	0.30–0.31	0.61
Wakhlu, 1963 (Shaw et al., 1972)	0.012–0.083	0.31	0.05	0.20
Singer, 1964	0.067–0.380	0.91–1.37	0.20–0.25	0.44–0.76
Shukla, 1970	0.102–0.121	1.27–1.52	0.02–0.13	0.46
Moss, 1972	0.033–0.076	0.15–0.76	0.152	0.61
Crabbe, 1974	0.06–0.37	0.08–0.12	0.15	0.3
Sreetharan, 1983 (4B, 7A, 7B, 8A, 8B, 9A, 10A, 10B, 11A, 11B, 12B)	0.037–0.290	0.08–0.90	0.08–0.20	0.27–0.51
Tim, 1986	0.025–0.122	0.31	0.10	0.25
Hager and Schwalt, 1994	0.027–0.202	0.50	0.40	0.50
Johnson, 2000		0.02–0.61	0.05–0.61	0.91–1.83
Zachoval et al., 2012a	0.036–0.191	0.50	0.25	1.00
Goodarzi et al., 2012	0.115–0.195	0.60	0.25	0.25
Major, 2013	0.057–0.163	0.50	0.25	1.00

2.2 Review on the Numerical Investigation of Flow Over the Broad-crested Weir

The numerical investigation of flow over the models of hydraulic structures was an interesting method to estimate the flow parameters of a given geometry. It is a time-saving system and the most economical in terms of investigation cost and accuracy of results. By using numerical simulation, we can analyze the impact of high flood on model, which was impossible for experimental investigation due to limited space in the laboratory. The design and simulation of flow over various shapes of models is economic and reliable in numerical simulation. Many researchers have used numerical analysis to validate the experimental data and for the final design of real projects. In most cases, 2D width-averaged Reynolds-averaged Navier Stokes (RAN) equations were used where applicable, along with computational fluid dynamics (CFD) with FLUENT and the OpenFOAM toolbox. The governing equations are obtained by applying the energy equation between the head measurement section when the fluid is considered ideal or frictionless.

Haun et al. (2011) studied the validation of two CFD models, 3D flow and SSIIM2 on a trapezoidal broad-crested weir. According to his investigation, for the same program to investigate flow over the identical shape of the broad-crested weir, SSIIM 2 required more cells than Flow-3D to achieve the same expected accuracy. When the result has been compared with the results obtained from a laboratory test using different discharges, the deviation between the computed and observed water level at upstream was between 1 % and 3.5 %. While the difference between the results from the two CFD models was between 1 and 1.5 %. However, the result obtained from both the CFD programs is quite similar to the results from the physical model test provided by Sargison and Percy (2009). The deviation between the programs seems to be the same order of magnitude as compared to the physical model. The discharge coefficient obtained from the numerical and physical models was also analyzed in his study.

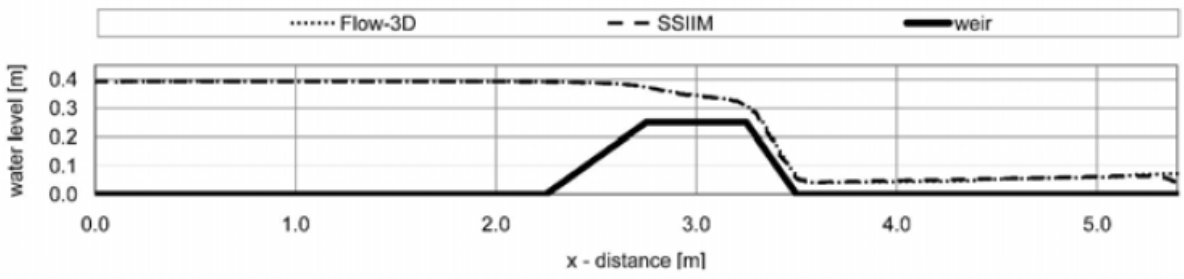

Figure 2-4 Longitudinal free water profile for Q = 0.0181m^3/s (Haun et al. 2011)

Al-Hashmi et al. (2016) presented the relationship of energy dissipation, the height of the weir, the upstream water surface ratio, making a step at the downstream of the weir and the Froude number, in the determination of most of the slope of the broad-crested weir to get maximum energy dissipation through different models. They carried out experimental investigations on a broad-crested weir by varying the downstream bed slope of the flume from 0 to 0.004. Computational fluid dynamics software with FLUENT toolbox was used for validation of the result of the physical model and they found good agreement.

The discharge parameters for vertical face weirs both with a square edge and rounded entrance were extensively analyzed by Azimi et al. (2013). Experimental and numerical flow modeling over a rectangular broad-crested weir has been conducted by Sarker and Rhodes (2004). A good agreement was found in the upstream water level; whereas all

other numerical results, like rapidly varied flow profile over the crest, differed slightly from the results of the physical model study.

Zachoval et al. (2014) investigated 3D computational fluid dynamics (CFD) simulation together with laboratory models in order to determine the free surface profile of broad-crested weirs. Simulations were performed using the volume of fluid (VOF) free surface model and three turbulence models of the RNG k-ε, standard k-ε and the large eddy simulation (LES) to find the water level profile and streamlines. They also selected RNG k-ε turbulence model with a low percentage of errors and found good agreement between experimental data and numerical simulations.

3 Methodology and Material Used

3.1 Discharge Equation and Broad-crested Weir Characteristics

The flow equation of any hydraulic structure depends on its boundary conditions on the upstream, and the downstream faces. The Equations vary mainly due to different head losses resulting from the boundary conditions. The flow equations represent a relationship of the discharge in terms of the energy head (the elevation of the water above the weir). For the accuracy of the reading, many researchers have stated that the water surface elevation above the weir should be measured at a distance 4-5 times the energy head upstream of the weir. Broad-crested weir flow occurs when the upstream head above the crest is between the limits of about 0.05 m and 0.5 m of the crest length in the direction of the flow. In the case of a large approach head, a thick wall or a flat stoplog can act like a sharp crest so that the flow springs from the upstream corner. If the upstream head is too small relative to the top profile length, the stoplog can act as a broad crested weir Sargison and Percy (2009).

3.2 Discharge Equation for a Broad-crested Weir

The discharge relation for flow over a broad crested weir can be obtained by a combination of continuity and Bernoulli's equation. The Figure 3-1 below shows the ideal flow of water over a broad-crested weir with a round edge including the energy gradient line (EGL).

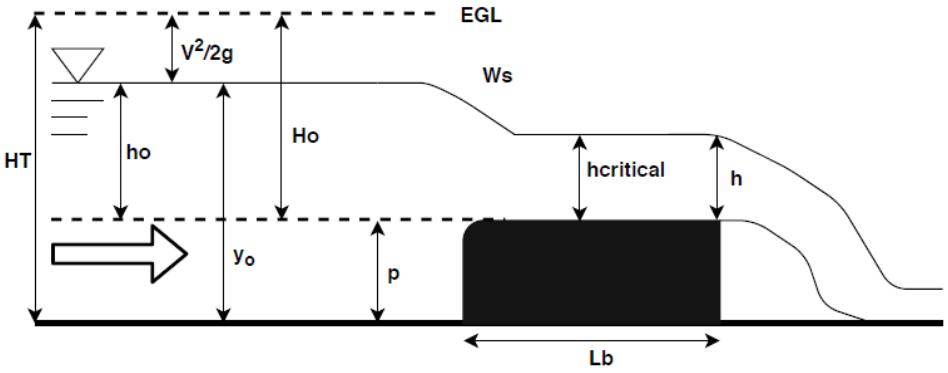

Figure 3-1 Definition sketch of a Broad-crested Weir

The discharge equation of a broad-crested weir at critical flow condition will be given as:

$$Q = 1.705 * Cd * B * (Ho)^{\frac{3}{2}} \qquad \text{Eq. 3-1}$$

Where -

Q is the total capacity (m^3/s); Cd is a dimensionless discharge coefficient; B is the width of the weir in (m); and Ho is the total energy head obtained by- $h_o + \frac{v^2}{2g}$.

Commonly the flow over a broad-crested weir under free-flow conditions is described by Fritz and Hager (1998). They used the free-flow conditions for estimation of the discharge coefficient shown in Eq 3-2.

$$Q = Cd\ B\sqrt{2g}Ho^{3/2} \qquad \text{Eq. 3-2}$$

3.3 Experimental Investigation of Flow over a Broad-crested Weir

A physical model is a scaled-down version of a real prototype which will be used in the laboratory for the investigation of flow over a given model. The model size and dimensions depend on the availability of space in the laboratory. However, for a hydraulic structure like a broad-crested weir, ogee spillway and other small geometries depend on the dimension of the flume. In this study different experimental investigations and their findings were reviewed. Most researchers considered different conditions and criteria during their investigations. Among these, the literature prepared by Hager and Schwalt (1994) on the experimental investigation of water flow over a broad-crested weir was identified as the most relevant analysis with good experimental results. In their study, 14 extended series of observations were conducted. In all series, the water surface profile and the bottom pressure profile were measured. This experimental investigation was carried out on a rectangular broad-crested weir with a sharp upstream corner. They observed that the water profile for low discharge has a local minimum downstream from the sharp corner; whereas, for a larger discharge, the flow gradually decreases from the approach to the tailwater channel.

3.3.1 Consideration of Design Geometry for a Broad-crested Weir

The flow features over the broad-crested weir with a vertical wall and sharp-crested corner are analyzed experimentally. Many researchers set the limits of weir length to depend on the approach head and crest length. Govinda Rao and Muralidhar (1963) presented the classification of weirs depending on the relative width of the weir crest Ho/Lw as:

- $0 < Ho/Lw < 0.1$ for long-crested weirs;
- $0.1 < Ho/Lw \leq 0.4$ for broad-crested weirs;
- $0.4 < Ho/Lw < 1.5$ for short crested weirs; and
- $Ho/Lw > 1.5$ for sharp-crested weirs.

Fritz and Hager (1998) have investigated many experiments to study the hydraulic characteristics of broad-crested weirs with various geometries and designs. The earliest study focused on determining the discharge coefficient and revealing the influence of the geometries on the flow pattern. In their investigation, they used compound broad-crested weirs which have a small inner rectangular section for measuring low flows and then, they broaden to a wide rectangular section at higher flow depths. They used the data from their study in the design of hydraulic structures for flow control and measurement. A series of laboratory experiments were performed in order to investigate the effects of the width of the lower weir crest and step height of broad-crested weirs with a rectangular compound cross section on the values of the discharge coefficient (Cd) and the approach velocity coefficient. For this purpose, 15 different broad-crested weir models with rectangular compound cross sections for a wide range of discharges were tested.

The dependence of the discharge coefficient and the approach velocity coefficient on model parameters was investigated by Hager and Schwartz (1994). Results show that a discontinuity occurs in head-discharge ratings because the section width suddenly changes shape, experiencing a break in the slope when the flow enters the outer section. By using an equation of a free free-flow condition shown in Eq 3-1 above, the values of Cd obtained from the experiments on compound broad-crested weirs are lower than those of a broad-crested weir with a rectangular cross-section because of its contraction effects.

3.3.2 Experimental Set-up

The experimental measurements were conducted by Hager and Schwartz (1994) in a horizontal rectangular channel 499 mm wide and 700 mm high. The total length of the channel was 7 m, with the front side made of the glass, and the bottom and back side made of black PVC. The broad-crested weir with a weir height (p) of 401 mm and crest length (L_w) 500 mm as shown in Figure 3-2 below was located at 4.828 m downstream of the inlet. By using various approaches, they obtained an excellent, smooth and wave-less flow and carried out experiments of good quality and accuracy.

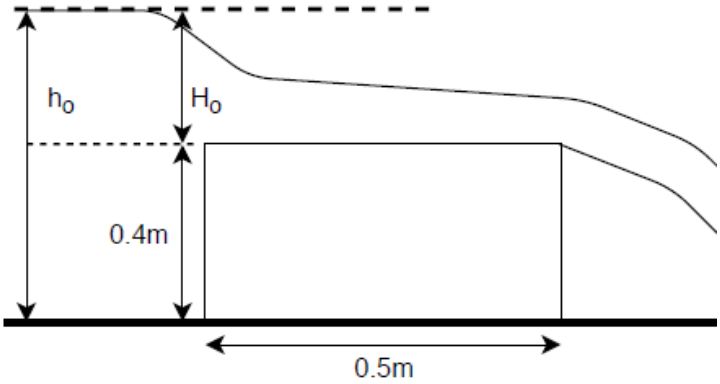

Figure 3-2 Broad-crested weir, notation

3.4 The Materials Used for Experimental Investigation

The materials used to investigate the experimental analysis of flow over a broad-crested weir carried out by Hager and Schwalt (1994) are:

- Rectangular flume: the experiment set-up was carried out in a rectangular laboratory flume.
- Weighing scale: this was applied in measuring the quantity of water that passes over the weir model. in their experiment, a 90º V notch was used as discharge measuring material.
- Stop-watch: a digital stopwatch was used to measure the rate of time a certain amount of water is collected in the tank attached to the weighing scale.
- Monometers: used to inject dye to the flow.
- Miniature propeller: a miniature is used for velocity measurement at the selected points and they only observed the streamwise components.
- Point gauge: the point gauge was used to measure the water depth above the crest of the weir model in the laboratory rectangular flume.

3.5 Analysis of Experimental Result

After they carried out an extended experiment, Hager and Schwalt (1994) tabulated the results and main characteristics of the models as shown in Table 3-1 below. From the typical free water surface, they observed that the profile for low discharge has a local minimum downstream from the sharp edge; whereas for a larger discharge, the flow gradually decreases from the approach to the tailwater channel. In their analysis, all cases are referred to as typical or usual flow over the broad-crested weir as $0.1 < Ho/Lw < 0.40$. They presented a series of free surface profiles in the vicinity of the weir. The profiles are numbered by the Run number ascribed to them as shown in Figure 3-3 below.

Table 3-1 Main flow characteristics of extended experiments Hager and Schwalt (1994.)

Run	Q (l/s)	h_o (mm)	H_o (mm)	Cd	F_o	Re
1	8.25	50.8	50.9	0.324	0.0174	4.13x10^4
2	4.55	34.2	34.2	0.325	0.0101	2.27x10^4
3	3.32	27.8	27.8	0.323	0.0076	1.67x10^4
4	3.77	30.3	30.3	0.323	0.0085	1.90x10^4
5	6.26	42.1	42.1	0.327	0.0136	3.11x10^4
6	10.90	60.7	60.7	0.329	0.0222	5.39x10^4
7	17.81	84.1	84.4	0.328	0.0337	8.83x10^4
8	25.98	107.9	108.4	0.329	0.0458	12.86x10^4
9	37.59	138.2	139.2	0.327	0.0607	18.71x10^4
10	54.83	176.2	178.0	0.330	0.0800	27.05x10^4
11	68.07	202.1	204.7	0.332	0.0930	33.36x10^4
12	3.60	29.3	29.5	0.322	0.0082	1.83x10^4
13	3.15	27.0	27.0	0.321	0.0072	1.60x10^4
14	4.19	32.2	32.3	0.326	0.0094	2.09x10^4

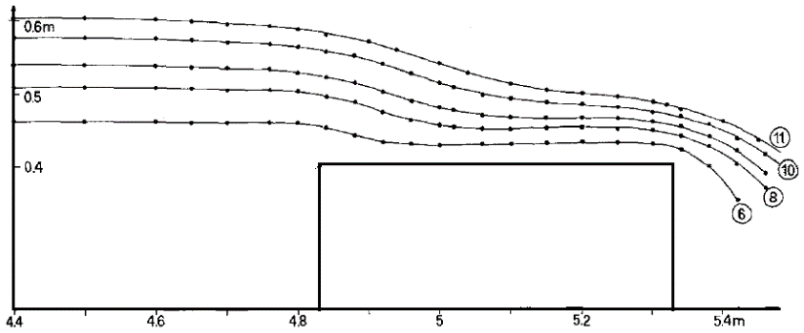

Figure 3-3 Free water profiles from Hager and Schwalt (1994)

An investigation of the discharge coefficient was done based on the design criteria set by Govinda Rao and Muralidhar (1963). The following Figure 3-4 shows the values of the investigated discharge coefficient varied from 0.321 to 0.332 with a corresponding relative length (Ho/lw) of 0.05 to 0.409. These values were obtained when the length was between 0.5 m and 2 m. The maximum discharge coefficient obtained from the experimental investigation was 0.332 at the inflow rate of 68.07l/s, which is labeled as Run (11) on Figure 3-3 above, of the free water surface.

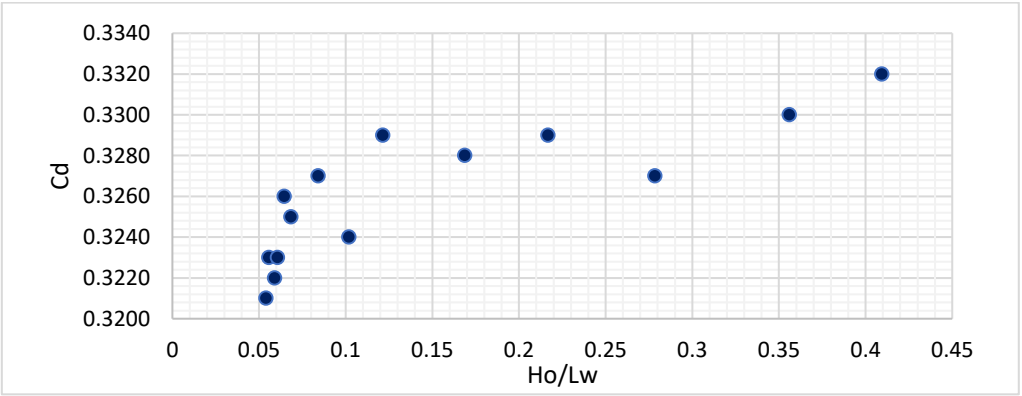

Figure 3-4 Experimental discharge coefficient

3.6 Numerical Modeling and 2D width-averaged RANS Set-up

3.6.1 Formulation and Numerical Simulation of Computational Fluid Dynamic (CFD)

Fluid motion is described with non-linear, transient, and second-order differential equations. The fluid equations of motion must be employed to solve these equations. The science of developing these methods is called computational fluid dynamics (CFD). Computational fluid dynamics (CFD) is a branch of fluid mechanics that uses numerical analysis and data structures to analyze and solve problems that involve fluid flows. It is the use of applied mathematics, physics and computational software to visualize how a gas or liquid flows as well as how the gas and liquid affects objects as it flows past.

CFD modeling employs specially developed numerical techniques to solve the equations of motion for fluids to obtain transient, 2D, 3D solutions to multi-scale, multi-physics flow problems. It involves the solution of the equations of fluid flow over a region of interest, with the specified conditions on the boundary of that region. The set of governing equations of fluid flow, which are solved by OpenFOAM toolbox in the Reynolds-averaged Navier-Stokes equations. These equations describe how the velocity, pressure, temperature, and density of moving fluid are related. The computers used to perform the calculations required to simulate the free-stream flow of the fluid, and the interaction of the fluid with surfaces defined by boundary conditions. The governing equations are the combination of continuity and momentum equation for incompressible flow.

A numerical solution of these equations involves approximating the various terms with algebraic expressions. The resulting equations are then solved to yield an approximate solution to the original problems and the process is called the simulation method. The average values of flow parameters such as pressure and velocity are determined for each cell by using the grinding system. The representation of the boundary conditions is also an important step in a correct solution.

3.7 Methodology Used

In this thesis, several methodologies were used to investigate the flow over different shapes of a broad-crested weirs. Some of them are:

- Governing equation and turbulence Modeling;
- Free surface modeling;
- Numerical schemes;
- Broad-crested weir parameters and simulation by different weir modification; and
- Boundary conditions.

3.7.1 Governing Equations and Turbulence Modeling

Based on the suitable approximations of the exact Navier-Stokes equations, turbulence modelling is an attempt to develop a various partial equation for turbulent flow calculations. At the approach of 2D width averaged Reynolds-averaged Navier-Stokes (RANS) equations, the starting point is the Reynolds decomposition of the flow variables into mean and fluctuation parts.

3.7.2 Reynolds Averaged Navier-Stokes Equations

The Reynolds-averaged Navier-Stokes equations (RANS) are time-averaged equations of motion for fluid flow. The idea behind the equations is Reynolds decomposition, whereby an instantaneous quantity is decomposed into its time-averaged and fluctuating quantities, an idea first proposed by Osbourne Reynolds Jackson and Launder (2007).

According to the concepts of Reynolds decomposition, the dependent variables are decomposed into mean and fluctuating parts;

$$u_i = \overline{u_i} + u' \text{ and } p = \overline{p} + p' \qquad \text{Eq. 3-3}$$

Where $\overline{u_i}$ is mean velocity and u' is an oscillation of velocity vary with time.

The RANS are obtained:

$$\frac{\partial \overline{u_i}}{\partial t} + \overline{u_j}\frac{\partial i}{\partial x_j} = -\frac{\partial \overline{p}}{\partial x_i} + \nu\frac{\partial^2 \overline{u_i}}{\partial x_j \partial x_j} - \frac{\partial \tau_{ij}}{\partial x_j} \qquad \text{Eq. 3-4}$$

$$\frac{\partial \overline{u_i}}{\partial x_i} = 0 \qquad \text{Eq. 3-5}$$

where $u_{i,j}$ are the velocity in x and y directions; x is the space dimensions; t is the time; and p is pressure.

3.8 Turbulence Models

Turbulence is one of the decisive parameters that cause scouring in the riverbed and threaten the foundation of hydraulic structures and characterized by fluctuating velocity. These fluctuations mix transported quantities such as momentum, kinetic energy, and species concentration, and cause the transported quantities to vary as well. Since these fluctuations can be small scale and high frequency, they are also computationally expensive to simulate directly in practical engineering calculations. Instead, the exact governing equations can be time-averaged and ensemble-averaged. Otherwise manipulated to remove the small scales, resulting in a modified set of equations that are computationally less expensive to solve and describe it Alfonsi (2009).

The Reynolds-averaged Navier-Stokes turbulence models have been classified as one equation, two equation model and the Reynolds stress model. One-equation model has been developed to provide the calculation of turbulent kinetic energy and to account for some non-local and history effects in effects in the definition of eddy viscosity. Whereas in two-equation models, two separate transport equations are solved for two independent quantities, directly related to the turbulence length and time scales. Therefore, choosing the right turbulent modeling scheme is the key to simulate the flow parameters accurately. In this study, turbulent flow conditions will be investigating over the various shapes of the broad crested weir by using the OpenFOAM toolbox. Besides the main turbulence schemes, the difficulties in modeling the flow close to the walls also will be solved by choosing the right wall function and boundary conditions.

3.8.1 K-ε Turbulence Model

I) The Standard K-ε Model

The baseline two-transport-equation model solving for kinetic energy (k) and turbulent dissipation (ε). Turbulent dissipation is the rate at which velocity fluctuations dissipate. In

the standard k- ε model, the eddy viscosity is determined from a single turbulence length scale, so the calculated turbulent diffusion is that which occurs only at the specified scale. The k- ε model uses the gradient diffusion hypothesis to relate the Reynolds stresses to the mean velocity gradients and the turbulent viscosity. Performs poorly for complex flows involving severe pressure gradient, separation, strong streamline curvature Hanjalić and Launder (1972).

Menter (1994) stated that this model is economical, reasonably accurate for many flows, especially for fully turbulent flows. However, it is to provide appropriate formula and is simple to implement and performs well for boundary layer flows. The k−ε model fails to accurately predict the flow with massive separation because the eddy viscosity is overestimated in the cases by two equations Menter (1994). This model expresses the turbulent viscosity in terms of turbulent kinetic energy (k) and its dissipation rate (ε). The following two transport partial differential equations are solved for the values of k and ε (Jackson and Launder 2007)

$$\frac{\partial}{\partial t}(\rho k) + \frac{\partial k}{\partial xi}(\rho k ui) = \frac{\partial}{\partial xi}\left[\left(\mu + \frac{\mu t}{\sigma k}\right)\frac{\partial k}{\partial xi}\right] + Gk - \rho\varepsilon \qquad \text{Eq. 3-6}$$

$$\frac{\partial}{\partial t}(\rho\varepsilon) + \frac{\partial \varepsilon}{\partial xi}(\rho\varepsilon ui) = \frac{\partial}{\partial xj}[\left(\mu + \frac{\mu t}{\sigma\varepsilon}\right)\frac{\partial \varepsilon}{\partial xi}] + C1\epsilon\frac{\varepsilon}{k}Gk - C2\epsilon\rho\frac{\varepsilon^2}{k} \qquad \text{Eq. 3-7}$$

Where the eddy viscosity μt, is computed by combining the turbulent kinetic energy (k) and rate of dissipation (ε), as follows in Eq 3-9 below.

$$\mu t = \rho C_\mu \frac{K^2}{\varepsilon} \qquad \text{Eq. 3-8}$$

$$Gk = \mu_t S^2 \qquad \text{Eq. 3-9}$$

$$S = \sqrt{2SijSij} \text{ and } Sij = \frac{1}{2}\left(\frac{\partial ui}{\partial xj} + \frac{\partial uj}{\partial xi}\right) \qquad \text{Eq. 3-10}$$

In the above equations, based on comparisons with physical experiments, the constants assume the values;

$$C_{\varepsilon 1} = 1.44, \quad C_{\varepsilon 2} = 1.92, \quad C_\mu = 0.09, \quad \sigma_K = 1.0, \quad \sigma_\varepsilon = 1.3$$

Where the constants σk and $\sigma\varepsilon$ are the Prandtl numbers for k and ε respectively Jackson and Launder (2007)

II) RNG K-ε Model

The RNG k- ε turbulence model is derived from the instantaneous Navier-Stokes equations, using a mathematical technique called, "renormalization group" RNG methods. It is similar in form to the standard k-ε models, but include the following refinements in the process of numerical simulation:

- The RNG model has an additional term in its epsilon equation that significantly improves the accuracy for rapid strained flows
- While the standard k-ε model is a high Reynolds number model, the RNG theory provides an analytical-derived differential formula for effective viscosity that accounts for low Reynolds-number effects.

These features make the RNG k-ε model more accurate and reliable for a wider class of flow than the standard k-ϵ model. Jackson and Launder (2007) derives an equation for the renormalization group by considering additional terms and transport equations.

$$\frac{\partial}{\partial t}(\rho k) + \frac{\partial k}{\partial xi}(\rho k ui) = \frac{\partial}{\partial xj}\left[(a_k \mu_{\epsilon ff})\frac{\partial k}{\partial xi}\right] + G_k - \rho\varepsilon \quad \text{Eq. 3-11}$$

$$\frac{\partial}{\partial t}(\rho\varepsilon) + \frac{\partial k}{\partial xi}(\rho\epsilon ui) = \frac{\partial}{\partial xj}\left[(a_\varepsilon \mu_{\varepsilon ff})\frac{\partial \epsilon}{\partial xi}\right] + G_{1\varepsilon}\frac{\varepsilon}{k}G_k - G^*_{2\varepsilon}\rho\frac{\varepsilon^2}{k} \quad \text{Eq. 3-12}$$

$$G^*_{2\varepsilon} = G_{2\varepsilon} + \frac{C_\mu \rho \eta^3 (1-\frac{\eta}{\eta_o})}{1+\beta\eta^3} \quad \text{Eq. 3-13}$$

$$\eta = \frac{sk}{\varepsilon} \quad \text{Eq. 3-14}$$

In the above equations G1ε, G2ε and $C\mu$ are constants and equal to 1.42, 1.68 and 0.0845, respectively. ak and $a\varepsilon$ equal to 1.393, η_o is equal to 4.38, $\mu\varepsilon ff$ equal to 1 and $\boldsymbol{\beta}$ equal to 0.012.

III) Realizable K- ε Model

The term "realizable" means that the model satisfies certain mathematical constraints on the Reynolds stresses, consistent with the physics of turbulent flows. It is a relatively recent development and differs from the standard k- ε model in two important ways:

- The realizable k- ε model contains a new formulation for the turbulent viscosity.
- A new transport equation for the dissipation rate, ε, has been derived from an exact equation for the transport of the mean-square vorticity fluctuation.

3.8.2 K-Ω Turbulence Model

a) Standard K-Ω Model

A two-transport-equation model solving for kinetic energy k and turbulent frequency ω. This model allows for a more accurate near wall treatment with an automatic switch from a wall function to a low-Reynolds number formulation based on grid spacing. The k- ε model uses the gradient diffusion hypothesis to relate the Reynolds stresses to the mean velocity gradients and the turbulent viscosity. This model performs significantly better under adverse pressure gradient conditions Wilcox (2008).

The main advantages of this model are a superior performance for the wall-bounded boundary layer, free shear, and low Reynolds number flows and Suitability for complex boundary layer flow under adverse pressure gradient and separation. It can be used for transitional flows (though tends to predict early transition). However, separation is typically predicted to be excessive and early and it requires mesh resolution near the wall.

b) KomegaSST (K-Ω)

The KomgaSST turbulence model is a two-equation eddy -viscosity model which has become very popular. The shear stress transport (SST) formulation combines the best of two worlds. The use of a k-ω formulation in the inner parts of the boundary layer makes the model directly usable down to the viscous sub-layer. Hence the SST k-ω model can be used as a low Reynold's number turbulence model without any extra damping functions. The SST formulation also switches to a standard k-ε behavior in the free-stream and thereby avoids the common k-ω problems that the model is too sensitive to the inlet free-stream turbulence properties Menter (1994)

3.9 Analysis Method

3.9.1 OpenFOAM

OpenFOAM is a free and open source CFD toolbox. OpenFOAM stands for Open source Field operation and manipulation. It is used in academia and industry to solve a wide variety of computational problems. In contrast to any proprietary software, the source code of OpenFOAM is accessible and modifiable.

Advantages

- No license cost;
- The friendly syntax for partial differential equations;
- Unstructured polyhedral grid capabilities;
- Automatic parallelization of applications written using OpenFOAM high-level syntax;
- Wide range of applications and models ready to use; and
- Commercial support and training provided by the developers.

Disadvantages

- Absence of an integrated graphical user interface (stand-alone open-source and proprietary options are available); and
- The programmer's guide does not provide enough details, making the progress slow if you need to write new applications or add functionality.

3.9.2 OpenFOAM Solvers

OpenFOAM solvers include:

- Incompressible flow with RANS and LES capabilities;
- Compressible flow solvers with RANS and LES capabilities;
- Buoyancy-driven flow solvers;
- DNS and LES;
- Multiphase flow solvers; and
- Solver for combustion problems and conjugate heat transfer.

3.9.3 OpenFOAM utilities

OpenFOAM utilities are divided into:

- Mesh utilities
  - Mesh Generation: used to generate computational grids starting either from an input file (block-Mesh) or from a generic geometry specified as STL file which is meshed automatically with hex-dominant grids (snappy-Hex-Mesh).
  - Mesh Conversion: they convert grids generated using other tools to the OpenFOAM formats.
  - Mesh Manipulation: they perform specific operations on the mesh such as localized refinement, the definition of a region and others.
- Parallel Processing Utilities: this used to provide tools to decompose, reconstruct and re-distribute the computational case to perform parallel calculations,
- Pre-Processing Utilities: tools to prepare the simulation cases.
- Post-processing utilities: tools to process the results of simulation cases, including a plugin to interface OpenFOAM and Para view.

3.10 Boundary Conditions

Boundary conditions are one of the most significant numerical analyses of the flow field to determine the boundaries of the numerical model; they are matched appropriately to the physical conditions of the problem. In the OpenFOAM simulation of flow over a broad-crested weir, the inlet velocity is estimated from the Reynolds number. For turbulent flow conditions, the value of the Reynolds number can be assumed to be greater than 4000. Then the turbulence kinetic energy and energy dissipation will be calculated from the velocity. For a given simulation to analyze the impact of one parameter, we must set another variable constant. Therefore, the constant flow parameters were used for different shapes of the weir to see the influence of change in the geometry of weirs and for better investigation. The turbulent kinetic energy and rate of dissipation can be determined from the following equations:

$$\mathrm{Re} = \frac{d * u}{v} \qquad \text{Eq. 3-15}$$

$$k = \frac{3}{2}(u * Ti)^2 \qquad \text{Eq. 3-16}$$

$$\varepsilon = 0.09^{3/4}\frac{k^{3/2}}{0.07d} \qquad \text{Eq. 3-17}$$

where

Re is the Reynolds number for turbulent flow conditions (usually >4000);

d is the inlet length (m); u is the inlet velocity;

k is the turbulent kinetic energy;

Ti is the intensity of turbulence; and ε is the dissipation rate.

When setting boundary conditions for a CFD simulation, it is often necessary to estimate the turbulence intensity on the inlets, which requires some form of measurements or previous experience to estimate. Here are a few examples of estimating the incoming turbulence intensity:

- High-turbulence case (between 5% and 20%): cases with high-velocity flow inside complex geometries.
- Medium-turbulence case (between 1% and 5%): flow in not-so-complex geometries or low speed flows.
- Low-turbulence case (well below 1%): cases with fluid that remains stationary or very high-quality wind-tunnels (low turbulence levels).

Therefore, in this study, since turbulence intensity was not given in the experimental investigation, I assumed 5% and the same amount was applied for all simulations.

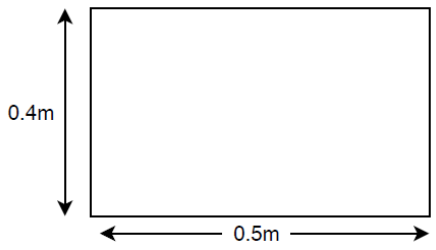

Figure 3-5 Rectangular shape of the broad crested weir

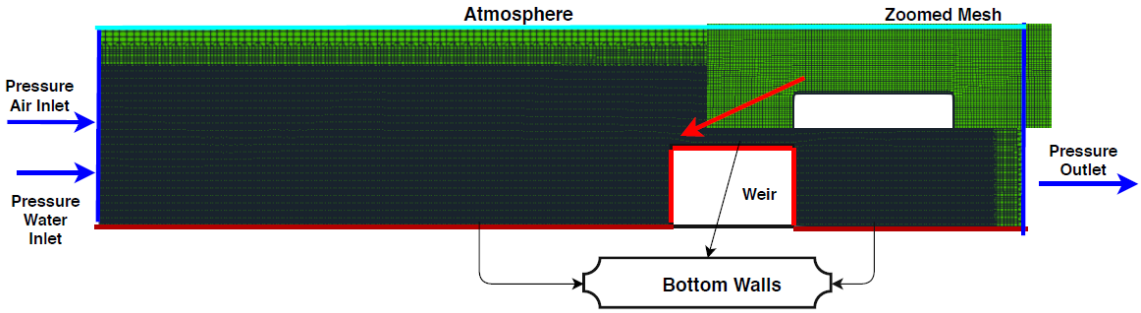

Figure 3-6 Mesh geometry and boundary condition with zoomed mesh on top of weir

The first step of the solution in the CFD software with the OpenFOAM toolbox is checking the mesh. It is also a good idea to check the mesh after performing the solution, in order to detect any mesh trouble before getting started with the problem of flow and the verification of the accuracy of meshing. Before starting the simulation, the flow must be initialized to provide an initial point for the simulation. The simulation will stop automatically when each variable meets its specified convergence measure and the message is (the solution convergences). When the convergence is checked that means the value is constant; we increased the iterations and the number of iterations was optimum.

3.11 Selection of Turbulence Models for Numerical Simulation

It is vital to select the correct turbulence model to obtain accurate data for a given numerical simulation of hydraulic structures. Therefore, for this study, the selection of the turbulence model is based on the least relative error on the water level between the numerical water surface and experimental water surface. The relative error will be computed by the mean relative error percentage (RE), root mean square errors (RMSE) and mean absolute errors (MAE). These error computation methods are used to evaluate the accuracy of data with the experimental investigation carried out by Hager and Schwalt (1994).

They are defined as follows:

Relative error percentage

$$RE = \frac{100}{N}\sum_{I=1}^{N}\left|\frac{h_{exp}-h_{num}}{h_{exp}}\right| \qquad \text{Eq. 3-18}$$

Root mean square error

$$RMSE = \sqrt{\frac{1}{N}\sum_{i=1}^{N}\left(h_{exp}-h_{num}\right)^2} \qquad \text{Eq. 3-19}$$

Mean absolute error

$$MAE = \frac{1}{N}\sum_{i=1}^{N}\left|h_{exp}-h_{num}\right| \qquad \text{Eq. 3-20}$$

where h_{exp} is the experimental head; h_{num} is the numerical head; N is the total number of points; and (i) is the number of points on the water's surface.

3.11.1 Numerical Water Surface from Different Turbulence Models

The numerical water surface profiles from all turbulence models, standard k-ε, standards k-ω, KomegaSST, Realizable k-ε, and RNG k-ε are shown in Figure 3-7, Figure 3-8, Figure 3-9, Figure 3-10 and Figure 3-11 respectively. From the figures, the water profile in each

model had a slight difference in the upstream and downstream of the broad-crested weir. However, we can observe the small variation of water surface among different models between the crest and in the downstream edge of the weir. Therefore, by comparing these water surface profiles with experimental data, we can select the best turbulence model. For better identification of the most relevant turbulence model, we need to plot and compare the numerical water surface and experimental water surface.

Figure 3-7 Numerical free water surface profile over a broad-crested weir by the standard K-ε turbulence model

Figure 3-8 Numerical free water surface profile over a broad-crested weir by standard K-ω turbulence model

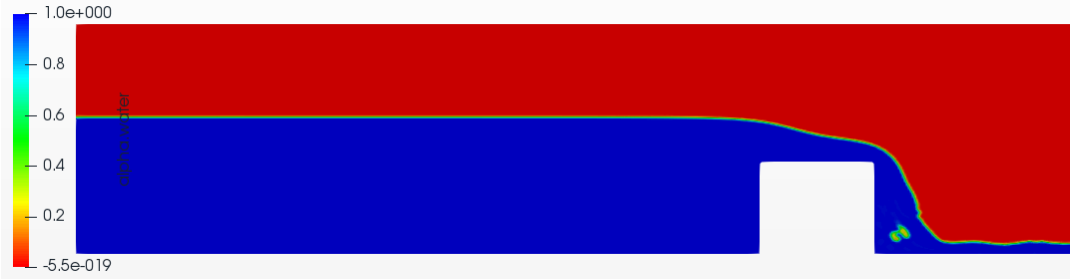

Figure 3-9 Numerical free water surface profile over a broad-crested weir by KomegaSST turbulence model

Figure 3-10 Numerical free water surface profile over a broad-crested weir by Realizable K-ε turbulence model

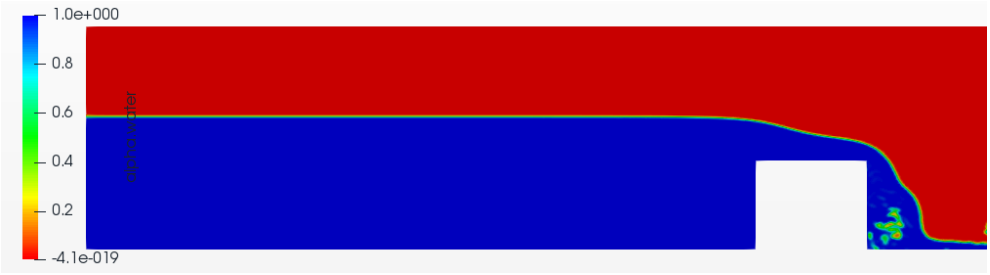

Figure 3-11 Numerical free water surface profile over a broad-crested weir by RNG K-ε turbulence model

3.11.2 Comparisons of Numerical and Experimental Water Surface

The result of relative errors obtained from the three methods must be compared and the turbulence model with the minimum relative errors will be used to set up the Reynolds-average Navier-Stokes equation for numerical simulation. Appendix A contains a summary of the water depth computed by different turbulence models. For reliability purposes, the same boundary conditions and input were used to analyze and compare with the experimental results. In the numerical simulation, it is very important to see the impact of the maximum flood on the discharge coefficient and to determine the capacity of the weir. Therefore, by considering this and relevant simulation criteria, the water surface investigated in the experimental analysis with the discharge of 68.07 l/s and the total energy head (Ho) of 0.2047 m plotted in Figure 3-3 above with Run (11) was selected for simulation and validation purposes.

Flow profiles over broad-crested weirs were obtained using different turbulence models. The numerical water surface results were plotted in Figure 3-12 below by the x-y plane; where x is the horizontal distance of the channel and y is the water flow depth along the channel. The entry of the water depth meets the weirs at 4.1 m. This figure indicates the comparison of the water surface profile obtained from the experimental work and predicted from five turbulence models, namely standard k-ε, Realizable k-ε, RNG k-ε, standard k-ω, KomegaSST k-ω. Based on the figures, the water level along the flow direction gradually decreases until it reaches a stability condition downstream of the flume. The simulations of all turbulence models indicated a good agreement with the experimental data. The simulation by the standard k-ε and standard k-ω models were almost the same as each other, but compared with the experimental data they indicated less agreement. However, KomegaSST k-ω and Realizable k-ε indicated the best similarity with the experimental data; and but the RNG k-ε model had the minimum similarity with the experimental data.

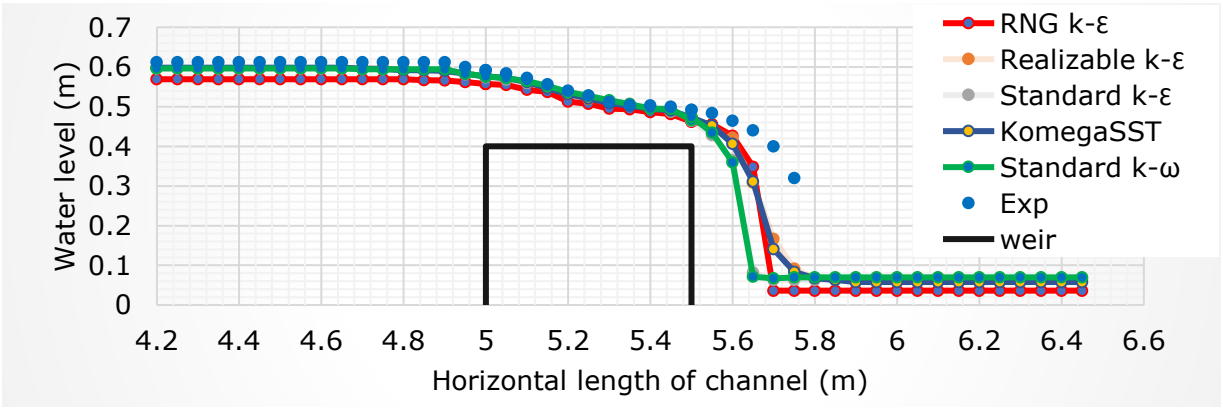

Figure 3-12 Comparisons of experimental and numerical water surface profiles computed by different turbulence models

3.11.3 Computation of Relative Errors for Water Level

At this stage, the best turbulence model was identified by using the plotted water surface in Figure 3-12 above. The water level was taken from the numerical results to identify the method which best fits the experimental data.

Table 3-2 below indicates that the relative percentage error for broad-crested weirs was about 11.187% to 6.933% in RE; 0.0957% to 0.06097% in RMSE; 0.0534% to 0.00307% in MAE; and 0.8119 to 0.908 of the goodness of fit (R2). These relative percentage errors were computed for the entire water surface profiles of all models; but in addition to this, it is also advisable to check the relative error of the head for all turbulence models.

Table 3-2 Relative percentage error of water level on the broad-crested weir

Percentage errors	Turbulence Method				
	Standard k-ε	Standard k-ω	KomegaSST k-ω	Realizable k-ε	RNG k-ε
RE (%)	9.905	9.677	7.137	6.933	11.187
RMSE (%)	0.0955	0.0957	0.0646	0.06097	0.0862
MAE (%)	0.0435	0.0423	0.0313	0.0307	0.0534
R^2	0.8306	0.823	0.9002	0.908	0.8119

For a better analysis, the head of water flow on the hydraulic structure will be constant if it is far from the obstruction or point of interest. In this analysis, 4.1 m to upstream of the weir is selected to compute the relative error of the head. From Table 3-3 below, the simulation by KomegaSST k-ω turbulence model has a minimum of 2.255% and the RNG k-ε model has higher relative errors of 7.026%.

Table 3-3 Relative errors of the head between numerical and experimental models for the broad-crested weir

Percentage errors	Turbulence Method				
	Standard k-ε	Standard k-ω	KomegaSST	Realizable k-ε	RNG k-ε
H_{exp} (cm)	61.2	61.2	61.2	61.2	61.2
H_{num} (cm)	59.56	59.63	59.82	58.68	56.9
RE (%)	2.6797	2.5654	2.255	4.1177	7.026

Based on the percentage error plotted in the histogram shown in Figure 3-13 below, the KomegaSST k-ω with the minimum relative error was identified as the best model for a numerical simulation of the water surface and other hydraulic parameters in this study. In case there is a special simulation consideration that doesn't allow us to use the KomegaSST model, we can also use models with minimum relative errors like the standard k-ε with 2.6797% relative errors, standard k-ω with relative errors of 2.5654% and realizable k-ε models with relative errors of 4.118%.

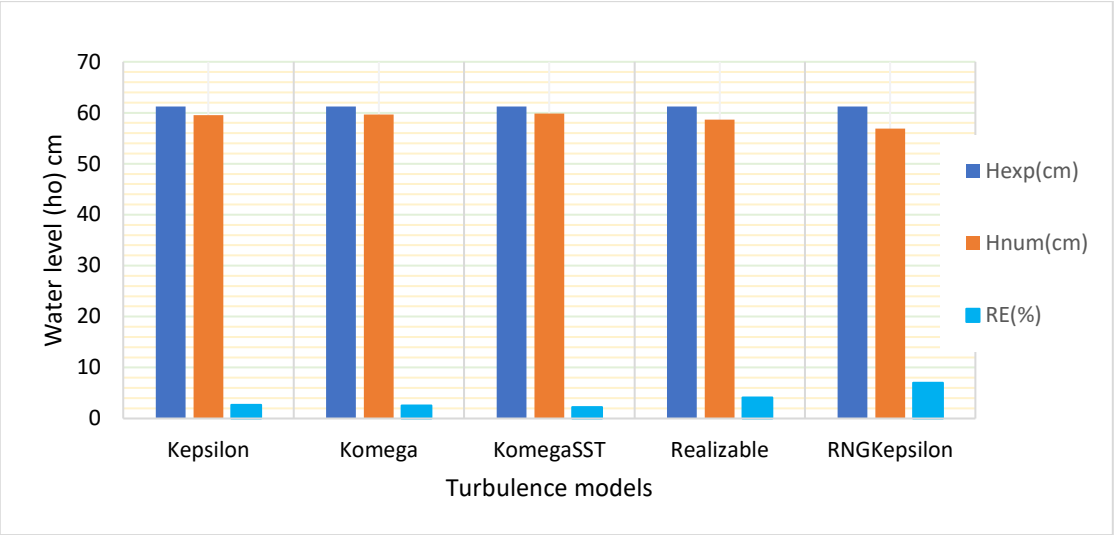

Figure 3-13 Relative errors of head from different turbulence models

3.12 Numerical Calibration and Set-up for a Sharp-edge Broad-crested Weir

After the identification of the best turbulence models, we need to calibrate the parameters for the square-edged weir until similar data to that from the experimental investigations are achieved. This will help us to analyze the impact of weir geometry on the discharge coefficient and flow parameters. Even though the main aim of this study concern natural rivers, there could be uncertainty of some parameters like the Reynolds number, velocity, degree of turbulence and turbulent kinetic energy. However, we can estimate those parameters from the design standards of hydraulic structures with different flow conditions. For instance, the flow is termed as having turbulent flow conditions, when the value of the Reynolds number is greater than 4000 for natural open channel flows. Therefore, these different ranges of Reynolds numbers were analyzed using the KomegaSST model to calibrate input data.

In this calibration process, the water surface, velocity distribution, pressure distribution, and discharge coefficient were computed. Table 3-4 below presents the values of the parameters used in the calibration and will be used further in the investigation of the detailed analysis with different geometry. The importance of the data calibration enables the investigator to get valid data and to optimize the best geometry of the broad-crested weir. The number cell used in this calibration process was 50,000. The ranges of inflow rate were also investigated; however, since the magnitude of discharge investigated in an experimental analysis by Hager and Schwartz (1994) was very small, it was identified that it will be better to go with a higher discharge of Q= 0.06807m^3/s.

3.12.1 Sensetivity Analysis

In this calibration, a sensitivity analysis was investigated by increasing numbers of cells, (means a refinement of geometry), time steps, applying of ranges of Reynolds number for turbulent flow conditions, and using different values of intensity of turbulence. When the geometry was more refinement, the accurate data will obtain, but it increases the time steps of simulations. However, the impact of the intensity of turbulence was high compared to other parameters. After checking the sensitivity analysis, the following Table 3-4 was prepared for the further simulation of flow over different shapes of broad-crested weirs.

Table 3-4 Parameters used in the calibration of the numerical model

Parameters	Value	Units
Reynolds number	33.36e-4	-
Viscosity	1.15e-6	m^2/s
Velocity	0.3836	m/s
Degree of turbulence (Ti)	5	%
Turbulent kinetic energy (k)	6e-4	-
Rate of dissipation (ε)	3.044e-6	-
Omega(ω)	0.0551	-
Number of Cells	50,000	

3.13 Validation of Experimental Results

The process of validation for the case of a broad-crested weir was started by Sarkar and Rhodes (2004). They compared the position of the free surface profile over a weir in a flume with that predicted by a CFD simulation. For a single flow rate, they considered, the agreement was good, but they asserted that further work was required at higher flow rates.

It is very important to check the set-up of the numerical model and validate the available data from experimental investigations by using the selected turbulence model. Based on the dimensions of the selected literature, several simulations were done to check the data quality and accuracy of physical modeling carried out on a sharp-edged broad-crested weir. In the experimental investigation, the ranges of the discharge (3.15 to 68.07 l/s) were used. The different types of flow patterns were dependent on the relative length of the weir Ho/Lw. Govinda Rao and Muralidhar (1963) classified the flow as a broad-crested weir, if the value of the relative length is between $0.1< Ho/Lw <0.4$. Therefore, by considering this design limitation and changing different flow parameters and the meshing of the geometry, the simulations on the geometry of a sharp-edge broad-crested weir were done to determine the discharge coefficient. The refinement of the mesh/geometry was also applied and helps us to get a sharp water surface and to obtain more accurate results.

3.13.1 Validation of Approach Flow Depth and Total Energy Head

The approach flow depth is the water depth above the crest of the weir and the total energy head is the summation of the pressure head and the velocity head. As we can see from Figure 3-14 below, the simulated and experimental water depth were in good agreement. In the experimental investigation, many researchers used the approach water depth to compute the discharge coefficient, but that way of calculating will lead to the wrong conclusion of the capacity and coefficient. However, the Hager experiment took into consideration the impact of the ignorance of the velocity head. In this validation, it shows a very good fit between the computed total energy head obtained from experimental results and simulated values.

Table 3-5 Validation of numerical and experimental data flow depth and total energy head

Q	Velocity (m/s)	Pressure (Pa)	Cd Sim	Cd Exp	ho Sim(m)	Ho Exp(m)	Ho Sim (m)	Ho Exp (m)
68.07	0.38364	5868.9	0.3413	0.332	0.1983	0.2002	0.2009	0.2047
54.83	0.31107	5616.41	0.3400	0.33	0.1725	0.1762	0.1744	0.178
37.59	0.21516	5256.87	0.3352	0.327	0.1359	0.1382	0.1369	0.1392
25.98	0.14789	4968.97	0.3349	0.329	0.1065	0.1079	0.1071	0.1084
17.81	0.10154	4740.09	0.3335	0.328	0.832	0.0841	0.0835	0.0844
10.9	0.06198	4515.87	0.3312	0.329	0.603	0.0607	0.0604	0.0607
8.25	0.04749	4416.9	0.3301	0.324	0.502	0.0509	0.0503	0.0509

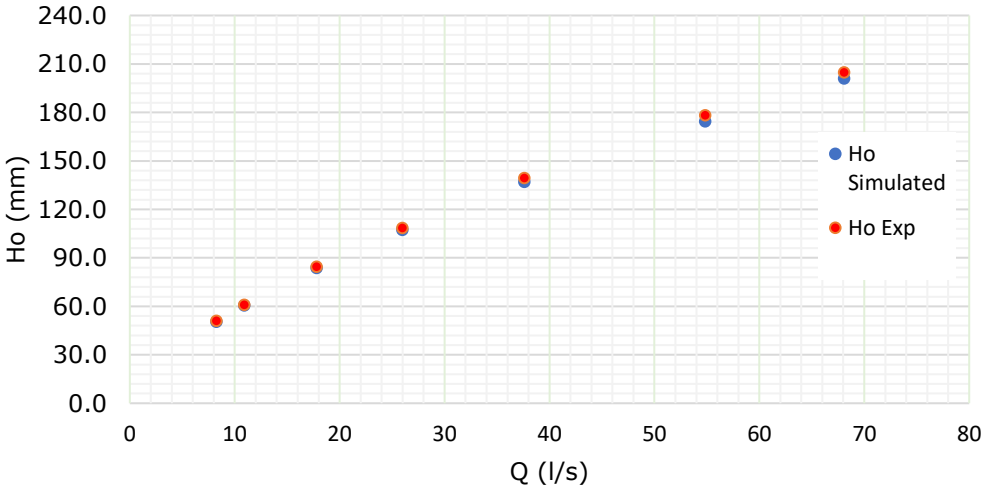

Figure 3-14 Validation of total energy head (Ho)

3.13.2 Validation of Discharge Coefficient

Most of the time computation of the discharge coefficient was done by using different discharge equations based on the objective of the research. In this study, as well as in an experimental investigation of Hager and Schwalt (1994), the discharge equation for the free water surface was considered. The discharge coefficient was computed with ranges of discharge from 8.25 l/s to 68.07 l/s and relative length (Ho/Lw) from 0.1 to 0.4. Table 3-6 below indicates a good agreement with the experimental data, but with a very small percentage of errors. This implies the correct set-up of the numerical model and the high accuracy of the experimental data.

Now, after the calibration and validation of the experimental data, we need to modify our weir geometry and run simulations. The weir geometry with a high discharge coefficient will be selected as the most economical weir in terms of capacity, planning, construction, and operation.

Table 3-6 Validation of discharge coefficient with ranges of relative length (Ho/lw)

Ho/L	Cd sim	Cd Exp	Percentage error (%)
0.406	0.337	0.332	1.373
0.3496	0.339	0.33	2.657
0.273	0.336	0.327	2.848
0.214	0.336	0.329	1.994
0.166	0.336	0.328	2.517
0.121	0.331	0.329	0.552
0.101	0.332	0.324	2.450

4 Design and Numerical Simulations

4.1 Selection of Design Criteria for Broad-crested Weir

The design of different shapes of weir geometry has been done depending on the practical design recommendations scheduled as limitation conditions of the broad-crested weir by the ASTM International Designation Standard Guide for Selection of Weirs and Flumes. Many researchers have used different design criteria to design broad-crested weirs. Most of them categorize the types of weir based on their water flow profile, energy head and crest length. Table 4-1 below describes the main, commonly used design considerations for broad-crested weirs.

Table 4-1 Basic design considerations and criteria of the broad-crested weir

Researchers	ASTM International Designation	(Govinda Rao and Muralidhar 1963)	Crabbe (1974) and Singer (1964)
Basic Assumptions and design criteria	$Lw \geq 1.75Ho$	$2.5 \leq Lw/Ho \leq 10$	$0.178 \leq Lw/Ho \leq 12.5$
	$R \geq 2.25Ho-Lw$	$R \geq 0.2Ho$	$R \geq 0.2Ho$
	$0.05 \leq Ho/Lw \leq 0.57$	$0.1 \leq Ho/Lw \leq 0.4$ 0.2	$0.08 \leq Ho/Lw \leq 5.6$
	$P \geq 0.15m$	$P \geq 0.3m$	$Ho \leq p/2$
	$Ho/p \leq 1.5$	$0.006 \leq Ho/p \leq 4$	$0.006 \leq Ho/p \leq 4$

The assumptions used for broad crested weirs are: -

- The flow lines are parallel and hydrostatic pressure distribution over the crest;
- Boundary layer thickness is overlooked compared to flow depth over the crest;
- The velocity distribution follows a uniform pattern in the outer layer.

In addition to this geometrical limitation, the following assumptions were used in the modification and detailed investigation of flow over various shapes of weirs. The upstream and downstream inclined cut are dependent on the value of the radius and the radius is assumed as (0.2 to 0.5) Ho. Table 4-2 summarizes the parameters which will be used in the modification of the weir's geometry. The energy head of 0.2047 m was selected from the literature study. For the uniformity of simulation, the weir height (p) and bottom length (Lb) were kept constant in each weir's modifications.

Table 4-2 Determination of parameters for modification of weir geometry

Ho=0.2047m	Computed Values of Parameters			
a (m)	a1= 0.2Ho	a2 = 0.3Ho	a3 = 0.4Ho	a4 = 0.5Ho
	0.0409	0.0614	0.0819	0.1024
b1 =1.5a1	0.0614	0.0921	0.1228	0.1535
b2 =2a2	0.0819	0.1228	0.1638	0.2047
b3 =3a3	0.1228	0.1842	0.2456	0.3071
b4 =4a4	0.1638	0.2456	0.3275	0.4094

4.2 Numerical Set-up of an Upstream Inclined-edge Broad-crested Weir with Various straight cut

The main aim of modifying the geometry of a broad-crested weir is to obtain the most economical weir dimension with a high discharge coefficient, which increases the discharge capacity. To get such a kind of geometry, it is important to see the impacts of upstream and downstream inclination on the flow conditions over the broad-crested weir. Table 4-3 below describes the geometries of 15 different models with the upstream and downstream inclined edge of the weir. In all cases, the same weir width and length was used and the simulation on each weir was analyzed. The minimum crest length was determined based on the design criteria manual and from the limit boundary of different works of literature.

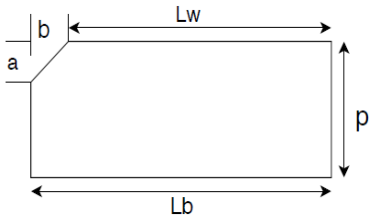

Figure 4-1 Models with the upstream inclined cut of the broad-crested weir

In this case, the minimum crest length was determined from Crabbe's (1974) and Singer's (1964) broad-crested weir design criteria. They classify the flow over the weir as broad crested if the relative length was between ($0.08 \leq Ho/Lw \leq 5.6$). Table 4-3 below shows the dimensions for all proposed geometry of broad-crested weirs in upstream straight cut and as well in both up and downstream straight cut. Thus, throughout all numerical simulations, the minimum and maximum limits of crest length were limited to these design criteria. However, for analyzing the impact of a very short crest length on the discharge coefficient, all modifications of weir geometry were also taken into consideration and simulation was done for each case.

Table 4-3 Dimensions of models with the u/s and d/s inclined cut of the broad-crested weir.

Models	Width (m)	Length Lb (m)	Height p (m)	a (m)	b (m)	Lw for u/s cut Lw = Lb-b	Lw for both side cut Lw =Lb-2b
a1b1	0.5	0.5	0.4	0.02047	0.030705	0.4693	0.4386
a1b2	0.5	0.5	0.4	0.02047	0.04094	0.4591	0.4182
a1b3	0.5	0.5	0.4	0.02047	0.05118	0.4488	0.3977
a2b1	0.5	0.5	0.4	0.04094	0.06141	0.4386	0.3772
a2b2	0.5	0.5	0.4	0.04094	0.08188	0.4181	0.3363
a2b3	0.5	0.5	0.4	0.04094	0.10235	0.3977	0.2953
a3b1	0.5	0.5	0.4	0.06141	0.09212	0.4079	0.3158
a3b2	0.5	0.5	0.4	0.06141	0.12282	0.3772	0.2544
a3b3	0.5	0.5	0.4	0.06141	0.15353	0.3465	0.193
a4b1	0.5	0.5	0.4	0.08188	0.12282	0.3772	0.2544
a4b2	0.5	0.5	0.4	0.08188	0.16376	0.3362	0.1725
a4b3	0.5	0.5	0.4	0.08188	0.2047	0.2953	0.0906
a5b1	0.5	0.5	0.4	0.10235	0.15353	0.3465	0.193
a5b2	0.5	0.5	0.4	0.10235	0.2047	0.2953	0.0906
a5b3	0.5	0.5	0.4	0.10235	0.235405	0.2646	0.0292

After an investigation of numerical simulation on the upstream cut by using the KomegaSST turbulence model, the results of the discharge coefficient, total pressure, water level, velocity head, and the total energy head were obtained and tabulated in Table 4-4 below. The comparison of the simulated discharge coefficient with the sharp edge of the experimental result was plotted on a histogram with a Cd value on the y-axis and weir models on the x-axis as shown in Figure 4-2 below. From these simulations, the increment of capacity was observed as the modification of the weir geometry was made from a sharp edge to upstream inclined edge. The maximum discharge coefficient was 0.3918 with a model a_4b_3 with the weir model of crest length 0.2953 m. This indicates that the new geometry of the weir can increase the capacity by 15.26%.

Table 4-4 Discharge coefficient comparison of 15 upstream cut models.

Models	(P_rgh) (Pa)	h_o (m)	Velocity (m/s)	H_o (m)	Cd simulated
a1b1	5794.62	0.1907	0.2305	0.1934	0.3614
a1b2	5779.31	0.1891	0.2311	0.1918	0.3658
a1b3	5755.29	0.1867	0.2321	0.1894	0.3728
a2b1	5718.15	0.1829	0.2336	0.1857	0.3842
a2b2	5737.00	0.1848	0.2328	0.1876	0.3783
a2b3	5735.40	0.1846	0.2329	0.1874	0.3788
a3b1	5716.79	0.1828	0.2336	0.1855	0.3846
a3b2	5729.89	0.1841	0.2331	0.1869	0.3805
a3b3	5718.87	0.1830	0.2335	0.1857	0.3839
a4b1	5726.35	0.1837	0.2332	0.1865	0.3816
a4b2	5700.25	0.1811	0.2343	0.1839	0.3898
a4b3	5694.25	0.1805	0.2345	0.1833	0.3918
a5b1	5791.66	0.1904	0.2306	0.1931	0.3622
a5b2	5790.00	0.1902	0.2307	0.1929	0.3627
a5b3	5718.70	0.1829	0.2335	0.1857	0.3840

where

P_ rgh is the total pressure obtained from numerical simulation;

h_o is the water level obtained by- $ho = \frac{P\_rgh}{1000*9.81}$;

v is the approach velocity calculated by; $\frac{Q}{(h_o+p)}$, p is the height of the weir;

H_o is the total energy head; $Ho = ho + \frac{V^2}{2g}$, $\frac{v^2}{2g}$ is the velocity head and the discharge coefficient Cd is calculated by using the discharge equation of free surface flow.

$$Cd = \frac{Q}{B*\sqrt{2g}(H_o)^{3/2}} \qquad \text{Eq. 4-1}$$

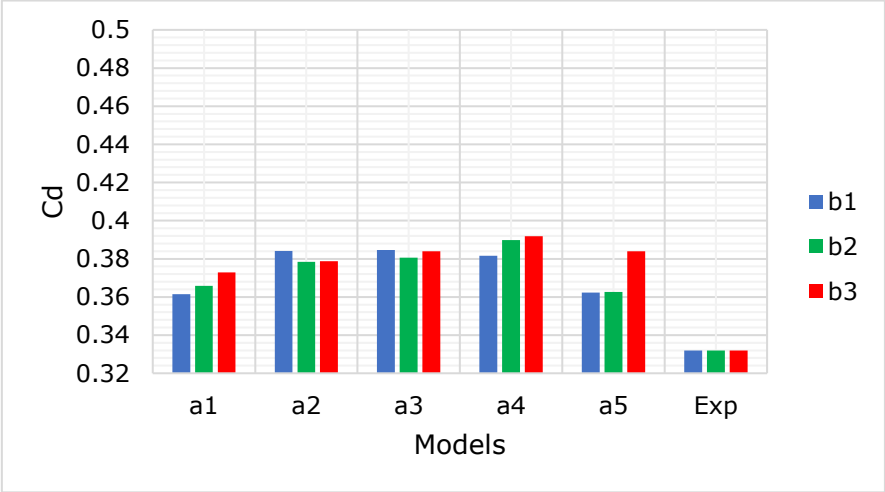

Figure 4-2 Comparison of the discharge coefficient for 15 models with upstream straight cut and the experimental result

4.3 Numerical Set-up for both Up and Downstream Inclined Edges with Various Straight Cuts

From the upstream straight cut, we observed that the value of the discharge coefficient was in keeping and increased by 15.25%. Hence, in this case, both upstream and downstream edges were changed to a straight cut. Thus, 15 different models were developed as shown in Figure 4-3 below and the result of the numerical simulation tabulated in Table 4-5 below. As we can see from this output, the discharge coefficient and weir modification have direct relationships. The peak Cd of 0.4827 was obtained from a model of a5b3 with the crest length of 0.0292 m as shown in Figure 4-4 below. However, this crest length is less than the minimum design criteria and it is too small a crest length to investigate with the ranges of discharge. In addition to this, even if it has a higher discharge coefficient, it will be very difficult to obtain the critical depth and parallel streamline on the top weir crest for a small crest length. Then the class of the weir will be changed from broad crest to a long-crested or sharp-crested weir depending on the energy head. On the other hand, the weirs with the small crest length do not reflect the characteristics of the broad-crested weir, but they can be described as sharp-crested weirs. As a result of this, I decided to optimize the crest length and Cd values for detailed analysis. Thus, from both upstream and downstream straight cuts, the model named as a4b2 which

has the Cd value of 0.4156 was selected with the crest length of 0.173 m and an increment of discharge coefficient by 20.211%.

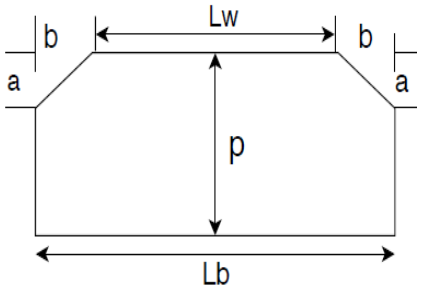

Figure 4-3 Model with the up and downstream inclined cut of the broad-crested weir

Table 4-5 Dimensions of models with the up and downstream inclined cut of the broad-crested weir

Models	P_rgh	h_o (m)	Velocity (m/s)	H_o (m)	Cd simulated
a1b1	5756.84	0.1868	0.2320	0.1896	0.3724
a1b2	5756.24	0.1868	0.2320	0.1895	0.3725
a1b3	5769.94	0.1882	0.2315	0.1909	0.3685
a2b1	5724.26	0.1835	0.2333	0.1863	0.3823
a2b2	5720.90	0.1832	0.2334	0.1859	0.3833
a2b3	5711.75	0.1822	0.2338	0.1850	0.3862
a3b1	5860.00	0.1973	0.2279	0.2000	0.3436
a3b2	5852.00	0.1965	0.2282	0.1992	0.3457
a3b3	5660.56	0.1770	0.2359	0.1799	0.4029
a4b1	5660.56	0.1770	0.2359	0.1799	0.4029
a4b2	5624.29	0.1733	0.2375	0.1762	0.4156
a4b3	5571.49	0.1679	0.2397	0.1709	0.4352
a5b1	5623.40	0.1732	0.2375	0.1761	0.4159
a5b2	5524.51	0.1632	0.2417	0.1661	0.4539
a5b3	5458.32	0.1564	0.2447	0.1595	0.4827

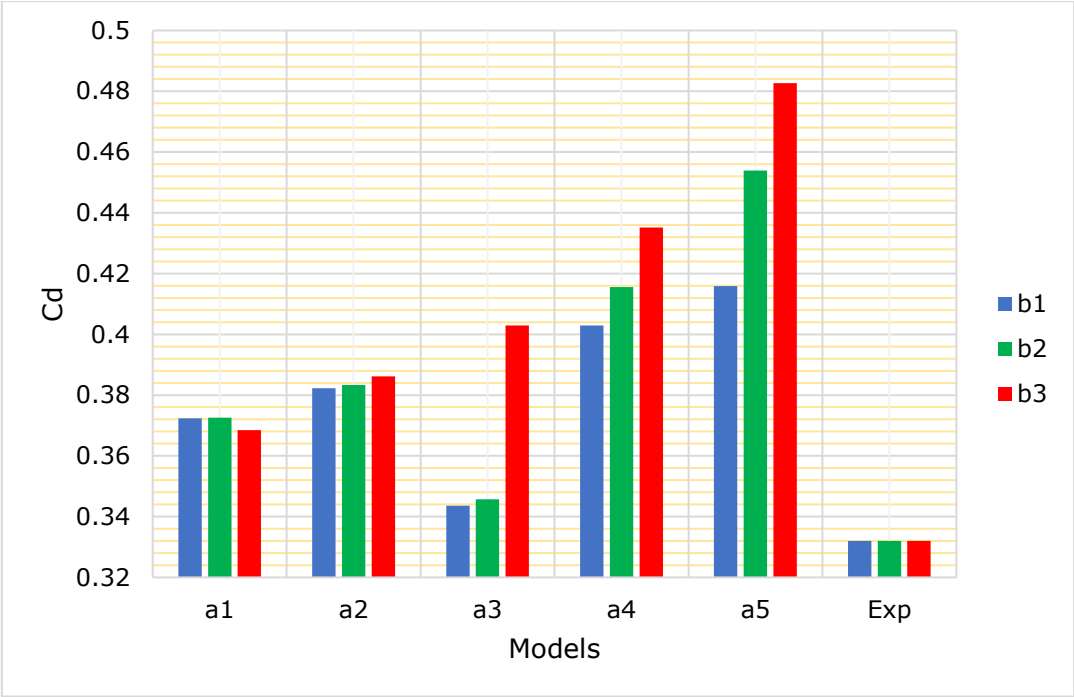

Figure 4-4 Comparison of discharge coefficient from 15 models with up and downstream cut

4.4 Numerical Set-up for Upstream Round Cut With Various Radiuses

The upstream round edge is the most commonly used shapes of the broad-crested weir in both numerical and experimental investigations. The upstream round edge tends to provide a good hydraulic characteristic by avoiding or minimizing the separation zone on the top of weirs. In this weir design, the upstream edge was rounded with the radius (0.02047 m to 0.10235 m) shown in Table 4-6 below.

Table 4-6 Dimension of upstream and downstream round cut

Models	Weir width (m)	Weir length (m)	Weir height (m)	Radius (m)
R1	0.5	0.5	0.4	0.02047
R2	0.5	0.5	0.4	0.04094
R3	0.5	0.5	0.4	0.06141
R4	0.5	0.5	0.4	0.08188
R5	0.5	0.5	0.4	0.10235

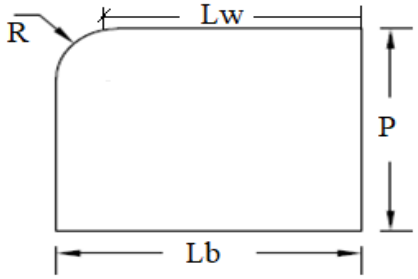

Figure 4-5 Model with the upstream round cut of the broad crested weir

Round edge weirs were the best solution to avoid the formation of recirculation on the top of a broad-crested weir, which will lead to a wrong discharge reading, the formation of scouring on the top of weir, and cavitation at the downstream. It was also the most studied areas of investigation by many researchers. The simulated discharge coefficient also increases as the sharp edge is changed to round edges. The maximum Cd value from this type of weir modification was 0.3829 with the round cut radius of 0.0819 m as shown in Table 4-7 below.

Table 4-7 Simulated parameters of upstream round cut

Models	P_rgh	ho(m)	Velocity(m/s)	Ho(m)	Cd simulated
R1	5787.83	0.1900	0.2307	0.1927	0.3633
R2	5765.21	0.1877	0.2317	0.1904	0.3699
R3	5724.50	0.1835	0.2333	0.1863	0.3822
R4	5722.25	0.1833	0.2334	0.1861	0.3829
R5	5766.56	0.1878	0.2316	0.1906	0.3695

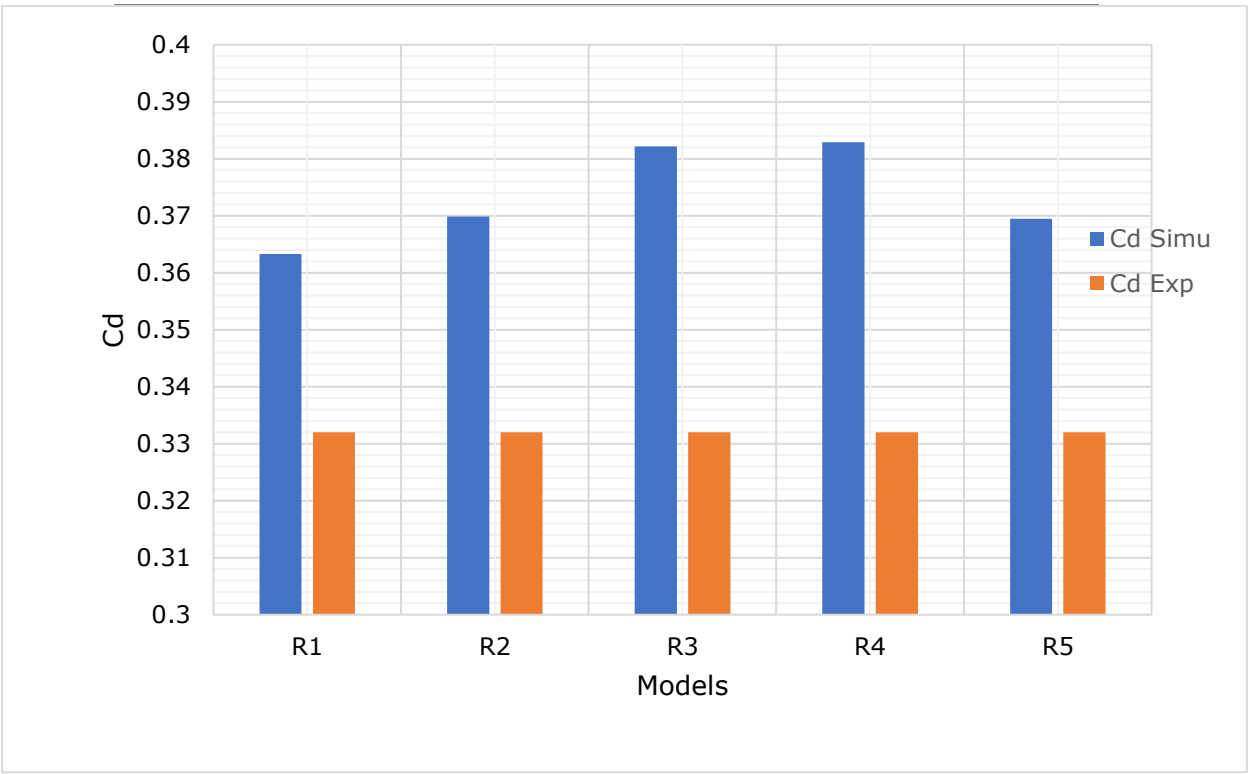

Figure 4-6 Comparison of discharge coefficient from five models with upstream round cut

4.5 Numerical Set-up for Upstream and Downstream Round Cut Edge With Various Radiuses

Many variations in weir shape exist for broad-crested weirs. A few alternative geometries for the downstream face of a round-nosed rectangular weir are shown in Figure 4-7 below. These alternative geometries consist of ways to reduce flow separation (round edges, ramps, streamlining) and are generally meant to increase the discharge coefficient Julian (2014). In this simulation, five different models were analyzed with both up and downstream round edges with different round radiuses. The increment of the discharge coefficient was also observed and the maximum Cd value of 0.388 was obtained when the

weir has both sides round-edged with a radius of 0.1023 m as shown in Figure 4-7 and below.

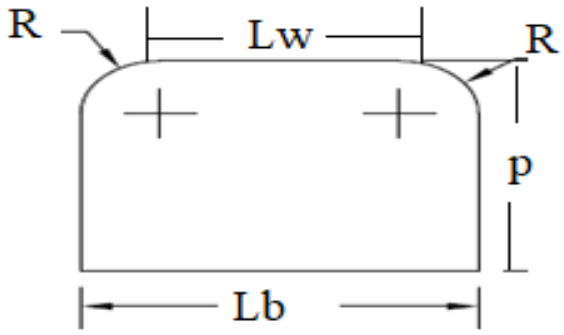

Figure 4-7: Model with the up and downstream round cut of the broad-crested weir

Table 4-8 Simulated parameters of upstream and downstream round cut

Models	P_rgh	ho (m)	Velocity (m/s)	Ho (m)	Cd simulated
R1	5776.22	0.1888	0.2312	0.1915	0.3667
R2	5761.69	0.1873	0.2318	0.1901	0.3709
R3	5743.80	0.1855	0.2325	0.1883	0.3763
R4	5734.80	0.1846	0.2329	0.1874	0.3790
R5	5705.69	0.1816	0.2341	0.1844	0.3881

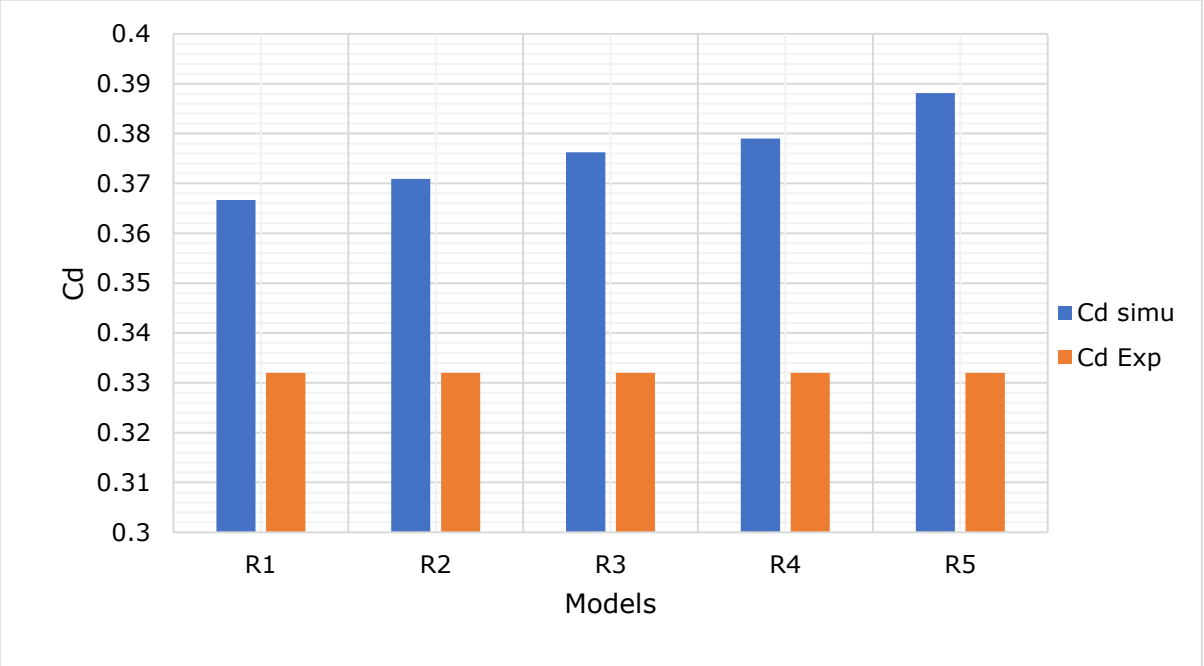

Figure 4-8 Comparison of discharge coefficient from five models with both up and downstream round cut against the experimental result

4.6 Result and Discussion

4.6.1 Comparison of Water Surface Profiles and Discharge Coefficient

During the selection of the best weir geometry from all cases, we need to compare different numerical parameters of the best models from all cases with the experimental data achieved by Hager and Schwalt (1994) on the square-edged broad-crested weir. The numerical water surface of the best models was plotted in Figure 4-9 below. For better comparison, the water surface was plotted together with the experimental water surface of the sharp-edged broad-crested weir as shown in Figure 4-10 below. However, Appendix C: Shows the comparison of the water level for all best models with the experimental. From this figure, we can observe that the weir model of a4b2 shows the maximum discharge coefficient and a small water level compared with a sharp-edged weir. The observed water surface is also smooth on the crest and towards downstream. Therefore, we can identify that model a4b2 is the better geometry for a weir with a 20.211% increment of discharge coefficient.

Table 4-9 Variation of Cd and Ho for best models from all weir modifications

Modification	Upstream straight cut	Both sides straight cut	Upstream round cut	Both sides round cut
Models	(a4b3)	(a4b2)	(R4)	(R5)
Q (l/s)	68.07	68.07	68.07	68.07
Ho Exp	0.2047	0.2047	0.2047	0.2047
Ho Simu	0.1832	0.1733	0.186	0.1844
Cd Simu	0.3918	0.4156	0.3829	0.388
Cd Exp	0.332	0.332	0.332	0.332
Increment in Cd	15.26%	20.211%	13.29%	14.43%

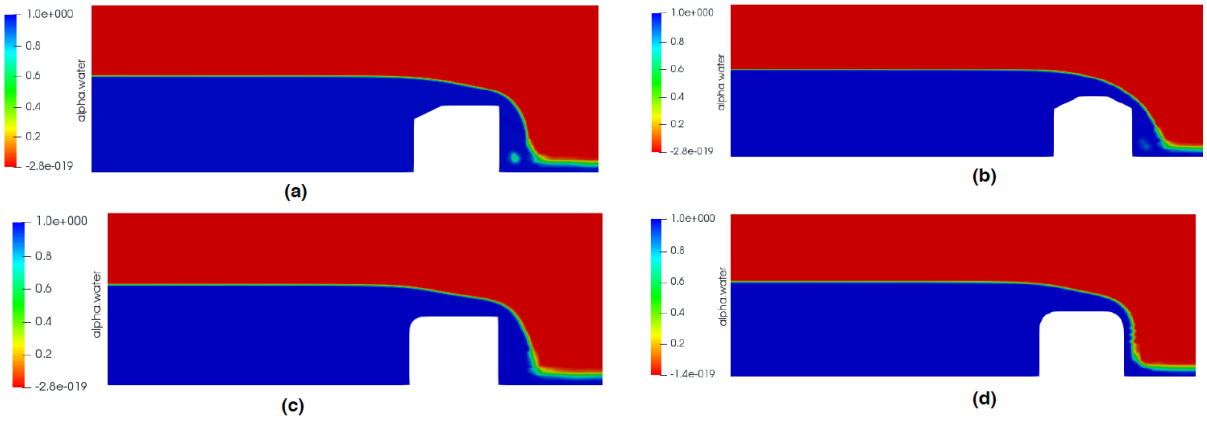

Figure 4-9 Numerical free water surface of best models (a4b3), a4b2, R4 and R5 in (a), (b), (c) and (d) respectively

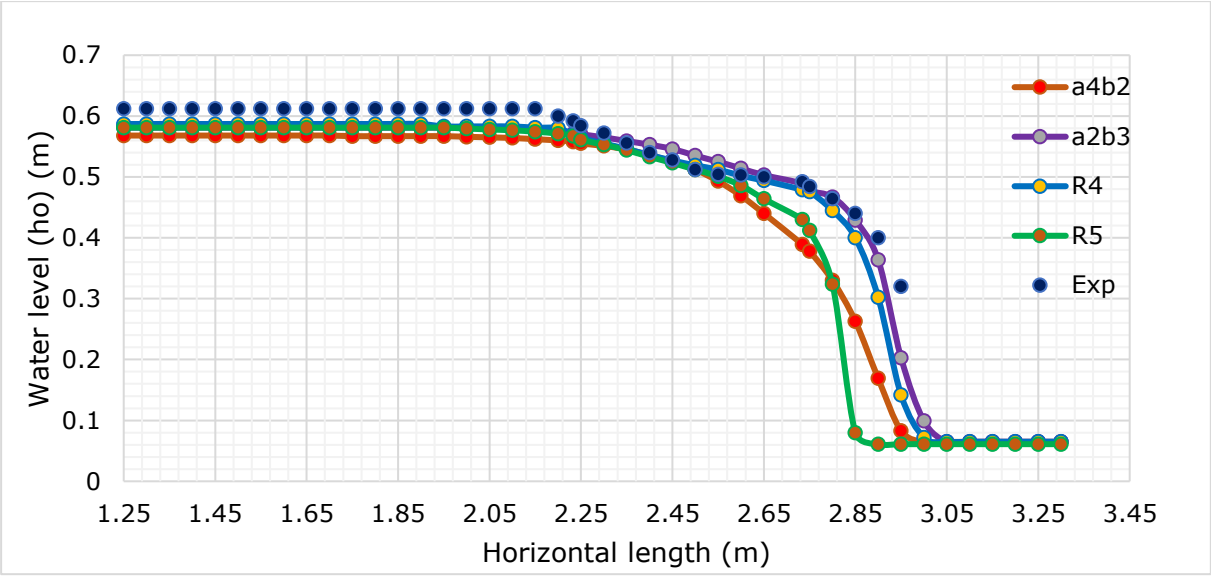

Figure 4-10 Comparison between experimental water surface on the square edge weir and simulated water surface from best models.

4.6.2 Comparison by Streamline Tracer

Streamlines are created by first creating tracer lines using the stream tracer filter. The tracer speed panel specifies the distribution of tracer points over a line source or point cloud. The distance the tracer travels and the length of steps the trace takes are specified in the text boxes in the mainstream tracer panel. The streamline is used for visualization of the formation of the separation zone for a given flow over hydraulic structures. Figure 4-11 below shows the formation of the recirculation zone on the top of a broad-crested weir with different shapes. We can see the long separation zone on the u/s edge of a square-edged broad-crest weir shown on Figure 4-11 (a). However, it is almost negligible or very small in models with both sides straight cut and the upstream round cut. We must avoid or minimize this as much as possible in the design of structures used for discharge measurement and flow regulation.

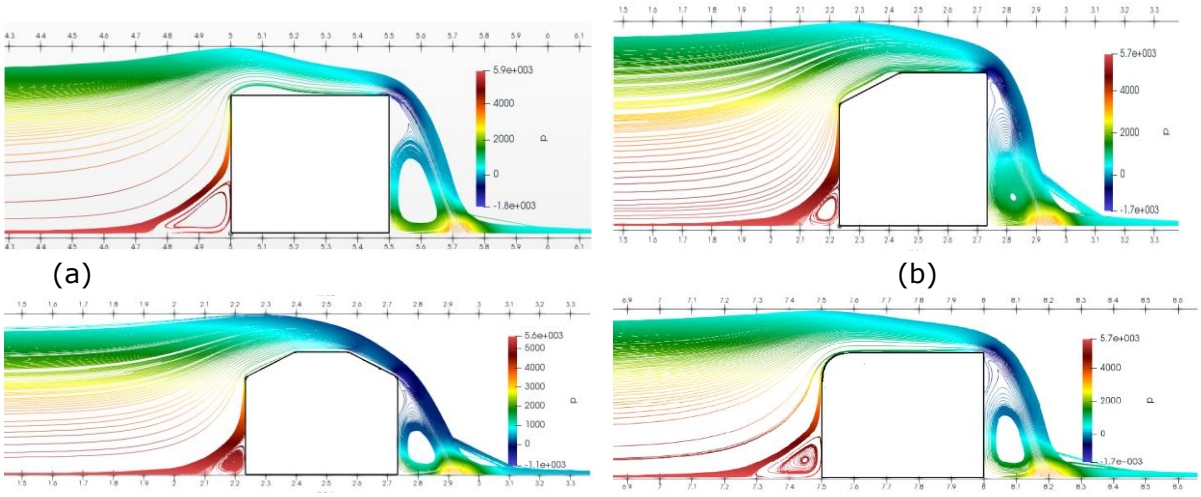

Figure 4-11 Streamline tracer for visualization of the recirculation zone on the sharp edge (a); upstream straight cut (b); both edge straight cut (c); upstream round cut (d)

4.6.3 Velocity and Pressure Distribution

Some typical velocity and pressure distributions are shown in Figure 4-12. The data in both velocity and pressure distribution showed consistently some rapid redistribution of pressure and velocity fields, at upstream and downstream ends of a broad-crested weir, and the flow rate rapidly varied. For the channel length of less than 0.5 m, the pressure gradient was typically less hydrostatic and the velocity in each model was increased as it reached the edge of the weir and then decreased towards the downstream end. The rapid flow redistribution at the upstream end of a turbulent boundary layer. However, in the discharge measurement, too much high-water turbulence at the top of the weir is not recommended. As we can see from the Figure 4-12 (a) and (b) below the model a2b4 has a lower velocity and pressure distribution among others.

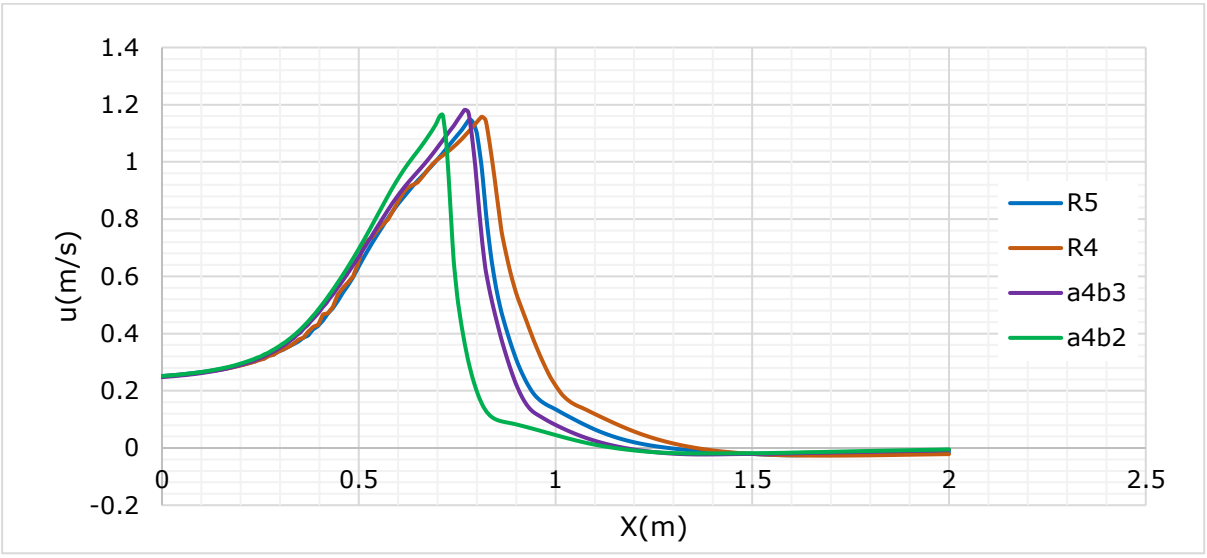

(a)

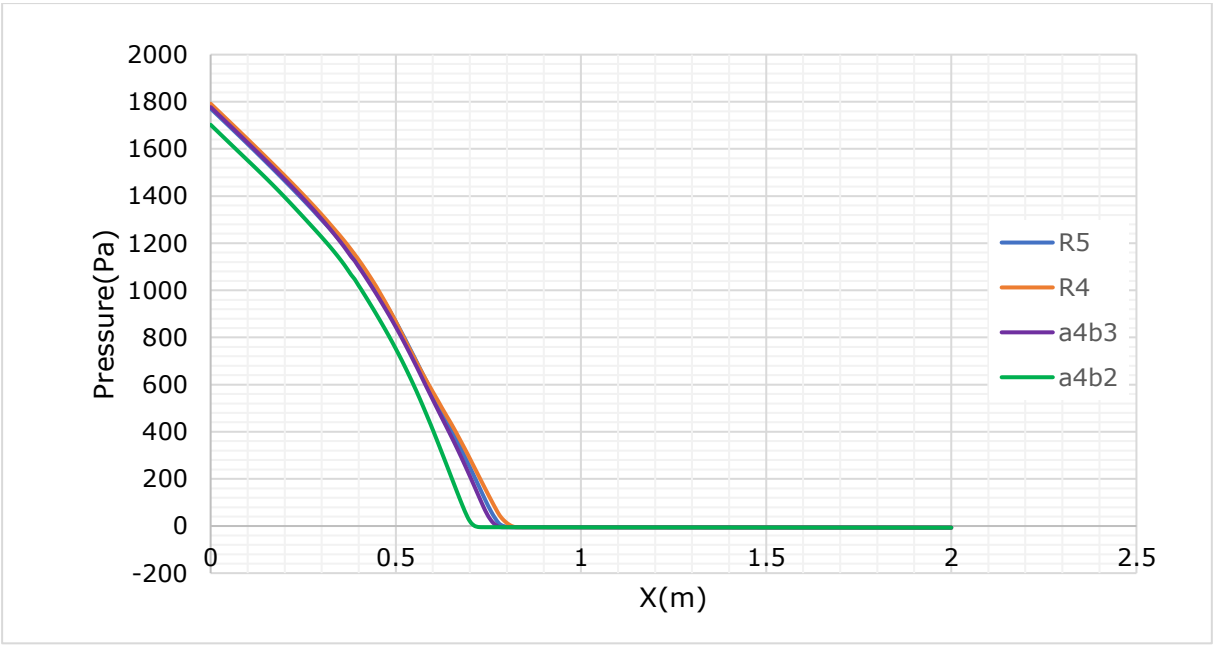

(b)

Figure 4-12 Comparison with velocity distribution (a); and pressure (b), for the discharge of Q=68.07l/s

4.6.4 Convergency Analysis

Checking for convergence has a major role in numerical simulations. Convergence means the flow conditions in a given channel or on a hydraulic structure will attain steady-state conditions. Typically, when assessing the convergence of steady state CFD analysis, the following three criteria should be monitored as the analysis progresses. They are residual values, solution imbalance, and quantities of interest.

The residual is one of the most fundamental measures of an iterative solution's convergence, as it directly quantifies the error in the solution of the system of equations. In a steady-state analysis, the solution field should not change from iteration to iteration for an analysis to be deemed converged. Monitoring quantities such as velocity distribution, total pressure, and alpha water can be used to evaluate whether our simulation was converged as shown in Appendix C.

In Figure 4-13 below, after approximating an accumulated time step of 8, there is no fluctuation seen in velocity and alpha water. This indicates that the flow of water became steady and there was good convergence of the numerical simulation. However, the velocity distribution of model a4b2 as we can see from the Figure 4-13 below in (a) shows small fluctuations throughout the time step. Hence, for better analysis and accurate interpretation, we need to simulate with more time steps.

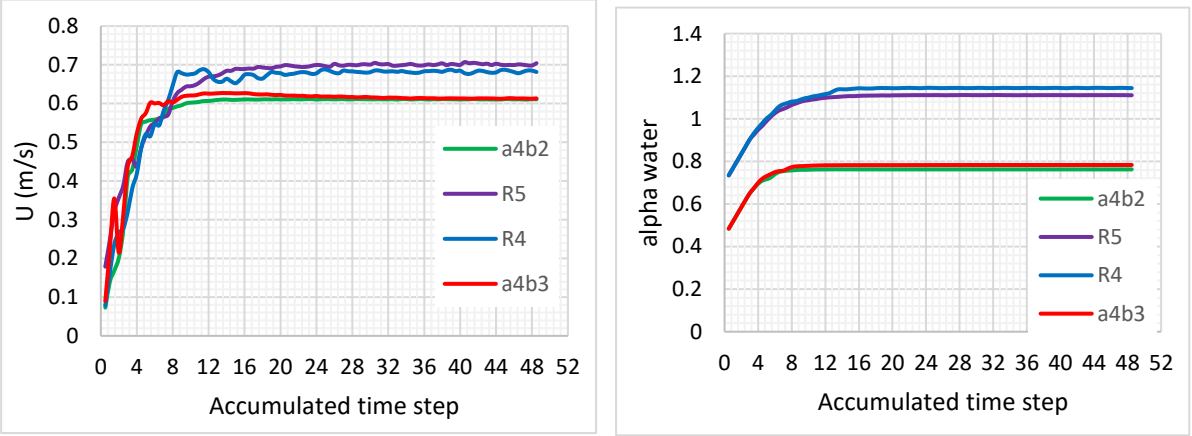

Figure 4-13 Convergence analysis by quantities of interest velocity (a), and alpha water (b)

4.6.5 Discussion of Existing Relationships for the Discharge Coefficient

The results of an investigation by different researchers on broad crested weirs showed that the upstream angles significantly affect a broad-crested weir's hydraulic performance in terms of free water surface, discharge coefficient, velocity profiles and flow separation zone. Despite computational fluid dynamics (CFD) becoming an important method to investigate hydraulic problems, less attention has been given to study the effect of the upstream angle on the hydraulic performance of a broad-crested weirs based on numerical simulations.

According to Horton et al. (1997) the discharge coefficient depends exclusively on the relative weir length Ho/Lw, provided the effect of viscosity and surface tension may be neglected. However, Fritz and Hager (1998) stated that the discharge coefficient of broad-crested weirs with vertical faces is very low. Hence, several investigators studied broad-crested weirs with sloped upstream and downstream faces. Fritz and Hager (1998), conducted on broad-crested weirs with upstream and downstream slopes satisfying 1V:2H,

to study the effect of slope faces on the flow regime. They found that such weirs' discharge capacity is 15% greater than that of broad-crested weir with vertical faces. They also developed an empirical formula to calculate the discharge coefficient, which is described as follows:

$$cd = 0.43 + 0.06\sin(\pi(\xi - 0.55)) \qquad \text{Eq. 4-2}$$

Where ξ is relative crest length; $\xi = \frac{Ho}{(Ho+L)}$ -with the value between 0< ξ<1.

Sargison and Percy (2009) investigated the flow over a trapezoidal broad-crested weir with varying upstream and downstream slopes. They found that increasing the upstream slope in the vertical direction reduced the discharge coefficient, and the effect of downstream slopes on the water's surface and pressure profiles over the broad-crested weir could be ignored. They modified Eq. 4-2 shown above to account for the influence of the upstream angle θ, which is described as follows:

$$Cd = 0.43 + 0.06 * \sin[\pi(\xi - 0.55)] - 0.0396\theta - 0.0029 \qquad \text{Eq. 4-3}$$

Govinda Rao and Muralidhar (1963), based on the results of their experimental investigation, suggested that in the range of $0 \leq \frac{ho}{Lw} \leq 0.1$, Cd is described by

$$Cd = 0.971\left(\frac{ho}{Lw}\right)^{0.022} \qquad \text{Eq. 4-4}$$

4.6.6 Equations of Discharge Coefficient Based on Weir Geometry

In this study, the impact of weir crest length and bottom width on the discharge coefficients was investigated. From all investigations, the maximum increment of the discharge coefficient was observed in the modification of broad-crested weirs with both upstream and downstream straight cut. As a result of this, the relationship between weir geometry and the corresponding value of Cd from all models of both sides straight cut was plotted against the ratio of Lw/Lb as shown in Figure 4-14 below. In this figure, we can see that the discharge coefficient was higher with the model of the straight cut a4 and gave the better Cd value for ranges of the Lw/Lb ratio (1 to 0.2), as compared to the other model's geometries. The highest Cd was 0.435 at the straight cut of a4 = 0.0819 m and Lw/Lb of 0.2.

In most layouts of broad-crested weirs the hydrostatic pressure is fully accomplished in the middle of the crest. However, in cases where the weir length is too small, it might be that the hydrostatic pressure is not fully accomplished Haun et al. (2011). For general design purposes the model with higher discharge coefficient was used to develop the equation of the discharge coefficient as a function of crest length and bottom length, as shown in Figure 4-15 below. By using Eq. 4-5 below, we can determine the discharge coefficient for a given geometry of the broad crested weir. The discharge coefficient equation based on the weir geometry is given as: -

$$Cd = -0.1057\left(\frac{L_w}{L_b}\right) + 0.4523 \qquad \text{Eq. 4-5}$$

where Cd is a discharge coefficient; Lw crest length; and L_b is the bottom weir length.

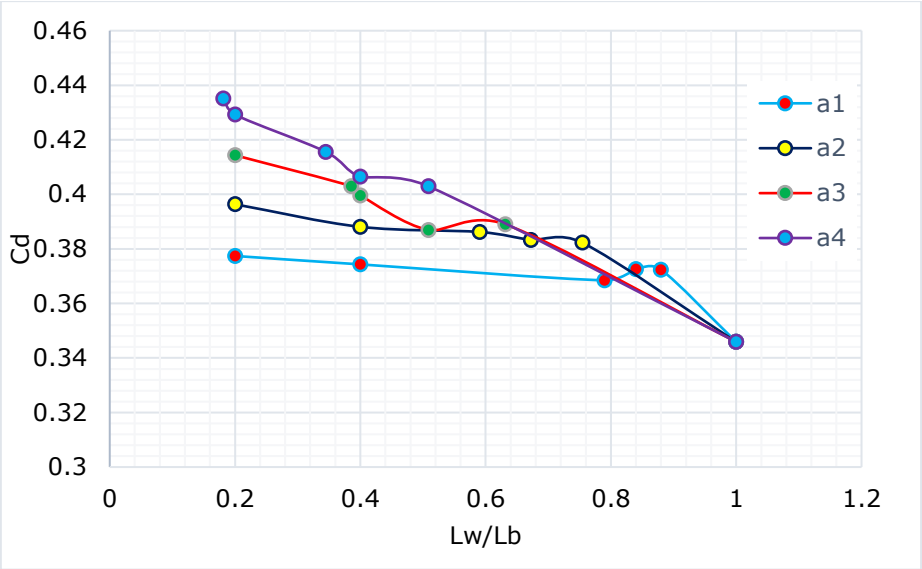

Figure 4-14 Comparison of Cd with the crest length to bottom length ratio (Lw/Lb)

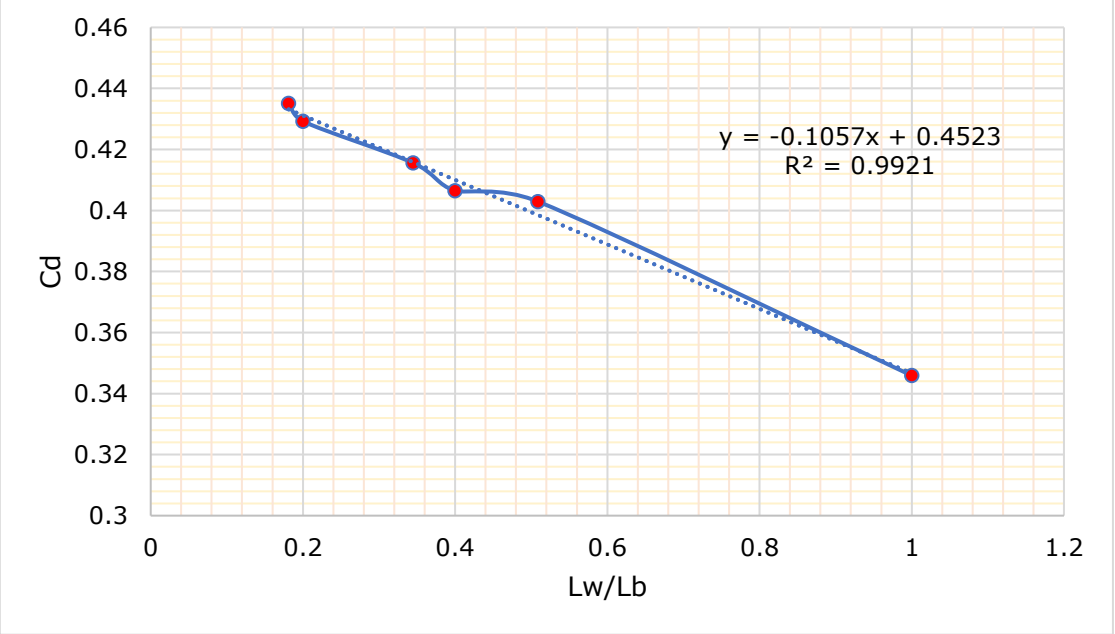

Figure 4-15 Variation of Cd with a combination of best weir geometry at the straight cut of a = 0.0819 m and b = 0.1638 m

4.7 Selection of the Most Economical Weir Geometry with High Capacity

Based on the design criteria of the broad crested weir, the minimum crest length should be attained. According to Govinda Rao and Muralidhar (1963), the minimum crest length of the weir to obtain the head of 0.2047m is 0.5m and the maximum is 2m. However, Crabbe et al.1974 expanded the application limits as proposed by Singer (1964) in terms of weir length and weir height, and then Sreetharan (1988) came up with limits as wide as $0.08 < Ho/Lw < 5.6$. and $0.006 < Ho/P < 4$. Therefore, according to Singer and Sreetharan, for broad-crested weirs the minimum crest length of 0.0366 m and a maximum crest

length of 2.55 m is required for attaining the maximum head of 0.2047 m. Farzin Poorescandar (2011) found that the ratio of crest length to the upstream head over crest Lw/Ho must be typically greater than 1.5 to 3 m. This research was very recent, and it modifies all broad-crested weir design criteria. Therefore, according to this principle, we need to provide the minimum crest length of 0.307 m and the maximum crest length of 0.6141 m to attain the head of 0.2047 m.

As a result of this, the weir geometry from all modifications with maximum discharge coefficient and with a cost-effective cross-section of the broad-crested weir was identified. For a better investigation, it was decided to set the minimum crest length to 0.17248m. According to Crabbe's and Singer's design criteria, we can simulate the flow over a broad-crested weir for the energy head (Ho) between 0.0138 m and 0.966 m with this crest length. The model which satisfies this criterion with a higher discharge coefficient of 0.4156 was the model (a4b2), with both sides inclined cut of 'a' value 0.08188 m and b = 2a = 0.16376 m as shown in Figure 4-16 below.

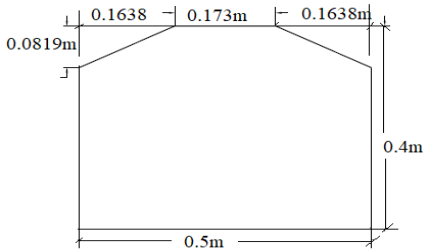

Figure 4-16 Selected broad-crested model's geometry based on discharge coefficient

4.7.1 Discharge Coefficient Based on the Ranges of Discharge Flow

Now, after identification of the best model depending on the Cd value, at detailed analysis will be made to get the relationship between the ranges of discharge and relative length (Ho/Lw). According to the design criteria of Crabbe and Singer, the maximum relative length of Ho/Lw is 1.187 m and is required for the design head Ho of 0.2047 m. Thus, we can run our simulations until we obtain the maximum design head, and even beyond the limit to analyze the impact of further simulation on the capacity.

The ranges of discharge for these simulations varied from 0.015 to 0.1 m^3/s. The required head of 0.2047 m was obtained with the discharge capacity of 0.085 l/s. This indicates the increase of capacity by 0.016 m^3/s with the new geometry. For the range of $0.35 \leq Ho/Lw \leq 1.3245$, the equation of the discharge coefficient was obtained by using a polynomial second-degree order relationship with a correlation value of R2 of 0.964 as shown in Figure 4-17 below.

$$Cd = -0.0243\left(\frac{H_o}{L_w}\right)^2 + 0.0804\left(\frac{H_o}{L_w}\right) + 0.3485 \quad \text{..... Eq. 4-6}$$

Where Cd a is discharged coefficient, Ho total energy head, and Lw weir crest length.

Finally, the water surface profile with the ranges of discharge from 0.015 m^3/s to 0.1 m^3/s was simulated and plotted in Figure 4-18 below. The observed water profiles were uniform upstream and downstream of the weir. This indicated that the simulation was done until the convergence criteria were attained. The selected model of the weir has high capacity with small geometry, and since it's simple geometry, it will be cost-effective in construction and operation.

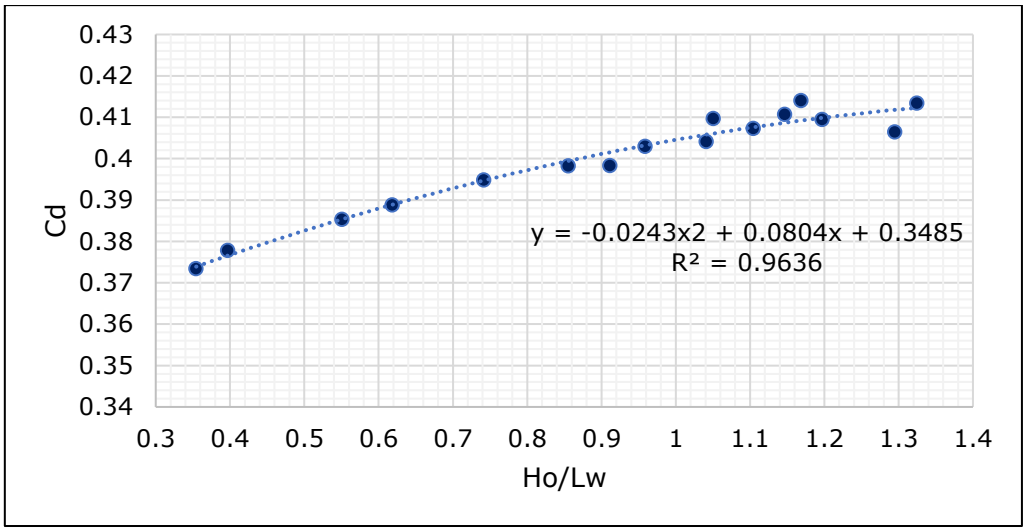

Figure 4-17 Relationship between discharge coefficient and relative length (Ho/Lw) of the a4b2 model

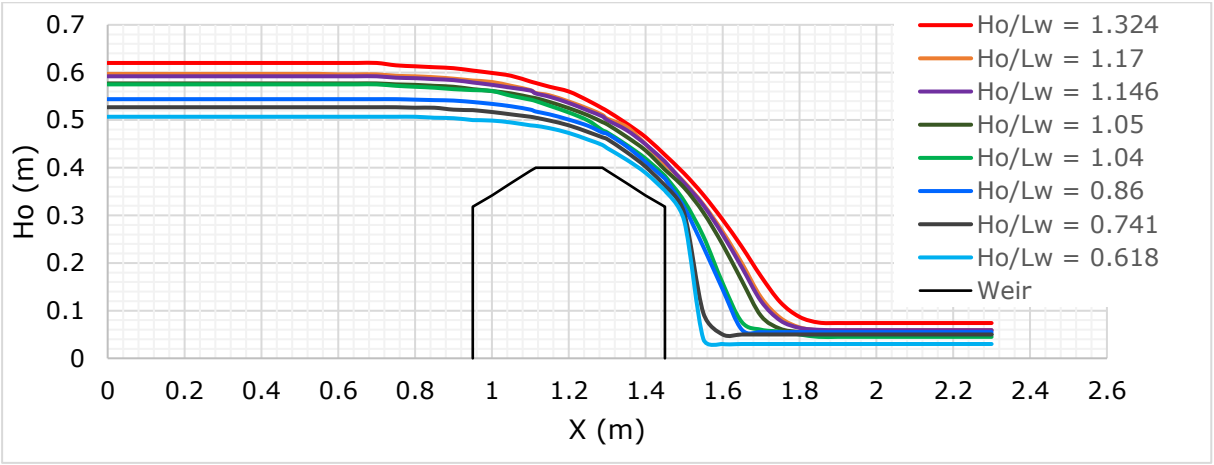

Figure 4-18 Water surface profile over the most economical broad-crested weir with ranges of discharge

4.8 Numerical Investigation of flow over the Broad-crested Weirs Based on Crest Inclination

In this case, the modification of the weir was done by varying the upstream straight and round cut with downstream crest inclination towards downstream with a range of inclination angles from 0° to 5°. In order to investigate the flow over a broad-crested weir with the required dimension, we need to know the relevant design criteria of such a weir.

According to Govinda Rao and Muralidhar's (1963) design criteria of abroad-crested weir with a boundary of 0.1 < Ho/Lw< 0.4, the minimum and the maximum allowable crest length were calculated based on this design criteria. Since the energy head of 0.2047 m was selected from the literature, the same assumptions during the weir modification were made in this case as well. However, in order to get this energy head, we need to run our simulation with the weir crest length between 0.5 m to 2 m. Depending on this limitation, the crest length of 1 m and height of 0.4 was selected for this case.

4.8.1 Numerical Simulation with Upstream Straight Cut and Crest Inclination of 0° to 5°

In this simulation, the modification of the weir was done on the upstream edge to the inclined and round cut. The effect of the crest inclination towards downstream on the discharge coefficient was also analyzed in both cases. The modification dimensions were assumed based on the selected total energy head. In Table 4-10 below, the values for both upstream straight cut and radius cut were tabulated. For investigation purposes, the same value for a straight cut (a) and round radius (R) was assumed. The crest inclination angle of 0° to 5° was taken from the suggestions of my supervisor's that it will be good for the designing of broad-crested weirs in the determination of capacity and reduction of the recirculation zone. Figure 4-19 (b) below shows the design layout of the weir with the upstream straight cut and inclination of the crest with the required angles. The small horizontal length (a) on the top edge of the weir was assumed to be equal on the radius.

The suggested design criteria were taken into consideration and 18 simulations were done with the same input parameters but with different inclinations and upstream straight cuts. In all cases, the values of the discharge coefficient, free water surface, velocity distribution, and pressure distribution were investigated.

Table 4-10: Computed dimensions of the broad-crested weir for modification of geometry

Parameters	Assumed relation Ho=0.2047m	Dimension (m)
Upstream Radius	$R1 = 0.2Ho$	0.04094
	$R2 = 0.3Ho$	0.06141
	$R3 = 0.4Ho$	0.08188
Upstream Cut (a)	$a1 = R1$	0.04094
	$a2 = R2$	0.06141
	$a3 = R3$	0.08188
Total crest length	Lw	1
Weir height	p	0.4
Weir bottom length	$Lb = Lw + R$	$1 + R$
Horizontal crest	r	$r = R$

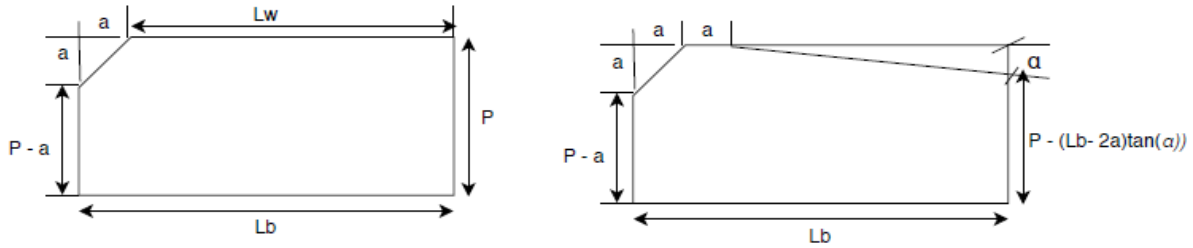

(a) (b)

Figure 4-19 Upstream inclined cut (a), and inclination of crest towards downstream (b)

From the simulated results with different modifications of weir geometry, the increment of discharge coefficient was observed as the angle (α) of inclination of the horizontal crest increases from 0˚ to 5˚ as plotted in Figure 4-20 below. This indicated that the capacity and crest inclination angle (α) have a direct relationship. However, the value of Cd from three models A1, A2, and A3 was almost nearly same. The proposed model A2 has a higher discharge coefficient of 0.4032 among the combinations of weir modifications. This weir

has the minimum horizontal crest length 0.06141 m, an inclined angle to 5° and upstream straight cut length of 0.06141 m.

Table 4-11 Simulated result of discharge coefficient for a straight cut with crest inclination (0° to 5°)

Models	Angles (α)	P_rgh	ho(m)	velocity (m/s)	Ho(m)	Cd Simu
A1	0	5795.02	0.1907	0.2305	0.1934	0.3613
	1	5760.33	0.1872	0.2319	0.1899	0.3713
	2	5714.96	0.1826	0.2337	0.1853	0.3852
	3	5693.05	0.1803	0.2346	0.1831	0.3922
	4	5683.96	0.1794	0.2350	0.1822	0.3951
	5	5665.85	0.1776	0.2357	0.1804	0.4012
A2	0	5782.55	0.1895	0.2310	0.1922	0.3648
	1	5747.46	0.1859	0.2324	0.1886	0.3752
	2	5722.02	0.1833	0.2334	0.1861	0.3830
	3	5697.77	0.1808	0.2344	0.1836	0.3906
	4	5675.09	0.1785	0.2353	0.1813	0.3981
	5	5659.85	0.1770	0.2360	0.1798	0.4032
A3	0	5790.37	0.1903	0.2306	0.1930	0.3626
	1	5738.22	0.1850	0.2327	0.1877	0.3780
	2	5867.54	0.1824	0.2338	0.1852	0.3858
	3	5701.51	0.1812	0.2342	0.1840	0.3894
	4	5690.56	0.1801	0.2347	0.1829	0.3930
	5	5661.31	0.1771	0.2359	0.1799	0.4027

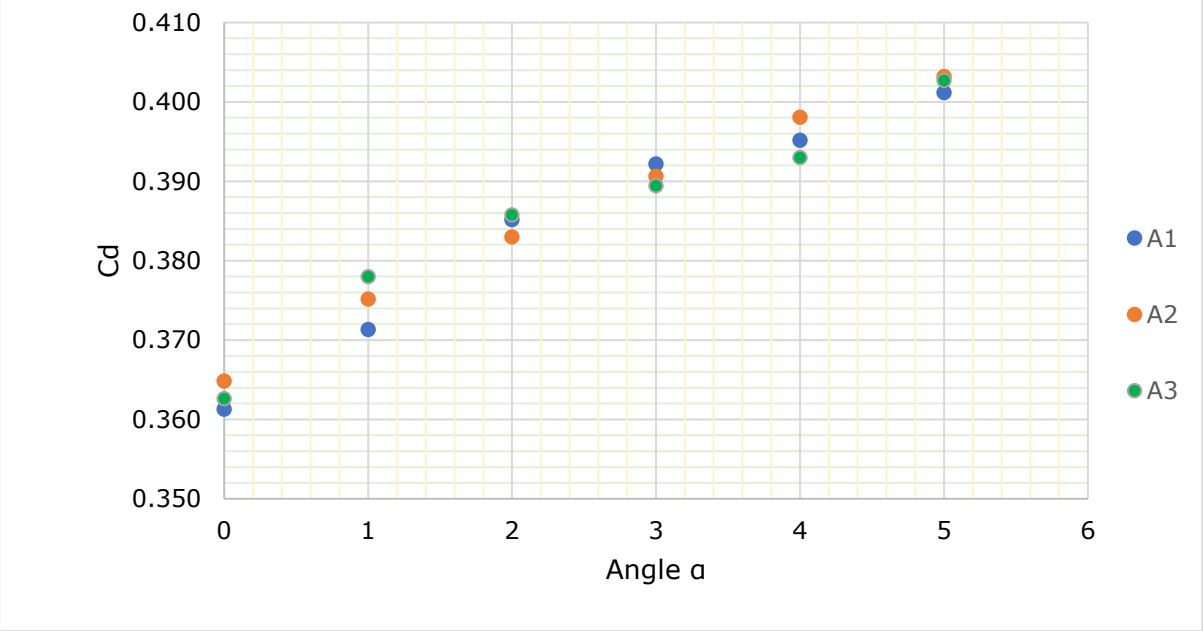

Figure 4-20 Result of discharge coefficient from simulations of u/s inclined cut with an inclination of (0° to 5°)

4.8.2 Numerical Simulation with Upstream Round Cuts and Crest Inclination of 0° to 5

The upstream round cut is the most efficient way of increasing capacity and accurate measurement of discharge, due to the low formation of the recirculation zone. The assumption made in Table 4-10 above was considered and 18 simulations were done to identify the best model of the weir. From the results of the numerical simulation shown in Table 4-12 below, the discharge coefficient was increased with the increased crest inclination in all round edge modifications. As a result of this, the maximum discharge coefficient of 0.40312 was obtained from the model 'R2' with an upstream round cut of R=0.06141m and crest inclination of 5°. Therefore, this modification of geometry was identified as the most economical dimensions of the broad-crested weir in terms of capacity, planning, design and operation.

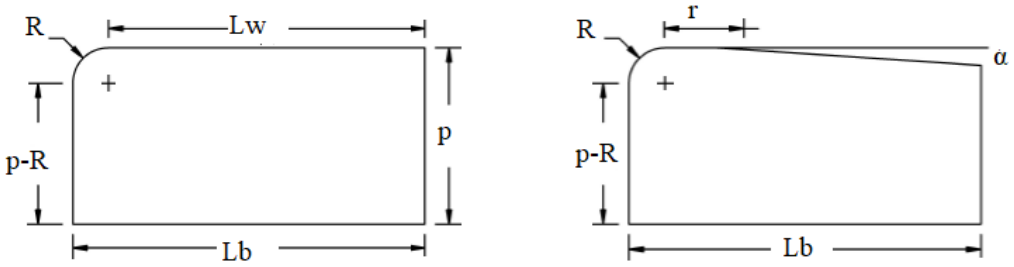

Figure 4-21 Upstream round cut (a), and inclination of crest towards downstream (b)

Models	Angle(α)	P_rgh (pa)	ho (m)	Velocity (m/s)	Ho (m)	Cd
R1	0	5799.05	0.1911	0.2303	0.1938	0.3601
	1	5736.68	0.1848	0.2328	0.1875	0.3784
	2	5719.58	0.1830	0.2335	0.1858	0.3837
	3	5694.9	0.1805	0.2345	0.1833	0.3916
	4	5685.8	0.1796	0.2349	0.1824	0.3945
	5	5672.84	0.1783	0.2354	0.1811	0.3988
R2	0	5783.21	0.1895	0.2309	0.1922	0.3646
	1	5720.57	0.1831	0.2335	0.1859	0.3834
	2	5710.17	0.1821	0.2339	0.1849	0.3867
	3	5690	0.1800	0.2347	0.1828	0.3932
	4	5671.08	0.1781	0.2355	0.1809	0.3994
	5	5660.06	0.1770	0.2360	0.1798	0.4031
R3	0	5762.92	0.1875	0.2317	0.1902	0.3706
	1	5734.48	0.1846	0.2329	0.1873	0.3791
	2	5724.06	0.1835	0.2333	0.1863	0.3823
	3	5702.37	0.1813	0.2342	0.1841	0.3892
	4	5688.46	0.1799	0.2348	0.1827	0.3937
	5	5673.88	0.1784	0.2354	0.1812	0.3985

Table 4-12 Simulated result of the discharge coefficient from u/s round cut with crest inclination (0° to 5°)

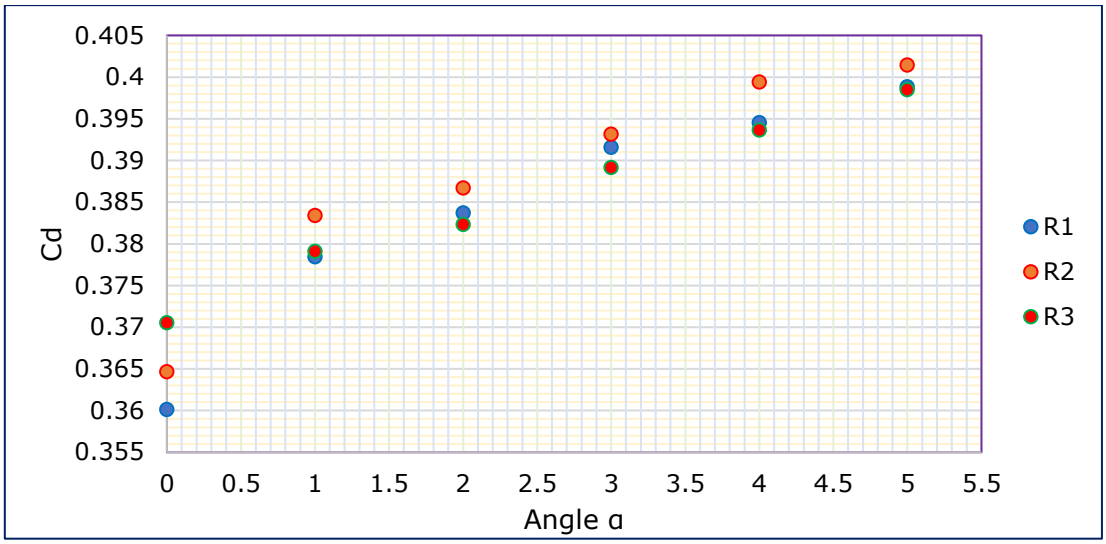

Figure 4-22 Discharge coefficient results from simulations of u/s round cut with crest inclination by (0° to 5°)

4.9 Result and Discussion

4.9.1 Illustration of a Separation Zone in Both Cases

Moss et al. (1972) carried out an experimental analysis of flow over a sharp-edged broad-crested weir and observed that the separation bubble and re-attachment occur on the top of the crest. They ran the model of the flow mechanism both with a constant static head and with circulatory motion in a bubble, which was bounded by a turbulent mixing zone.

Hager and Schwalt (1994) injected dye through various pressure taps close to the upstream weir corner in order to determine the extent of the corner separation region. Without access to the experimental technique and results, it is difficult to compare the CFD results against the experimental separation curve in any quantitative manner. It does, however, provide a useful insight into the behavior of the various turbulence models used in the numerical study.

As we can see from

Table 4-11 and Table 4-12 above, the simulated result of the discharge coefficient from both the straight and round cut with crest inclination towards downstream was nearly the same. To identify the best models, we need to consider different criteria and safety conditions. For instance, the formation of the recirculation zone in the design of hydraulic structures is not recommended. A sharp-edge weir has a higher separation zone than round-edge weir. It decreases as the corner of the weir changes from a sharp crest to inclined and round cut. The weir with the round cut and an inclined crest has an almost insignificant separation zone on the crest of the weir, as shown in Figure 4-23 (a), (b) and (c) below.

The characteristics of the square and round-edge rectangular broad-crested weirs are studied under free flow and submerged flow conditions by Ramamurthy et al. (1988b). They found that the best degree of rounding of u/s weir edges was when $0.094 < R/P < 0.25$, because this ratio reduces flow separation and it increases the Cd values (p = the height of the weir).

The formation of the separation zone will be large when the flow is with the large discharge and high velocity. Due to this reason, if we implement the inclined cut for our project, it may be easy in terms of construction and operation, but it will create a large separation zone. In real practice, too large a separation zone will create inaccuracy of the discharge measurement. Thus, in this simulation, we must avoid the separation zone by changing the upstream edge to more realistic shapes. On the other hand, broad crests with a round edge will have good hydraulic characteristics and have a minimum or negligible formation of the separation zone. However, it is quite a complicated and difficult structure to build as a real construction. For a beneficial investigation, the best models of A_2 and R_2 with a better Cd coefficient and small separation zone were selected from both cases for detailed analysis. Although, the very minimum or negligible separation zone was observed in the simulation with an upstream round-edge(R), minimum horizontal crest length $(r = R/2)$ and with a crest inclination of 5° towards downstream of the weir shown in Figure 4-23 (c) below. Since broad-crested weirs are widely used nowadays, it will be useful for the estimation of most cross sections of a weir to achieve better capacity in terms of inclination angle (α) by using the relationship between the discharge coefficient and the crest inclination as shown in Figure 4-24 and Equation 4-7 below.

As a result of this, I decided to select this geometry to investigate the simulation of flow with ranges of discharge to obtain the relationship between the discharge coefficient and relative length (Ho/Lw) and to develop the general equation which will be applied to estimate the capacity of the weir. Figure 4-23 below shows the formation of a separation zone of three different geometries of the broad-crested weir.

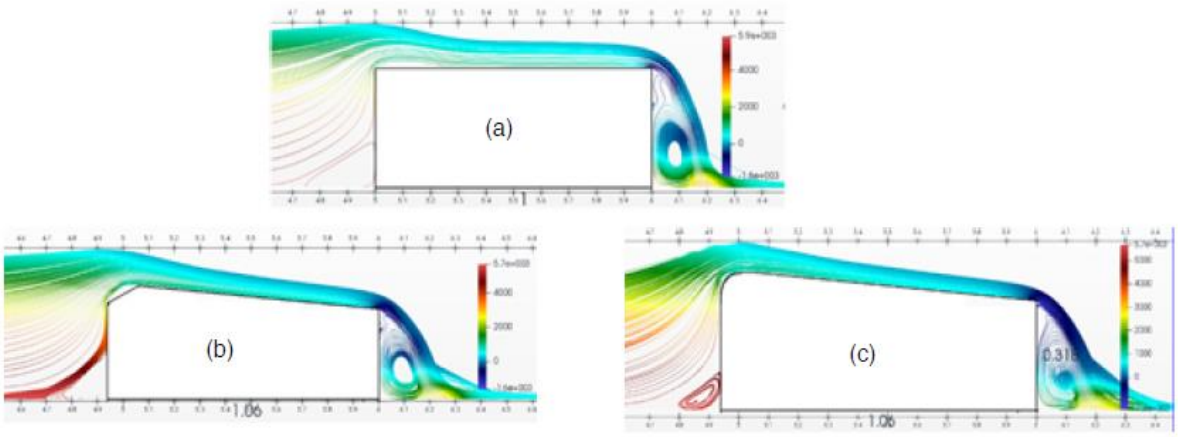

Figure 4-23 Separation zone illustration (a) with a sharp edge; (b) straight cut with inclined crest; and (c) round the edge with a small horizontal crest length of r = R/2 with the crest of inclination of 5°

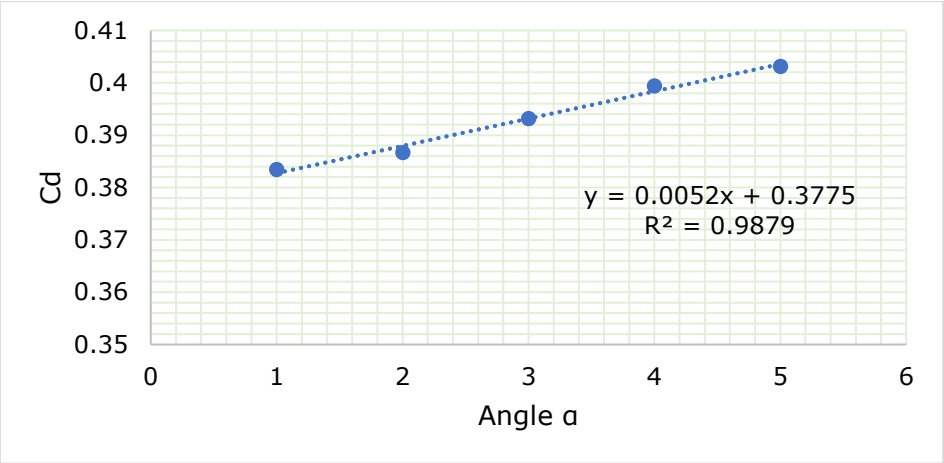

Figure 4-24 Discharge coefficient equation based on the inclination angle (α)

After the identification of the best model, the effect of crest inclination on the discharge coefficient was investigated. The Cd value becomes higher as the inclination angle increases. Since the maximum inclination angle of a 5° was recommended by my supervisor, the simulation was done up to 5° crest inclination. However, to see the impact of different inclination angles on the discharge coefficient, a range of angles was considered. The general discharge equation based on the inclination angle was developed as shown in Figure 4-24 and in the section view in Figure 4-26 below . The equation below will be useful to estimate the required discharge coefficient and capacity for a given inclination angle of (α)

$$Cd = 0.3775 + 0.0052(\alpha) \qquad \text{Eq. 4-7}$$

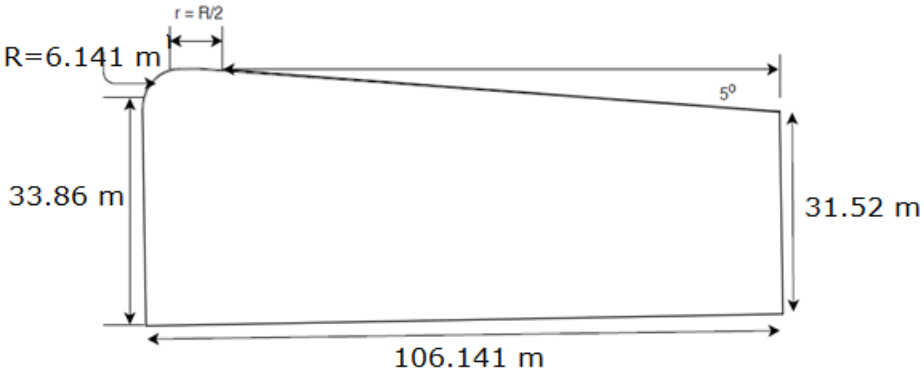

Figure 4-25 Final design of the most economical geometry of a broad crested weir

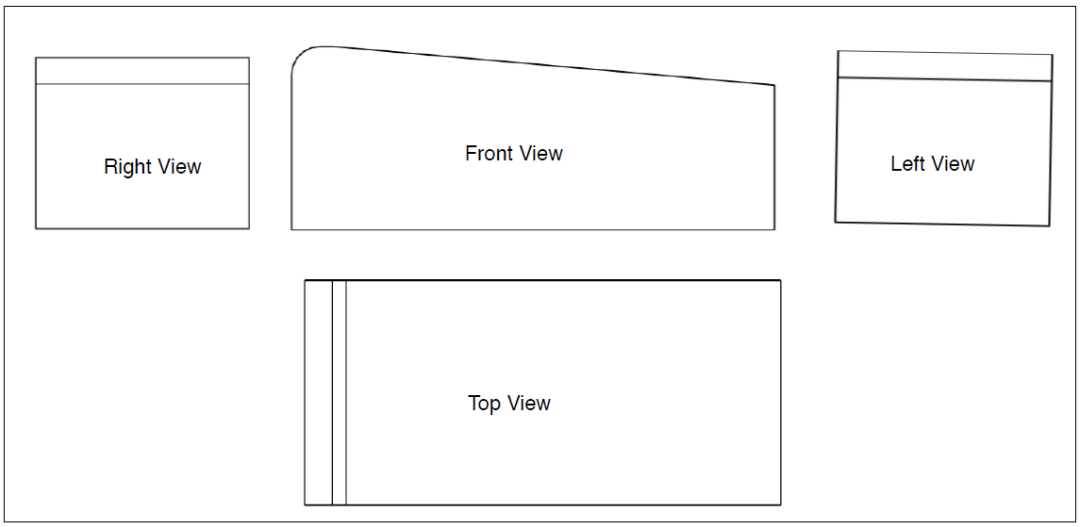

Figure 4-26 Section view of selected broad-crested weir

4.9.2 Convergence Analysis of the Selected Weir Geometry

Convergency is very important to obtain more accurate results from the CFD numerical simulation. It depends on the size of the mesh and running time steps. As the mesh of weir geometry receives more refinement, the water surface becomes sharp without too much fluctuation and the discharge coefficient and other flow parameters are also obtained with the required accuracy. However, for more refinement, we need to run our simulation for long time steps. In this case, for the selected weir geometry, the convergency criteria were analyzed until the stead-state conditions were attained.

Figure 4-28 to Figure 4-30 below shows the convergence by quantities of interest for the ranges of discharge from 0.025 m^3/s to 0.12 m^3/s, i.e. velocity, total pressure and pressure, respectively. From this convergence analysis, all quantities were converged after 10-time steps and uniform throughout the accumulated time steps. This indicated that, the simulation was carried out with good refinement and the result of the flow parameters obtained from the simulation was accurate. Therefore, the selected geometry weir has a good hydraulic efficiency with ranges of discharges and the proposed geometry can be applied to real projects.

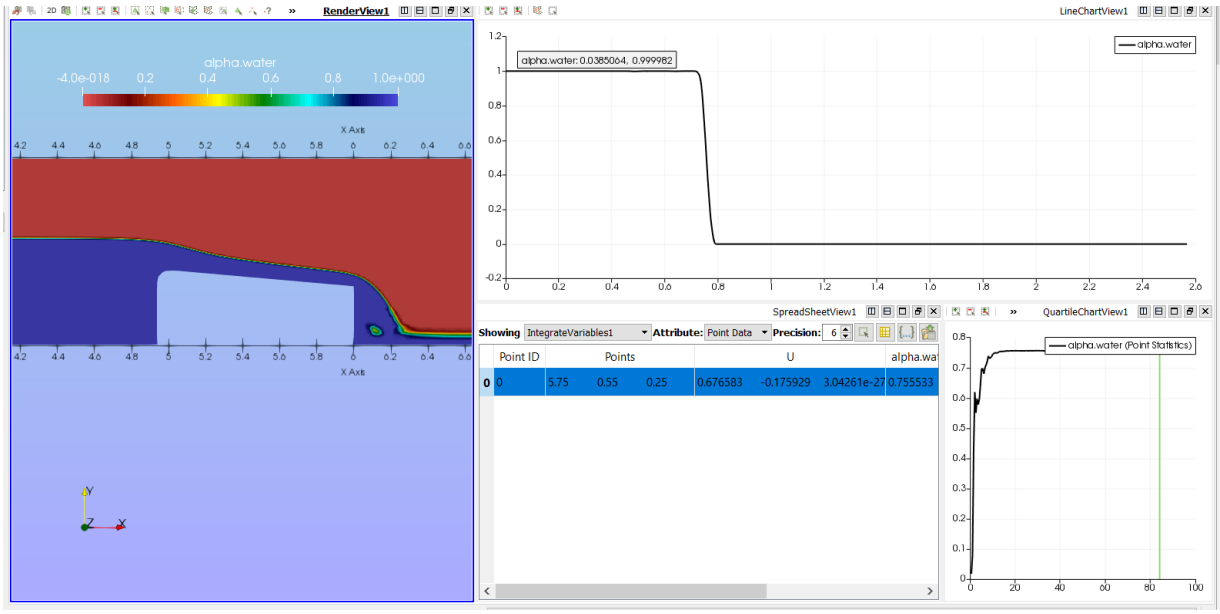

Figure 4-27 Convergency by alpha water for discharge of 0.068 m³/s

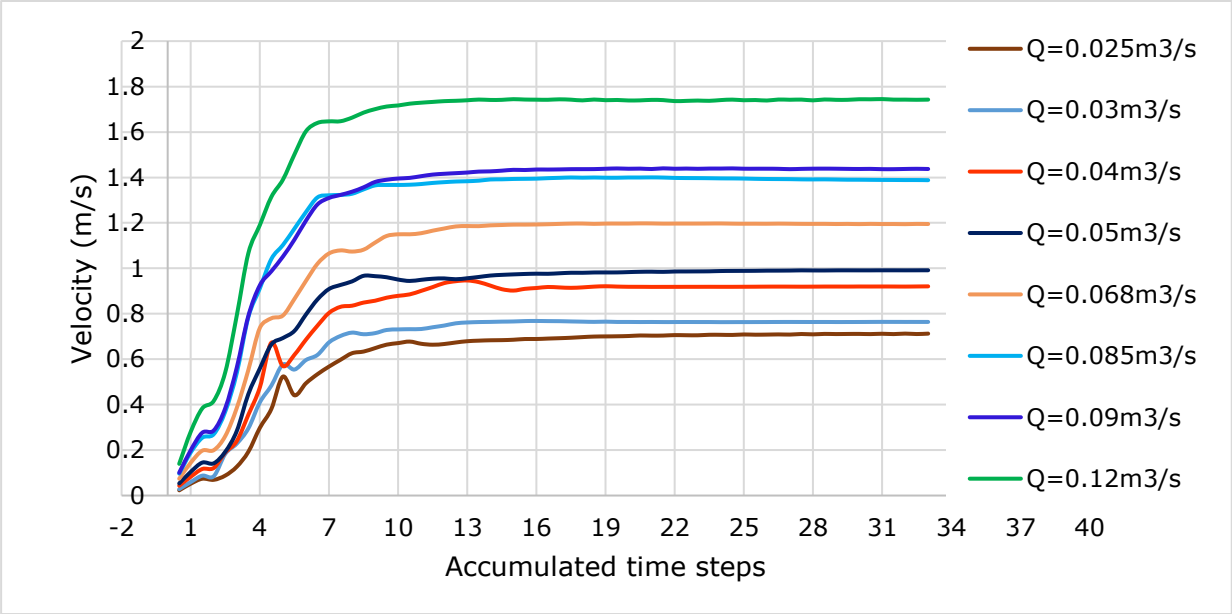

Figure 4-28 Convergency by velocity distribution for the ranges of Q from 0.025 m³/s to 0.12 m³/s

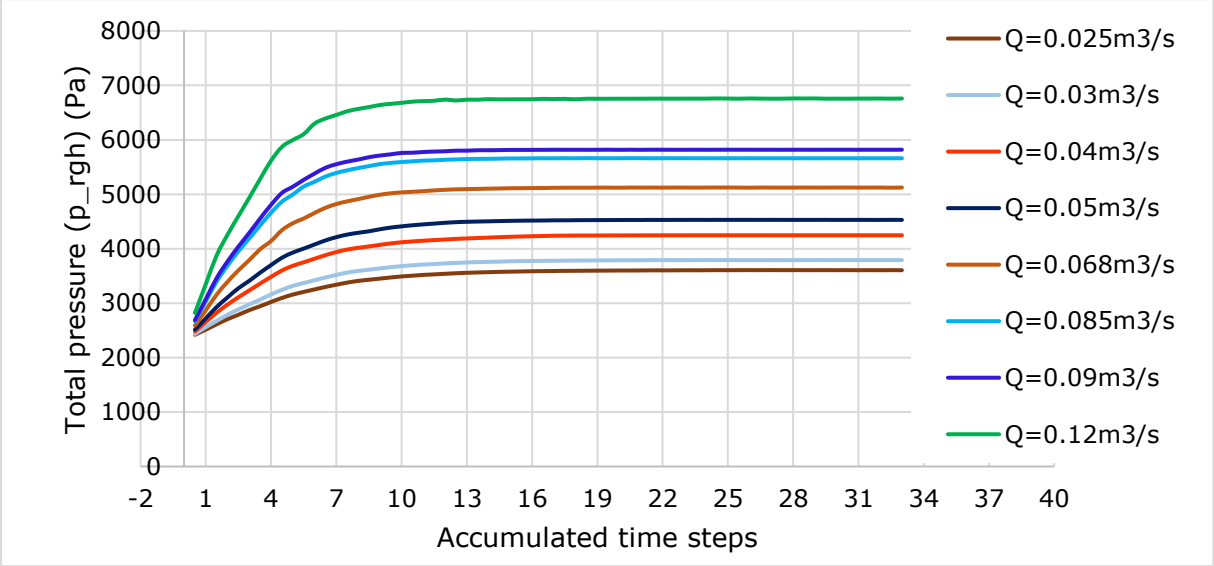

Figure 4-29 Convergency by the total pressure (P_rgh) distribution for the ranges of Q from 0.025 m /s to 0.12 m³/s

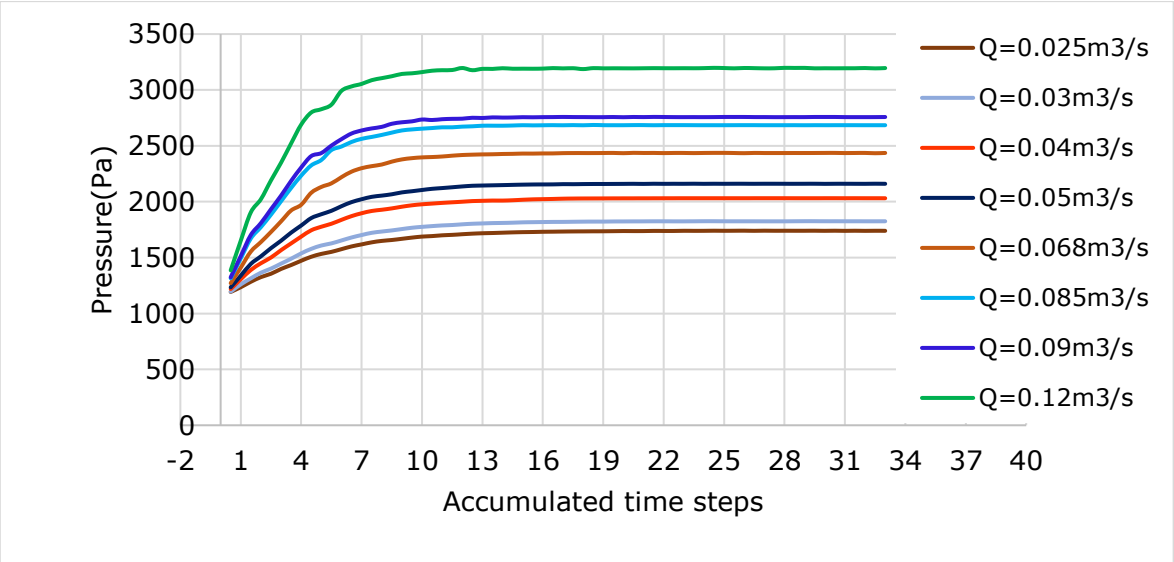

Figure 4-30 Convergency by pressure (P) distribution for the ranges of Q from 0.025 m^3/s to 0.12 m^3/s

4.9.3 Velocity and Pressure Distribution of the Selected Model

The pressure and velocity distribution for the selected shape of the weir was investigated by using ranges of discharge from 0.025 m^3/s to 0.12 m^3/s. The velocity distribution profiles are uniform and increases with the discharge both at the upstream and the downstream of the weir. However, the rapid-varied flow conditions were observed immediately as the water hit the weir edge at the horizontal distance of 4.9386 m and on the top of the weir crest as shown in Figure 4-31 and Figure 4-32 below. The maximum velocity of 1.66 m/s was observed when the simulation ran with a discharge of 0.12 m^3/s.

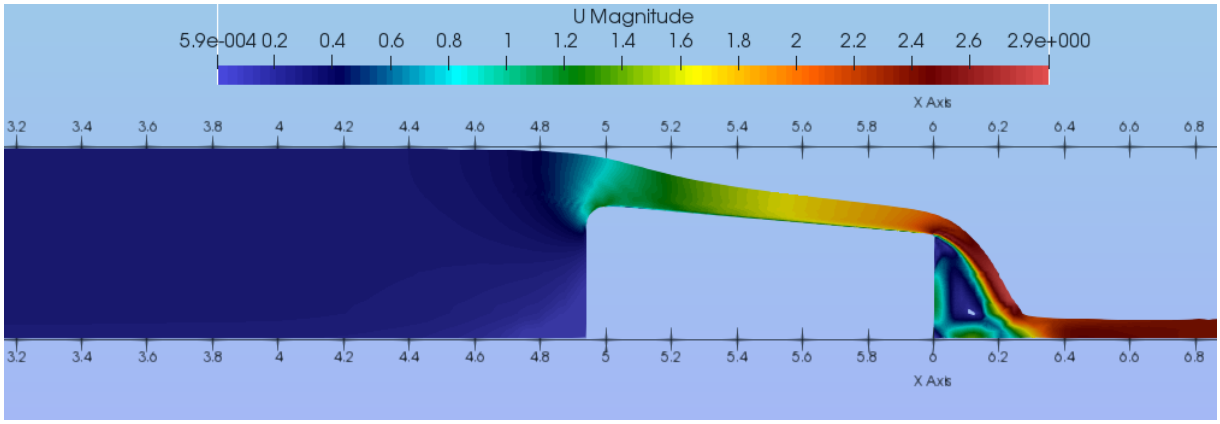

Figure 4-31 Velocity distribution profile for Q=0.06807 m^3/s

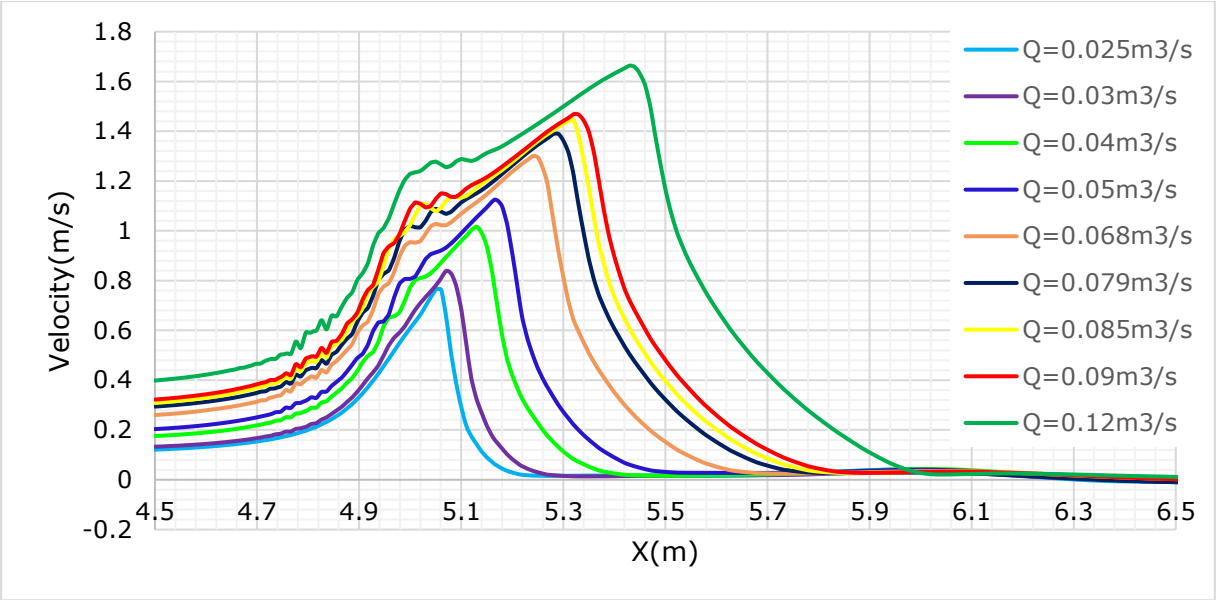

Figure 4-32 Velocity distribution for the ranges of Q from 0.025 m^3/s to 0.12 m^3/s

The pressure distribution is also not hydrostatic at the edge of the weir, but the parallel streamlines were observed on the inclined crest as shown in Figure 4-33 and Figure 4-35 below. The main influential factors which create the fluctuation of flow over the weir crest were large discharge, and high velocity. High hydrostatic pressure occurs behind the dam and varies with the discharge flow as shown Figure 4-34 and Figure 4-36. In the real field, the topographic features, slope of the river and bed roughness could be considered as additional factors. During numerical simulation, it is important to analyze the impact of high discharge flow, especially for a hydraulic structure used as a diversion, for flow measurement and regulation. However, since in the assumed design the energy head was Ho = 0.2047 m, we can investigate the numerical simulated data until the planned objective is obtained. The velocity and pressure distribution profiles for the ranges of discharge (0.025 to 0.12) m^3/s are shown in Appendix D.

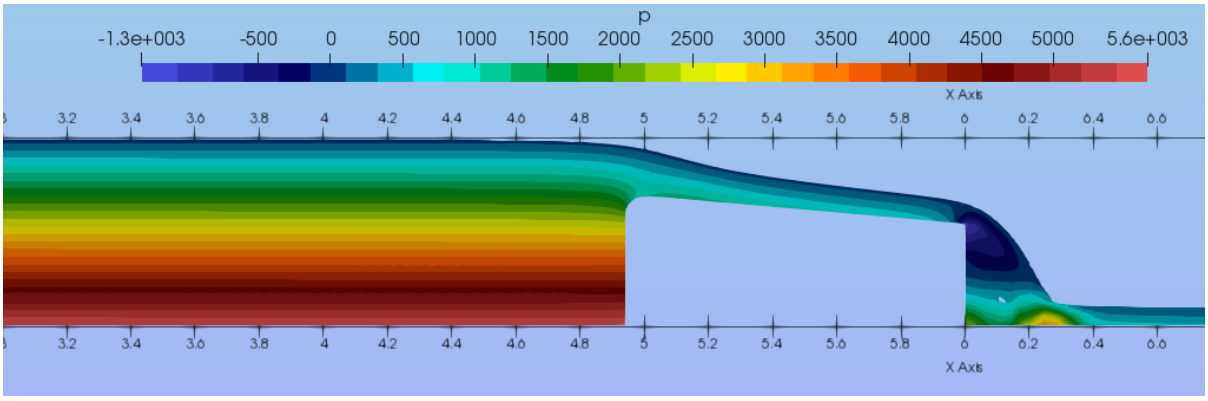

Figure 4-33 Pressure distribution profile for Q=0.06807 m^3/s

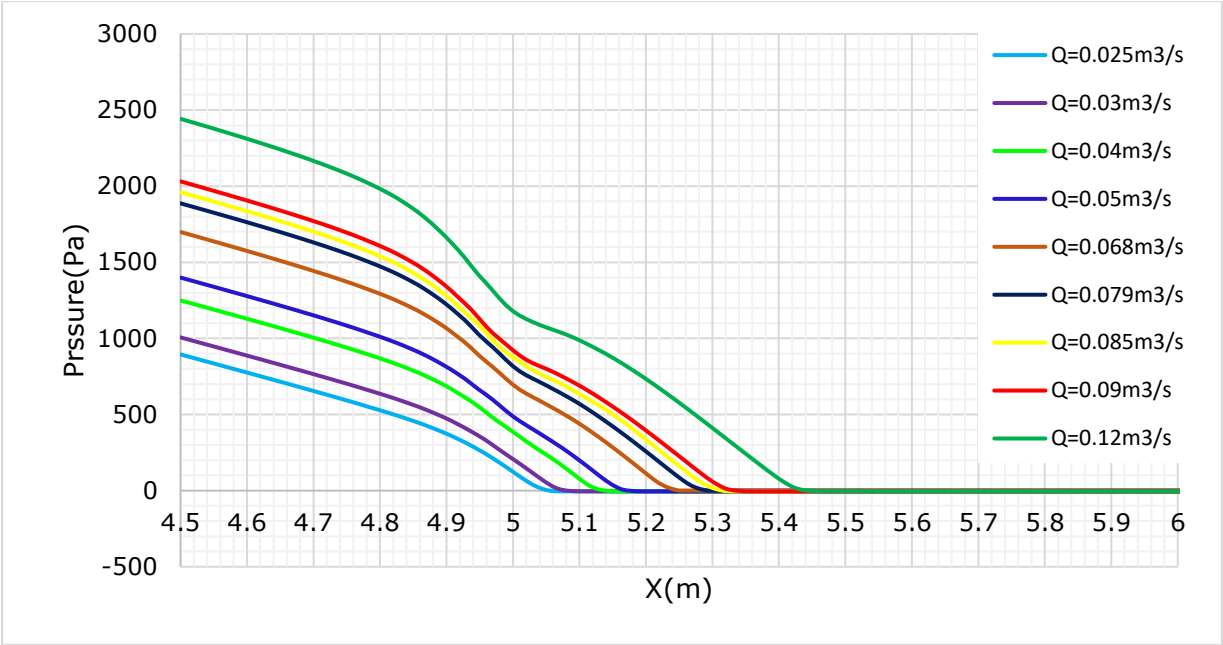

Figure 4-34 Pressure distribution for the ranges of Q from 0.025 m³/s to 0.12 m³/s

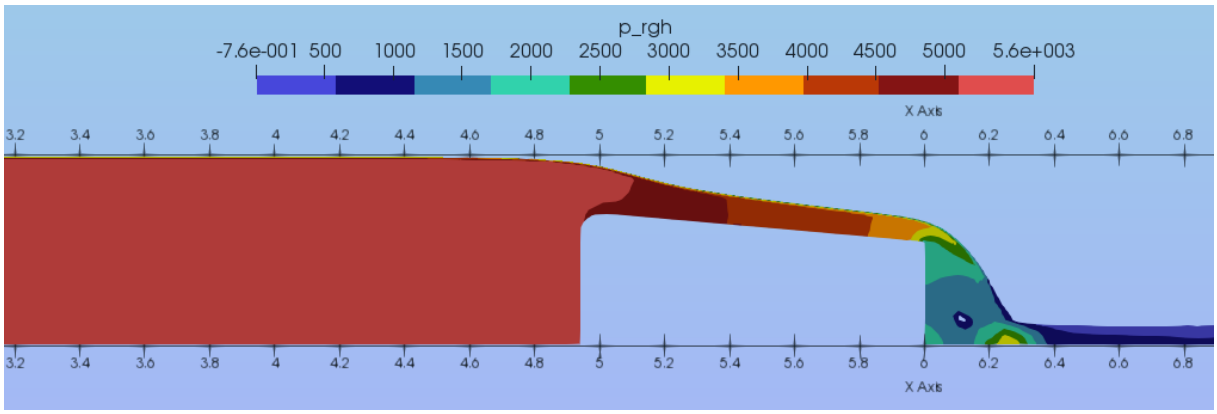

Figure 4-35 Total pressure distribution profile for Q=0.06807 m³/s

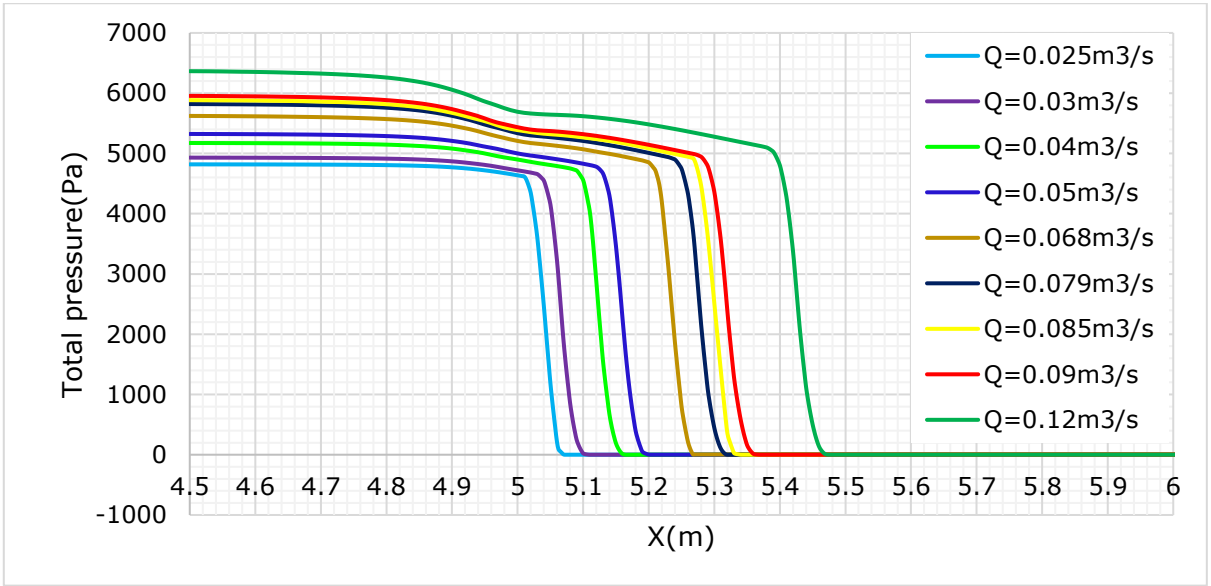

Figure 4-36 Total pressure distribution for the ranges of Q from 0.025 m³/s to 0.12 m³/s

4.10 Development of Relationship between Discharge Coefficient and Relative Head of the Selected Model

For the efficiency and safety of hydraulic structures, it is crucial to investigate with various ranges of discharge. When the inflow varies from minimum to maximum ranges, we can visualize the flow pattern upstream, on the crest, and downstream of the weir. In this simulation, the minimum discharge of 0.025 m^3/s and maximum discharge of 0.4 m^3/s was investigated and the critical depth was also located on each water surface, as shown in Figure 4-37 below. Parallel streamlines in each range of discharge were also observed on the crest. However, for the discharge, greater than 0.12 m^3/s, the formation of the separation zone was increased. The corresponding discharge coefficient also decrease for the relative length (Ho/Lw) greater than 0.266, as shown in Figure 4-38 below. This indicates the optimum discharge capacity of this weir is 0.12 m^3/s. When we compare this capacity with sharp-edged broad-crested weir of (Q=0.06807 m^3/s), the new weir geometry causes an increment in capacity by 43.3%. With the new design consideration for the new broad-crested weir it was presented as $0.095 \leq Ho/Lw \leq 0.266$.

Therefore, based on this design limitation, the equation of discharge coefficient, which is used for a general expression, the relationship between Cd and Ho/Lw was developed as shown in Figure 4-40 and Eq. 4-8 below-

$$Cd = 0.0396\left(\frac{H_o}{L_w}\right) + 0.3996 \qquad \text{Eq. 4-8}$$

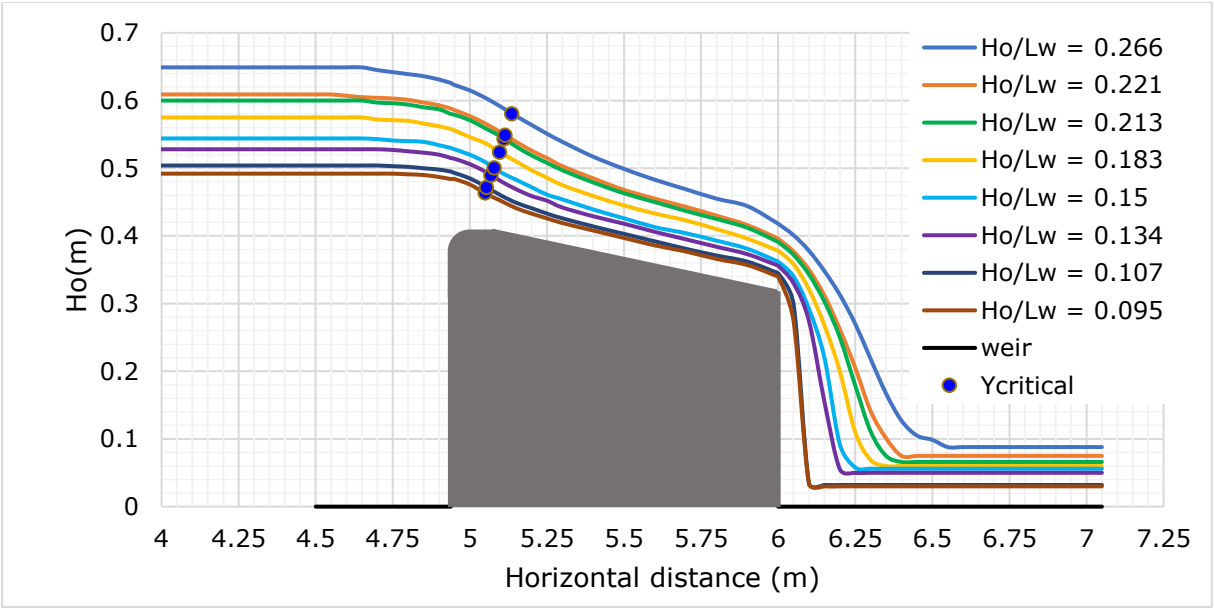

Figure 4-37 Investigation on the selected weir with ranges of Q from 0.025 m^3/s to 0.12 m^3/s

The relationship between the discharge coefficient and the relative head as shown in Figure 4-38 below, indicated the optimum point of Cd was at Ho/Lw of 0.266 for the selected weir model. From this model, we can conclude that the discharge coefficient of the selected model increases from 0.4034 to 0.4115, corresponding to the relative length (Ho/Lw) 0.095 to 0.266, and then gradually decreases with the increases in the discharge flow. Therefore, based on this figure, we can estimate the capacity of the weir based on the known value of the relative head.

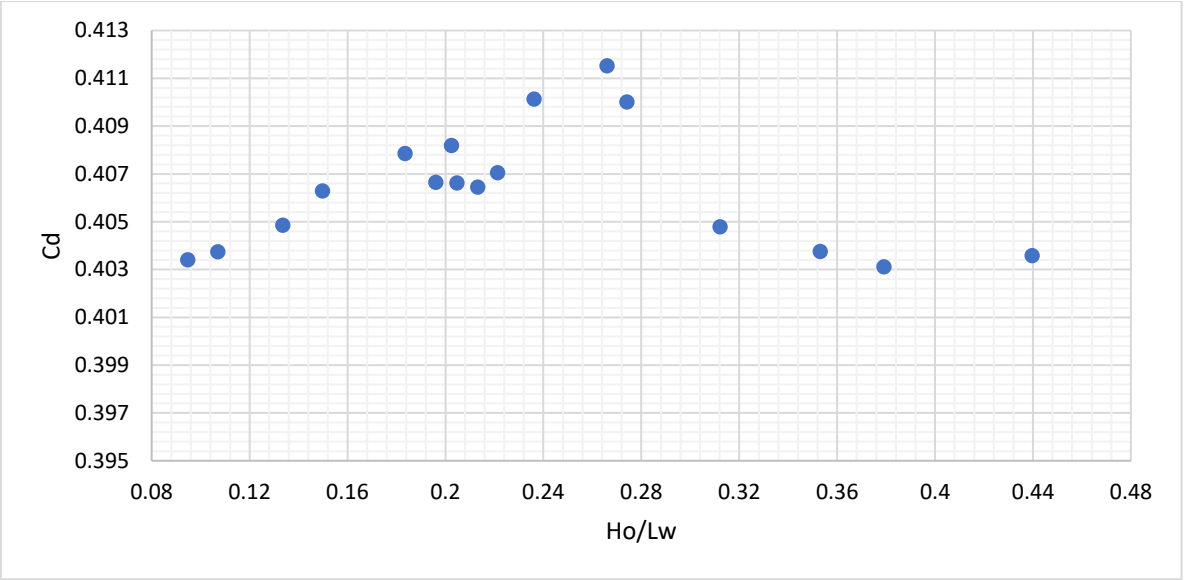

Figure 4-38 Relationship between Cd and relative length of new weir model

The relationship between the energy head and the ranges of the flow rate was plotted on the stage discharge curve shown Figure 4-39 below. As the magnitude of the overflow increases, the water level over the crest also increases. This is very important in a hydropower project and for flood protection, but from hydraulic point of view, we need to optimize the required head and release the excess water via the spillway to keep the safety of the structures. From this figure, we can determine the amount of discharge(m^3/s) needed for the given values of the energy head (m).

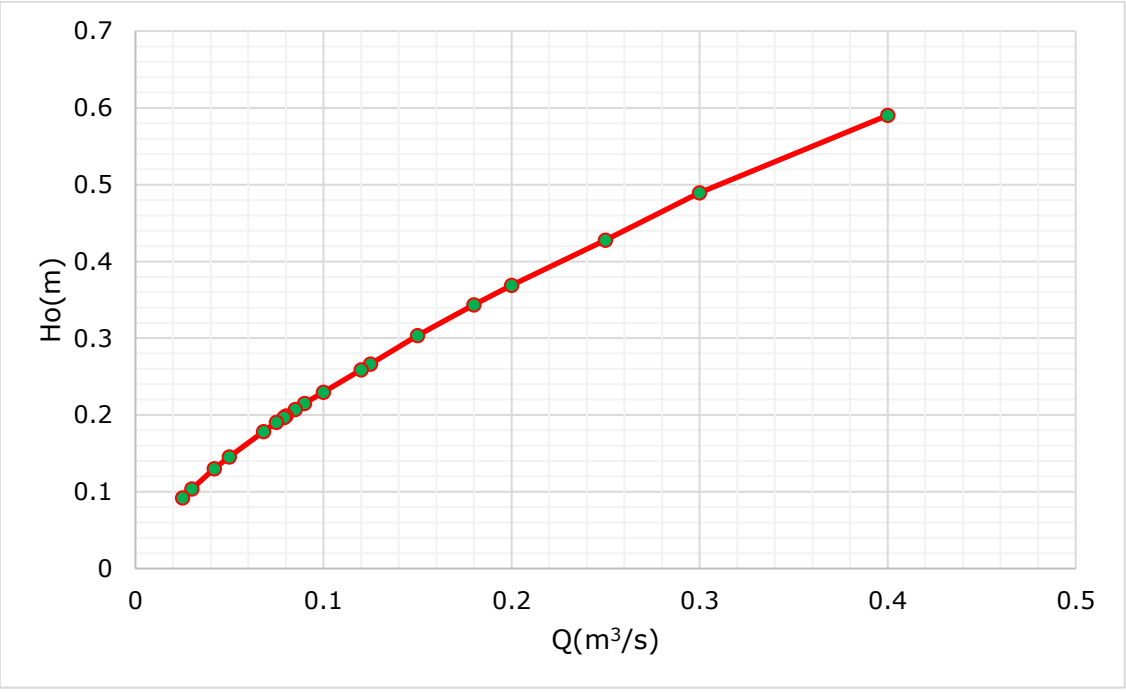

Figure 4-39 Stage discharge for the selected model

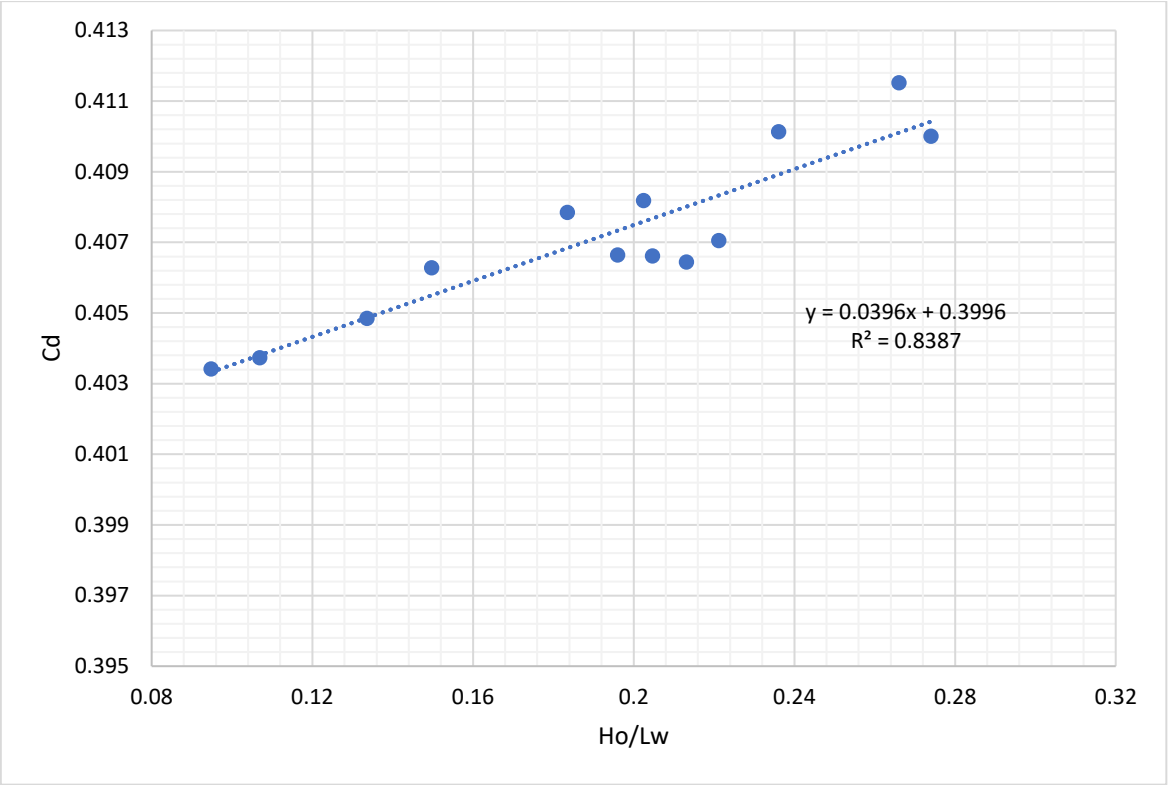

Figure 4-40 Relationship between Cd and relative length (Ho/Lw) of selected model

4.11 Source Errors in Numerical Simulation

CFD simulations have the following potential source of errors of uncertainties:

- Numerical errors: Results from the difference between the exact equations and the discretized equations solved by the CFD code.
- Modeling Errors: Results from the necessity to describe flow phenomena such as turbulence and multi-phase flows by empirical models
- User Errors: Result from incorrect use of CFD software and are usually a result of insufficient expertise by the CFD user.
- Application Uncertainties: related to insufficient information to define a CFD simulation. A typical example is insufficient information on boundary conditions.
- Software Errors: caused as a result of an inconsistency between the documented equations and the actual implementation in the CFD software.

5 Conclusions and Recommendations

5.1 Conclusions

In this study, a numerical investigation of flow over various shapes of the broad-crested weir was simulated by using CFD software with the OpenFOAM toolbox. The different turbulence models Standard k-ε, RNG K-ε, Realizable k-ε, Standard k-ω, and KomegaSST were compared to identify the best model. The KomegaSST was selected to predict water surface, flow parameters, and applied for all numerical simulations. By using a published experimental data set as a validation set, it has been shown that it is possible to build a CFD model which replicates the findings to acceptable levels of accuracy. The driver behind this paper was to test the free surface modelling capabilities of OpenFOAM and in that it proved successful. Modelling of more complex geometries and flow configurations can now be addressed with more confidence by the authors and others.

Two cases were considered to investigate the impact of different parameters on the discharge coefficient. In the first case, the modification of weirs was done on the square edge of a broad-crested weir with the up and downstream straight and round cut. The influential parameters like velocity distribution, pressure distribution, free water surface, the slope of the straight cut and radius were investigated.

According to the design limitation of Singer et al. (1964) and Crabbe et al. (1974), the extended ranges of broad-crested weirs $0.08 < Ho/Lw < 5.6$ were considered. By considering these, 40 simulations were done on different shapes of broad-crested weirs. The relationship between the discharge coefficient and the weirs geometry was analyzed. The observed simulated results indicate that the discharge coefficient was increasing as the weir geometry was modified from sharp-edged to the inclined and round edged. After a comparison of flow simulation with different conditions, the most economical geometry of the broad-crested weir was selected. This weir has a width of 0.5 m, a height of 0.4 m, and a crest length of 0.173 m. In addition to this, the weir has an up and downstream straight cut with a = 0.0819 m, and b = 0.1638 m, as shown in Figure 4 16 above.

The relationship between the discharge coefficient and the relative length developed when the range of discharge (12.5 to 100) l/s was investigated. However, since our maximum required energy head was 0.2047 m, the ranges of discharge used to develop the relationships were (12.5 to 85) l/s with the corresponding relative length of ($0.235 < Ho/Lw < 1.168$). Within this range, the increments of discharge capacity from 68.07 l/s to 85 l/s and the discharge coefficient from 0.332 to 0.416 were obtained, when the weir shape changes from sharp-edged to this new model with both edges straight cut. The equation of the discharge coefficient as shown in Eq 4-6 was developed to analyze the impact of high flood and minimum flow over the selected broad-crested weir. Good agreement was obtained when compared with the modified equation of the discharge coefficient by Sargison and Percy (2009) with a mean error of -1.68%.

The second case investigated the crest inclination towards downstream and Govinda Rao and Muralidhar's (1963) design limitation of the broad-crested weir. According to this design limitation, the broad-crested weir should have a relative length of ($0.1 < Ho/Lw < 0.4$). Since the minimum crest length for the energy head of Ho=0.2047 m was about 0.5

m, the dimension of the broad-crested weir was modified and the length of 1m was selected for this case; furthermore, the inclination of the crest (0° to 5°) was considered.

In this case, 36 simulations were investigated by changing the weirs to upstream straight cut and round cut with crest inclinations of 0° to 5°. In each simulation, different flow parameters were compared, and the increment of the discharge coefficient was observed. However, since a small length of straight cut and radius was used in the modification of the weir, the deviation of the simulated results between the straight cut and round cut was very small.

By considering the effect of weir shapes on the hydraulic characteristics and capacity, the broad-crested weir with a round edge and inclined crest of 5° was selected as the best model. This weir has a height of 0.4 m at the upstream end and 0.3152 m at the downstream end, a crest length 0.973 m, a bottom length of 1.061 m and a width of 0.5 m as shown in Figure 4-25 above. The selected model of the weir has a discharge coefficient of 0.40312. The general discharge coefficient in equation 4-7 was developed in terms of crest inclination angles (α).

The ranges of discharges (0.025m3/s to 0.12m3/s) were also investigated. The free water surface, pressure and velocity distribution, separation zone and discharge coefficient were analyzed. The required energy head of 0.2047 m was obtained with a discharge of 0.086 m^3/s. This indicates the capacity of the weir was increased by 20%, when a new model is used. However, the optimum discharge capacity, which has no problems with a recirculation zone was identified as 0.12 m^3/s. With this discharge, the capacity will be increased to 43.3%. Therefore, by using this maximum limit, the equation of the discharge coefficient was developed in terms of relative length (Ho/Lw) and with ($0.095 < Ho/Lw < 0.266$) as shown in Eq. 4-8. From the observed result during the numerical simulation, the selected weir geometry has a high capacity with good hydraulic efficiency.

In general, the time taken to produce steady-state free surface flows, even in 2D, is prohibitive when compared with other modelling techniques that are routinely applied for the prediction of flow around hydraulic structures; thus, CFD is increasingly becoming the most reliable and accurate modelling option.

Based on the results in both cases, we can conclude that the upstream weir design has a considerable effect on the flow pattern and discharge coefficient of sharp-edged broad-crested weirs. The performance of this structure is optimized by varying the upstream straight and round cut, both up and downstream edge straight and round cut, and modification of crest inclination towards downstream with ranges of angles.

Finally, from this study, the required broad-crested model with high capacity was discovered. The selected weir was economical and efficient in terms of planning, designing, implementation, construction, and operation. It can be used for new projects, replacements, extensions, and rehabilitation of old spillways, dams, and weirs.

5.2 Recommendations

Broad-crested weirs are widely investigated structures, both numerically and experimentally by different scholars and experts. During their investigations, they make several assumptions depending on the objective of the analysis. Most assumptions are based on experience and scaling from the same cases. Since the assumed data are used throughout the comparison of different parameters, it will influence the characteristics of flow over structures and capacity. As a result of this, the obtained result has a different degree of uncertainty and limitations.

For the flow measuring structure, it is highly recommended that the correct boundary conditions and all input parameters should be used in both experimental and numerical simulations. In this study, several numerical simulations were carried out by using the boundary conditions and geometry from the relevant literature. The boundary conditions obtained using in the numerical simulation are Reynold's number, inlet velocity, and geometry of a sharp-edged broad-crested weir. However, in the OpenFOAM toolbox solver, we need the degree of turbulence of the channel to determine the kinetic energy and the rate of dissipation. This indicates how the flow in the channel fluctuates, either in turbulent or laminar flow conditions. In this case, an intensity of turbulence of 5% was assumed and applied for the simulations. Meanwhile, as it has an impact on the discharge coefficient, I would recommend that the correct river flow conditions should be used for real projects.

Since Computational fluid dynamics is case sensitive software, the result obtained may also be affected by the size and shape of geometry, the size and number of cells, the distance of the inlet water from the point of interest (weir) and the slope and radius of weir modification. So, in this study, the geometry of the model used in the first case was a broad-crested weir with a height of 0.4 m, a width of 0.5 m and a thickness of 0.5 m. Due to the small size of the model, a large variety of simulated parameters from different modifications was not observed. In addition to this, it was difficult to see the impact of large modification on the capacity and other parameters such as parallel streamlines and location of critical depth on the crest of the weir. For better numerical investigation and to obtain more reliable results, the prepared models need to be big enough and with more refinement.

I would like to recommend for future interested researchers to further study on the simulation of the overflow of a broad-crested weir with ranges of crest inclination and calibration with real river conditions, by using more reliable experimental data.

Nowadays, using CFD is the most popular and accurate method to determine the flow conditions around hydraulic structures to the required accuracy. Additionally, the results of a study such as this one could be encapsulated in other models through a table of values or more sophisticated machine intelligence methods. With the confidence gained in this application, I would like to recommend using similar techniques and software to study the overtopping of embankment dams.

Reference

Alfonsi, G., 2009. Reynolds-Averaged Navier–Stokes Equations for Turbulence Modeling. *Applied Mechanics Reviews*, 62 (4), 040802.

Al-Hashimi, S. A. M., Madhloom, H. M., Nahi, T. N., and Al-Ansari, N., 2016. Channel Slope Effect on Energy Dissipation of Flow over Broad Crested Weirs. *Engineering*, 08 (12), 837–851.

Azimi, A. H. and Rajaratnam, N., 2009. Discharge Characteristics of Weirs of Finite Crest Length. *Journal of Hydraulic Engineering*, 135 (12), 1081–1085.

Azimi, A. H., Rajaratnam, N., and Zhu, D. Z., 2013. Discharge Characteristics of Weirs of Finite Crest Length with Upstream and Downstream Ramps. *Journal of Irrigation and Drainage Engineering*, 139 (1), 75–83.

Bos, M. G., 1972. DISCHARGE MEASUREMENT STRUCTURES, 475.

Crabbe, A. D. 1974. "Some hydraulic features of the square-edged broad-crested weir." *Water and Water Engrg.,* 78(10), 354-358.

Farzin; Poorescandar, S., 2011. Discharge relations for rectangular broad-crested weirs. *Tarım Bilimleri Dergisi*, 17 (4), 324–336.

Felder, S. and Chanson, H., 2012. VELOCITY AND PRESSURE MEASUREMENTS ON A BROAD-CRESTED WEIR: PHYSICAL MEASUREMENTS, 8.

Fritz, H. M. and Hager, W. H., 1998. Hydraulics of Embankment Weirs. *Journal of Hydraulic Engineering*, 124 (9), 963–971.

GOodarzi, E., Farhoudi, J., and Shokri, N., 2012. Flow Characteristics of Rectangular Broad-Crested Weirs with Sloped Upstream Face. *Journal of Hydrology and Hydromechanics.*

Govinda Rao, N. S. and Muralidhar, D., 1963. DISCHARGE CHARACTERISTICS OF WEIRS OF FINITE-CREST WIDTH. *La Houille Blanche*, (5), 537–545.

Hager, W. H., and Schwalt, M. _1994_. "Broad-crested weir." *J. Irrig. Drain. Eng.*, 120_1_, 13–26.

Hanjalić, K. and Launder, B. E., 1972. A Reynolds stress model of turbulence and its application to thin shear flows. *Journal of Fluid Mechanics*, 52 (4), 609–638.

Haun, S., Olsen, N. R. B., and Feurich, R., 2011. Numerical Modeling of Flow Over Trapezoidal Broad-Crested Weir. *Engineering Applications of Computational Fluid Mechanics*, 5 (3), 397–405.

Horton, R. E. 1907. "Weir experiments, coefficients, and formulas." Dept. of the Interior, U.S. Geological Survey, *Water-Supply and Irrigation Paper 200.* Government Printing Office, Washington, D.C.

Jackson, D. and Launder, B., 2007. Osborne Reynolds and the Publication of His Papers on Turbulent Flow. *Annual Review of Fluid Mechanics*, 39 (1), 19–35.

Julian, D. P., 2014. Erik Sutherland Trevor Taylor, 9. classification of weirs

Madadi, M. R., Hosseinzadeh Dalir, A., and Farsadizadeh, D., 2014. Investigation of flow characteristics above trapezoidal broad-crested weirs. *Flow Measurement and Instrumentation*, 38, 139–148.

Mahtabi, G. and Arvanaghi, H., 2018. Experimental and numerical analysis of flow over a rectangular full-width sharp-crested weir. *Water Science and Engineering*, 11 (1), 75–80.

Menter, F. R., 1994. Two-equation eddy-viscosity turbulence models for engineering applications. *AIAA Journal*, 32 (8), 1598–1605.

Moss, W. D., 1972. Flow separation at the upstream edge of a square-edged broad-crested weir. *Journal of Fluid Mechanics*, 52 (2), 307–320.

Ramamurthy, A. S., Tim, U. S., and Rao, M. V. J., 1988. Characteristics of Square-Edged and Round-Nosed Broad-Crested Weirs. *Journal of Irrigation and Drainage Engineering*, 114 (1), 61–73.

Sargison, J. E. and Percy, A., 2009. Hydraulics of Broad-Crested Weirs with Varying Side Slopes. *Journal of Irrigation and Drainage Engineering*, 135 (1), 115–118.

Singer, J. 1964. "Square-edged broad-crested weir as a flow measurement device. "*Water and Water Engrg.,* 68(6), 229-235.

Sreetharan, M. 1988. "Discharge characteristics of rectangular profiled weirs. "Proc. Nat. *ASCE Conf. Hydr. Engrg.,* S. R. Abt. and J. Gessler, eds., ASCE,

969-978, New York, N.Y.

Wilcox, D. C., 2008. Formulation of the k-w Turbulence Model Revisited. *AIAA Journal*, 46 (11), 2823–2838.

Zachoval, Z., Knéblová, M., Roušar, L., Rumann, J., and Šulc, J., 2014. Discharge coefficient of a rectangular sharp-edged broad-crested weir. *Journal of Hydrology and Hydromechanics*, 62 (2), 145–149.

Appendix A:

Numerical water surface from different turbulence models and experimental water surface.

Length (m)	RNG(k-ε)	Realizable(k-ε)	Standard(k-ε)	KomegaSST (k-ω)	Standard(k-ω)	Exp
4	0.5691	0.5968	0.5956	0.5982	0.5963	0.612
4.05	0.5691	0.5968	0.5956	0.5982	0.5963	0.612
4.1	0.5691	0.5968	0.5956	0.5982	0.5963	0.612
4.15	0.569	0.5968	0.5956	0.5982	0.5963	0.612
4.2	0.5691	0.5968	0.5956	0.5982	0.5963	0.612
4.25	0.5691	0.5968	0.5956	0.5982	0.5963	0.612
4.3	0.5691	0.5968	0.5956	0.5982	0.5963	0.612
4.35	0.5691	0.5968	0.5956	0.5982	0.5963	0.612
4.4	0.5691	0.5968	0.5956	0.5982	0.5963	0.612
4.45	0.5691	0.5968	0.5956	0.5982	0.5963	0.612
4.5	0.5691	0.5968	0.5956	0.5982	0.5963	0.612
4.55	0.569	0.5968	0.5956	0.5982	0.5963	0.612
4.6	0.5691	0.5968	0.5956	0.5982	0.5963	0.612
4.65	0.5691	0.5968	0.5956	0.5982	0.5963	0.612
4.7	0.5691	0.5968	0.5938	0.5961	0.5941	0.612
4.75	0.5691	0.5968	0.5938	0.5946	0.5942	0.612
4.8	0.5691	0.5930	0.5920	0.5916	0.5941	0.612
4.85	0.5672	0.5914	0.5920	0.5916	0.5944	0.612
4.9	0.5663	0.5905	0.5920	0.5901	0.5942	0.612
4.95	0.5622	0.5843	0.5812	0.5831	0.5830	0.6
5	0.5573	0.5750	0.5740	0.5767	0.5766	0.592
5.05	0.5545	0.5701	0.5686	0.5722	0.5717	0.584
5.1	0.5425	0.5608	0.5595	0.5623	0.5643	0.572
5.15	0.5371	0.5473	0.5470	0.5468	0.55197	0.556
5.2	0.5125	0.5313	0.5343	0.5312	0.5372	0.54
5.25	0.5071	0.5189	0.5253	0.5211	0.5274	0.528
5.3	0.4952	0.5103	0.5144	0.5092	0.5162	0.512
5.35	0.4930	0.5030	0.5072	0.5021	0.5064	0.504
5.4	0.4861	0.4955	0.4982	0.4953	0.4953	0.503
5.45	0.4810	0.4869	0.4874	0.4897	0.4941	0.509
5.5	0.4621	0.4709	0.4639	0.4724	0.4663	0.492
5.55	0.4551	0.4487	0.4278	0.4524	0.4346	0.484
5.6	0.4264	0.4213	0.3647	0.4062	0.3597	0.464
5.65	0.3481	0.3083	0.0815	0.3111	0.0714	0.44
5.7	0.0362	0.1667	0.0634	0.1406	0.0673	0.415

Appendix B:

Water surface profile of the most economical weir geometry with crest inclination of 5°.

Q	0.12	0.1	0.09	0.085	0.068	0.05	0.042	0.03	0.025
Ho/Lw	0.266	0.236	0.221	0.213	0.183	0.150	0.134	0.107	0.095
x					ho(m)				
4	0.649	0.621	0.609	0.6	0.575	0.544	0.528	0.504	0.492
4.05	0.649	0.621	0.609	0.6	0.575	0.544	0.528	0.504	0.492
4.1	0.649	0.621	0.609	0.6	0.575	0.544	0.528	0.504	0.492
4.15	0.649	0.621	0.609	0.6	0.575	0.544	0.528	0.504	0.492
4.2	0.649	0.621	0.609	0.6	0.575	0.544	0.528	0.504	0.492
4.25	0.649	0.621	0.609	0.6	0.575	0.544	0.528	0.504	0.492
4.3	0.649	0.621	0.609	0.6	0.575	0.544	0.528	0.504	0.492
4.35	0.649	0.621	0.609	0.6	0.575	0.544	0.528	0.504	0.492
4.4	0.649	0.621	0.609	0.6	0.575	0.544	0.528	0.504	0.492
4.45	0.649	0.621	0.609	0.6	0.575	0.544	0.528	0.504	0.492
4.5	0.649	0.621	0.609	0.6	0.575	0.544	0.528	0.504	0.492
4.55	0.649	0.621	0.609	0.6	0.575	0.544	0.528	0.504	0.492
4.6	0.649	0.621	0.607	0.6	0.575	0.544	0.528	0.504	0.492
4.65	0.649	0.621	0.605	0.6	0.575	0.544	0.528	0.504	0.492
4.7	0.645	0.617	0.604	0.597	0.572	0.543	0.528	0.504	0.492
4.75	0.642	0.615	0.603	0.596	0.571	0.541	0.527	0.503	0.492
4.8	0.639	0.612	0.601	0.594	0.57	0.54	0.525	0.502	0.491
4.85	0.636	0.608	0.597	0.59	0.566	0.539	0.523	0.5	0.49
4.9	0.631	0.601	0.593	0.587	0.562	0.534	0.52	0.498	0.487
4.938	0.626	0.596	0.588	0.58	0.558	0.53	0.515	0.495	0.484
4.95	0.623	0.594	0.586	0.579	0.556	0.528	0.514	0.493	0.484
5	0.615	0.585	0.577	0.571	0.546	0.52	0.506	0.485	0.476
5.05	0.604	0.574	0.566	0.559	0.537	0.509	0.495	0.473	0.463
5.1	0.591	0.565	0.553	0.547	0.523	0.494	0.481	0.46	0.452
5.15	0.577	0.552	0.539	0.532	0.51	0.483	0.469	0.449	0.441
5.2	0.564	0.538	0.526	0.519	0.497	0.472	0.459	0.441	0.433
5.25	0.551	0.526	0.515	0.508	0.486	0.461	0.452	0.433	0.426
5.3	0.539	0.513	0.503	0.497	0.475	0.454	0.442	0.426	0.419
5.4	0.517	0.495	0.485	0.479	0.459	0.439	0.429	0.414	0.408
5.5	0.499	0.478	0.468	0.463	0.445	0.426	0.418	0.403	0.397
5.6	0.483	0.464	0.455	0.45	0.433	0.413	0.406	0.392	0.386
5.7	0.469	0.451	0.443	0.437	0.423	0.404	0.395	0.381	0.377
5.8	0.455	0.438	0.43	0.425	0.41	0.393	0.384	0.371	0.366
5.9	0.444	0.423	0.416	0.412	0.396	0.381	0.373	0.362	0.357
6	0.418	0.401	0.396	0.391	0.378	0.362	0.356	0.345	0.34
6	0.418	0.401	0.396	0.391	0.378	0.362	0.356	0.345	0.34

Appendix C:

Numerical water surface and convergency of flow over various shapes of broad-crested weir.

The following figures shows the convergence of flow parameters with the best models selected from first case.

Model a4b2 with both sides straight cut

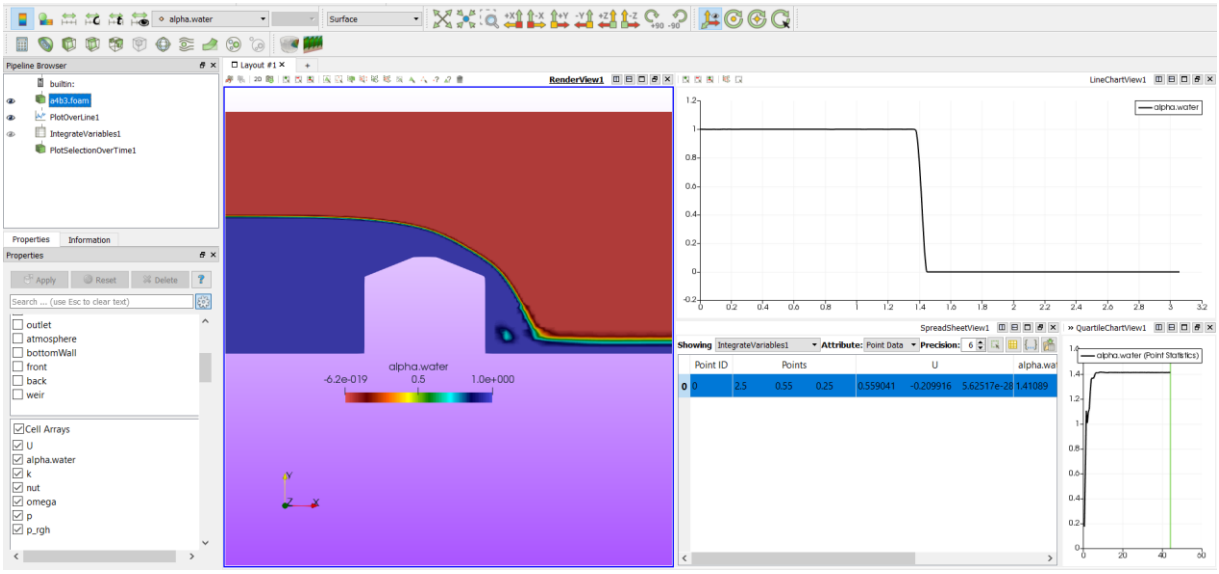

Model a4b3 with upstream straight cut

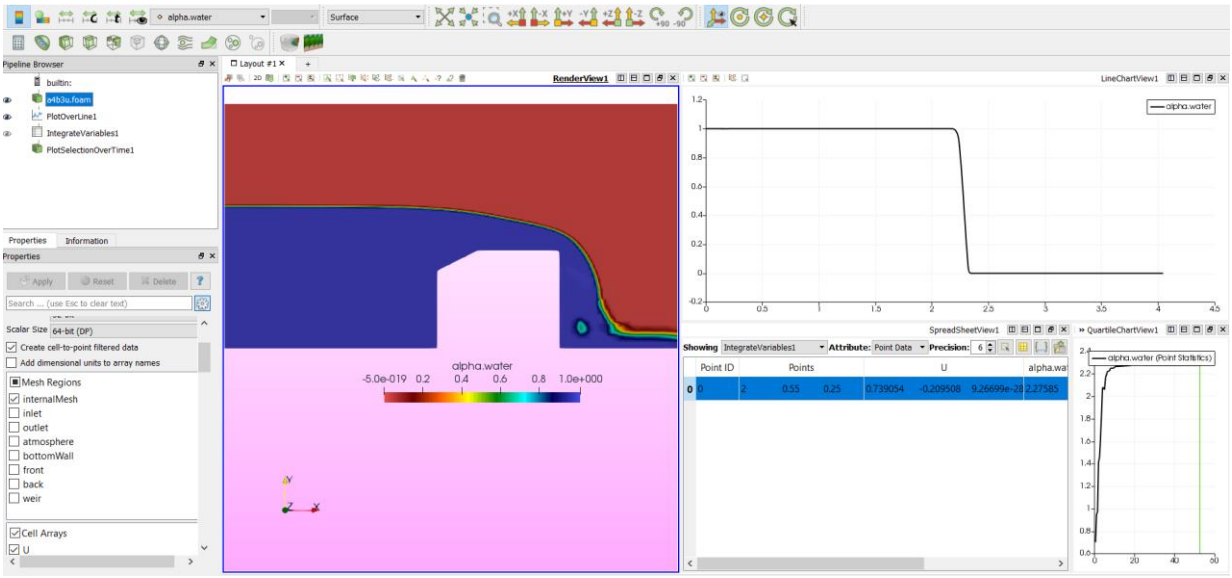

Model R4 with upstream round cut

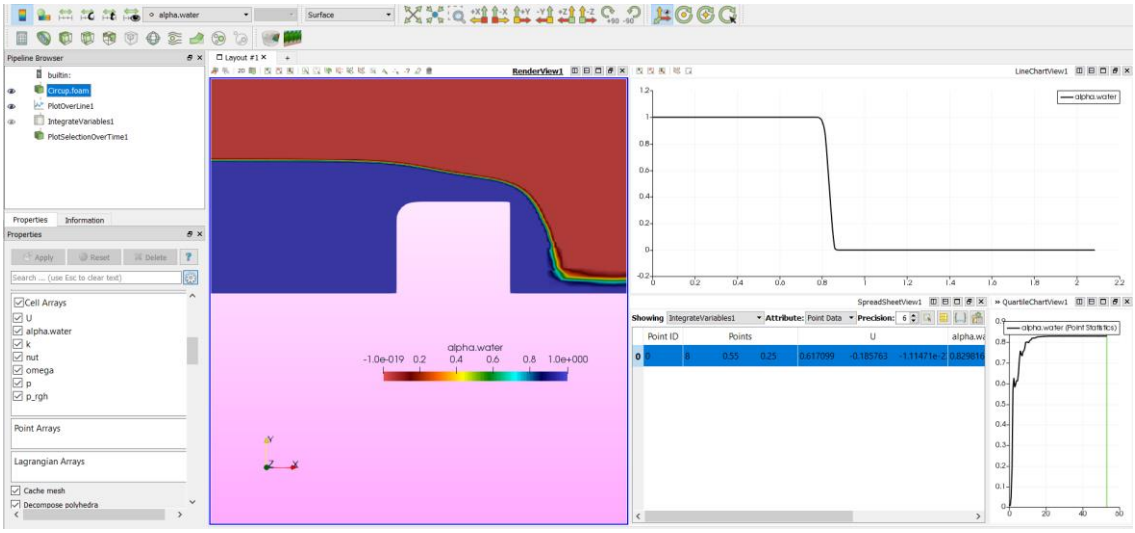

Model R5 with both sides round cut

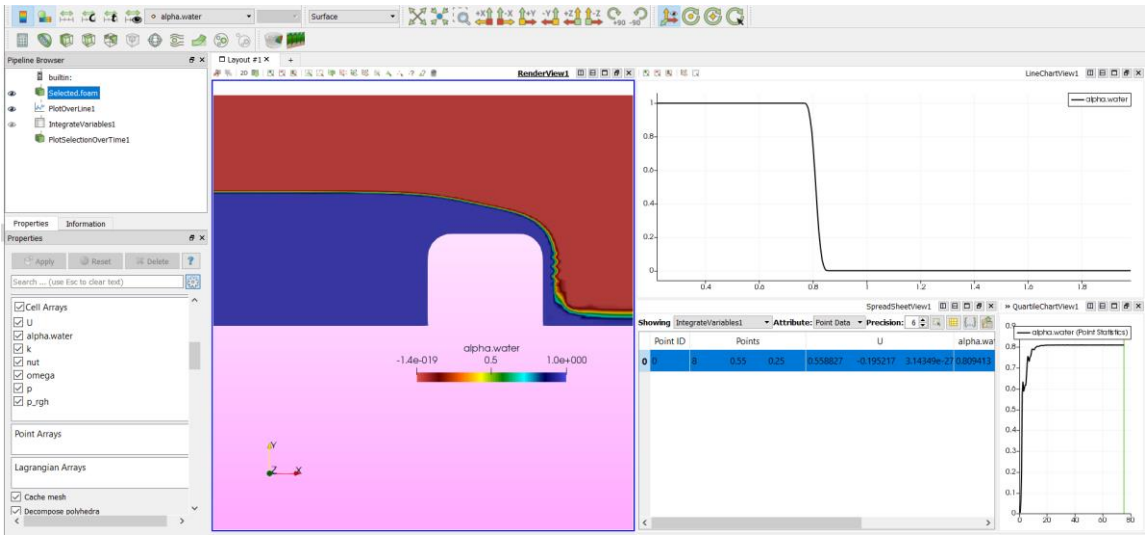

Comparison of experimental water surface and numerical water surface obtained from best models

Model a4b3 with upstream straight cut

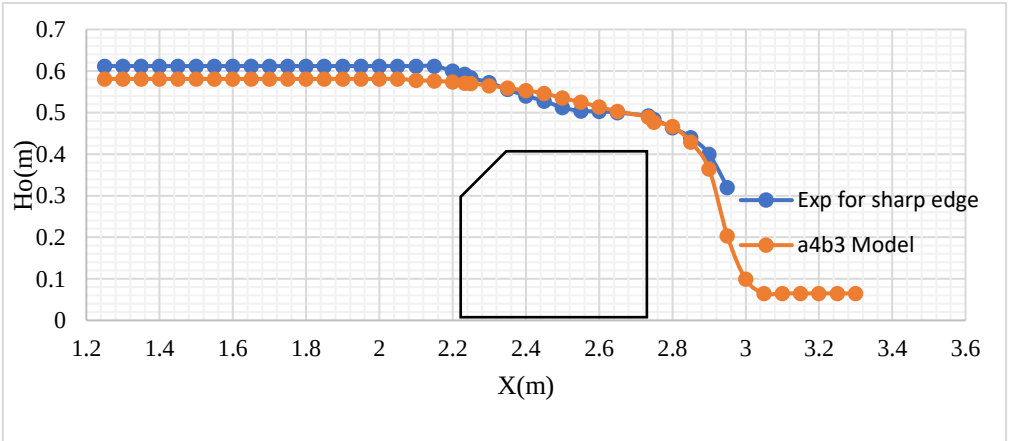

Model a4b2 with both sides straight cut

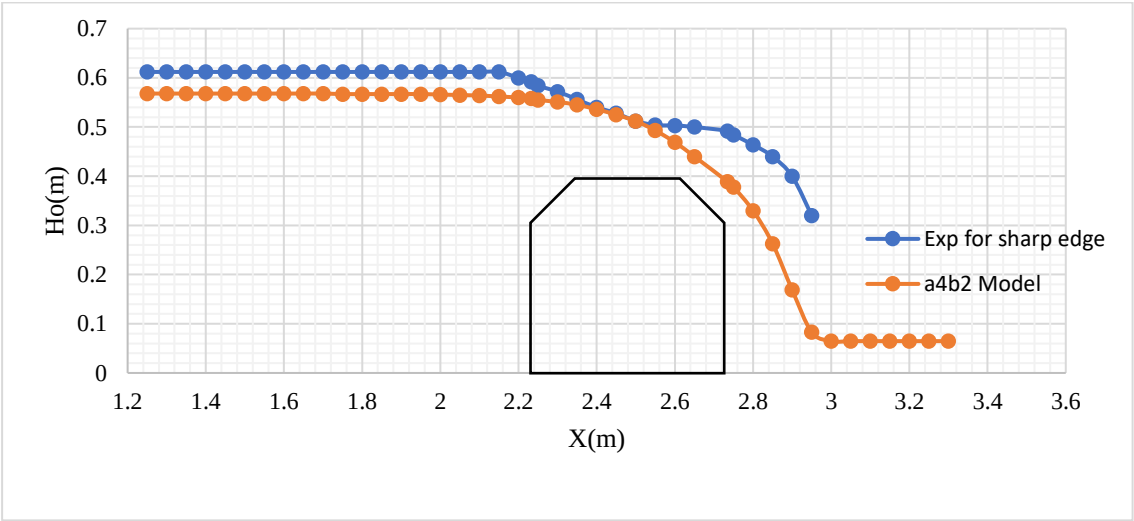

Model R4 with upstream round cut

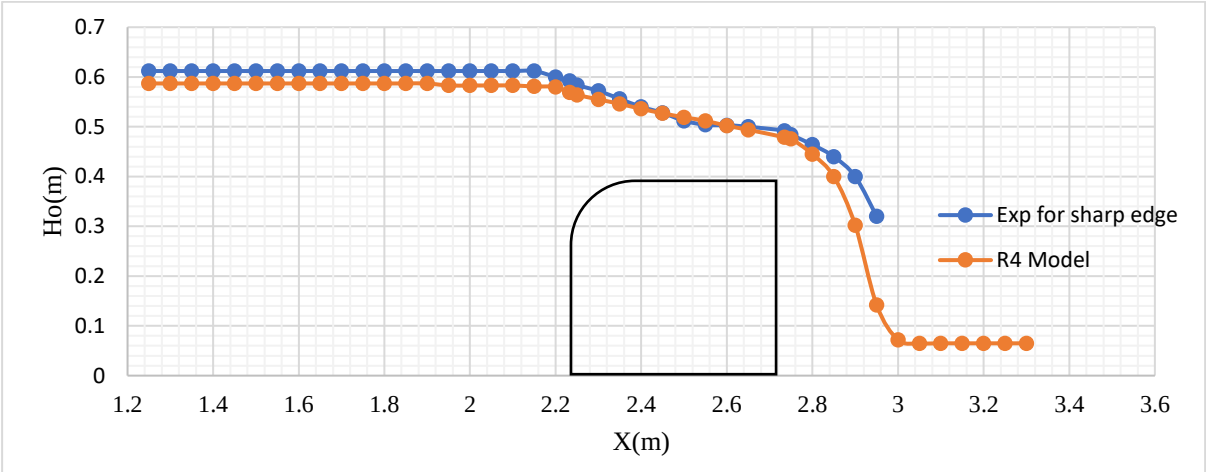

Model R5 with both sides round cut

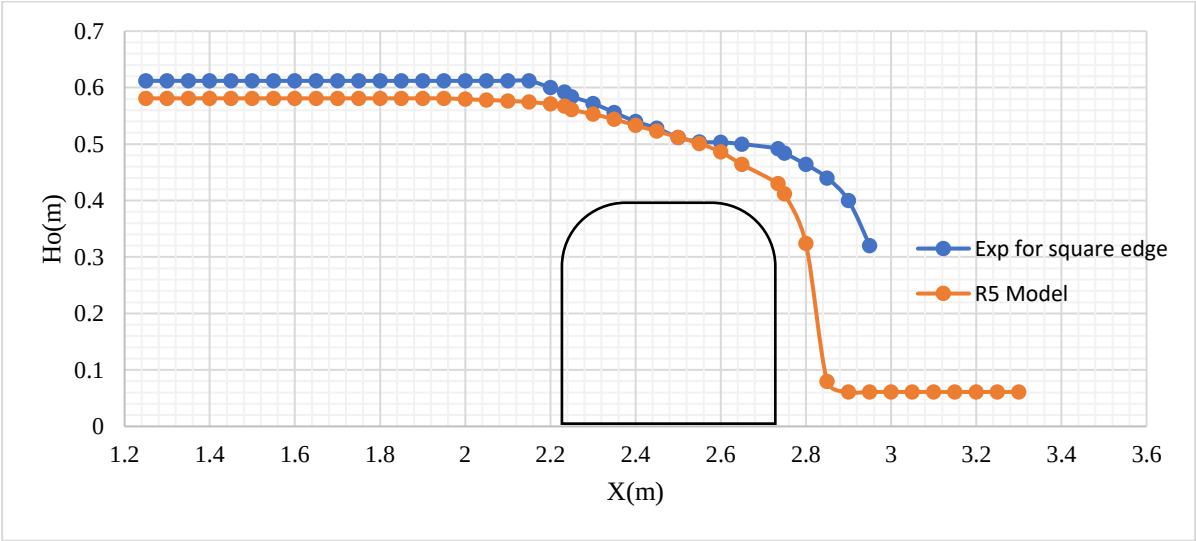

Appendix D:

Numerical water surface and convergency of flow over selected of a broad-crested weir.

Under this appendix, the numerical water surface and convergence of the selected broad-crested weir model with upstream round (R=0.0819 m) and crest inclination angle of 5°). Since several simulation was done in thesis, it is difficult to show the result for each case. However, the following figures were the represents the numerical investigation over selected model with Q=0.06807 m^3/s and for the ranges of discharge between 0.025 m^3/s and 0.12 m^3/s. The convergence profiles, free water surface, velocity, and pressure distribution were illustrated.

Convergence profile for selected weir geometry with Q=0.06807 m^3/s

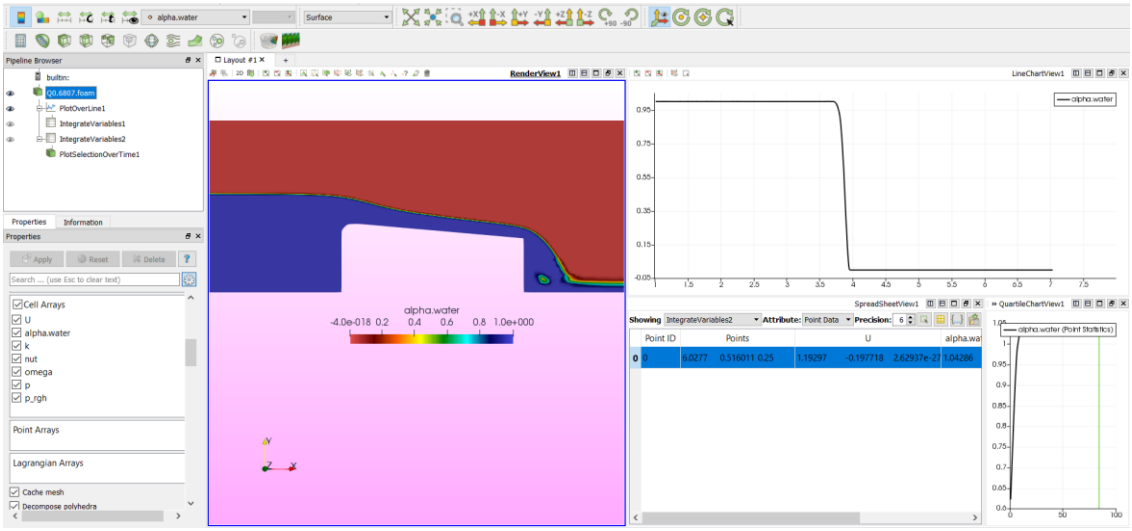

Numerical free water surface profile of flow over selected weir geometry with the Q (0.025 m^3/s - 0.12 m^3/s)

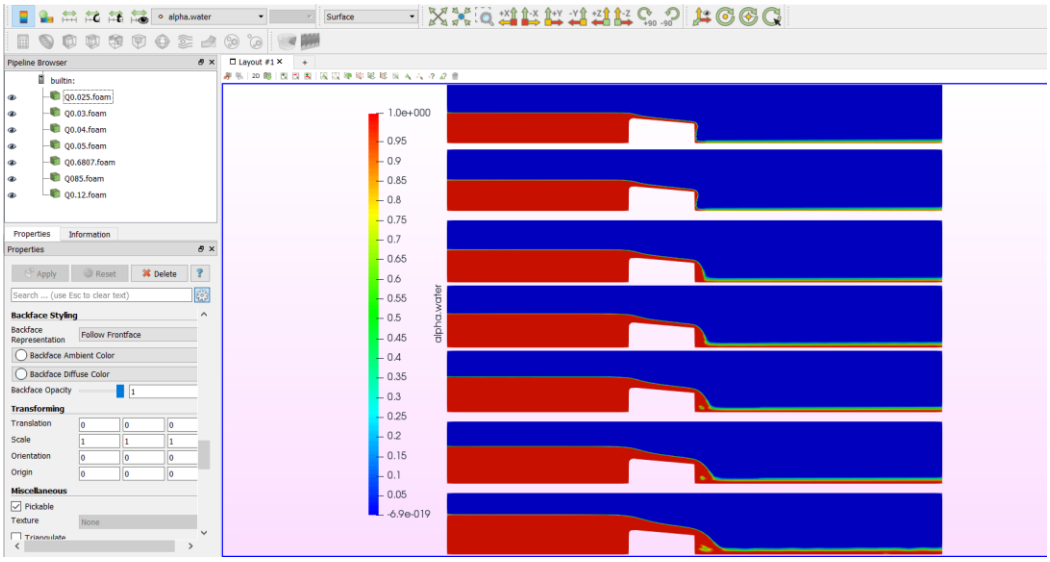

Numerical Velocity profile of flow over selected weir geometry with the Q = 0.025 m^3/s - 0.12 m^3/s

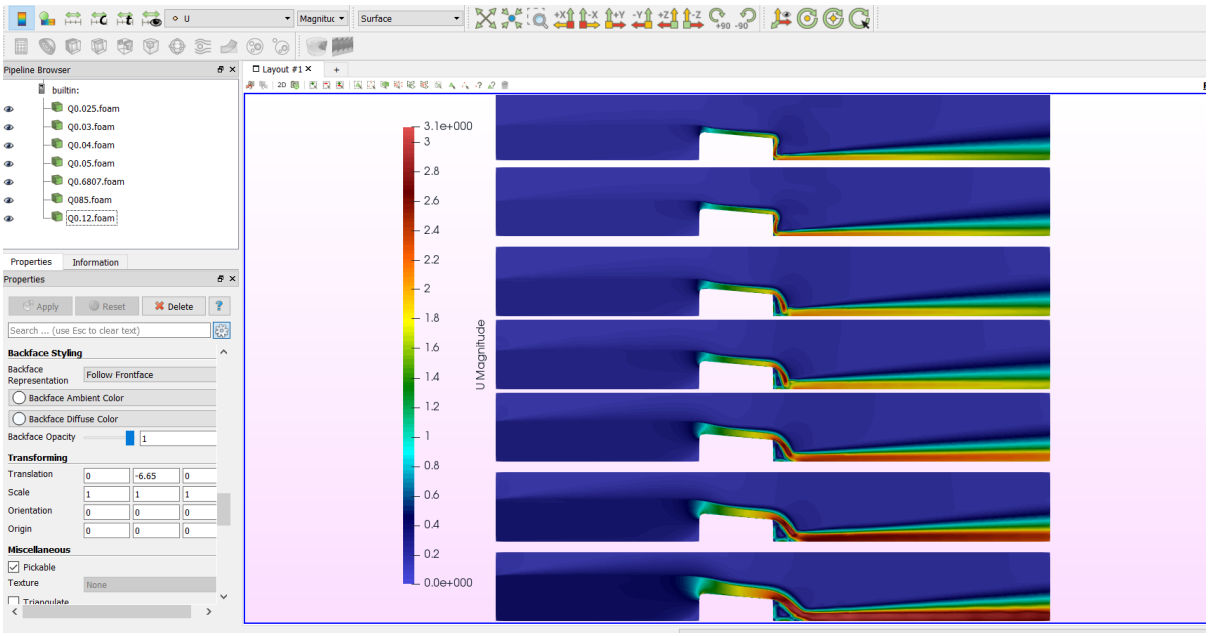

Numerical pressure profile of flow over selected weir geometry with the Q = 0.025 m^3/s - 0.12 m^3/s

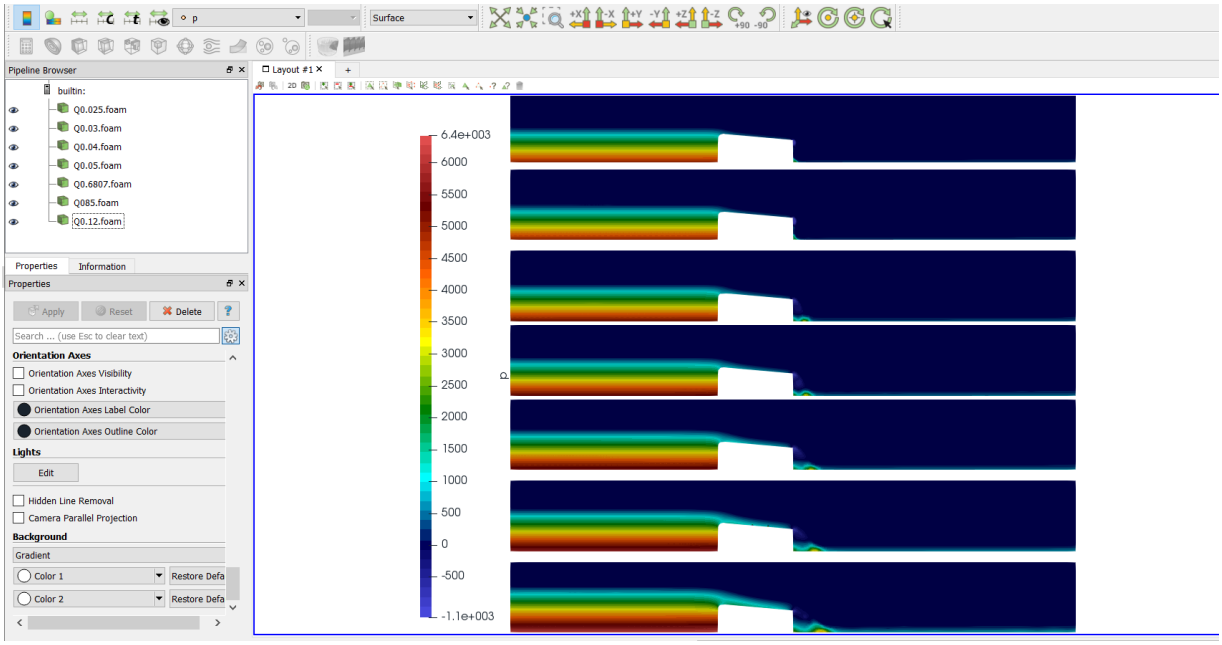

Total pressure profile of flow over selected weir geometry with the Q = 0.025 m^3/s - 0.12 m^3/s

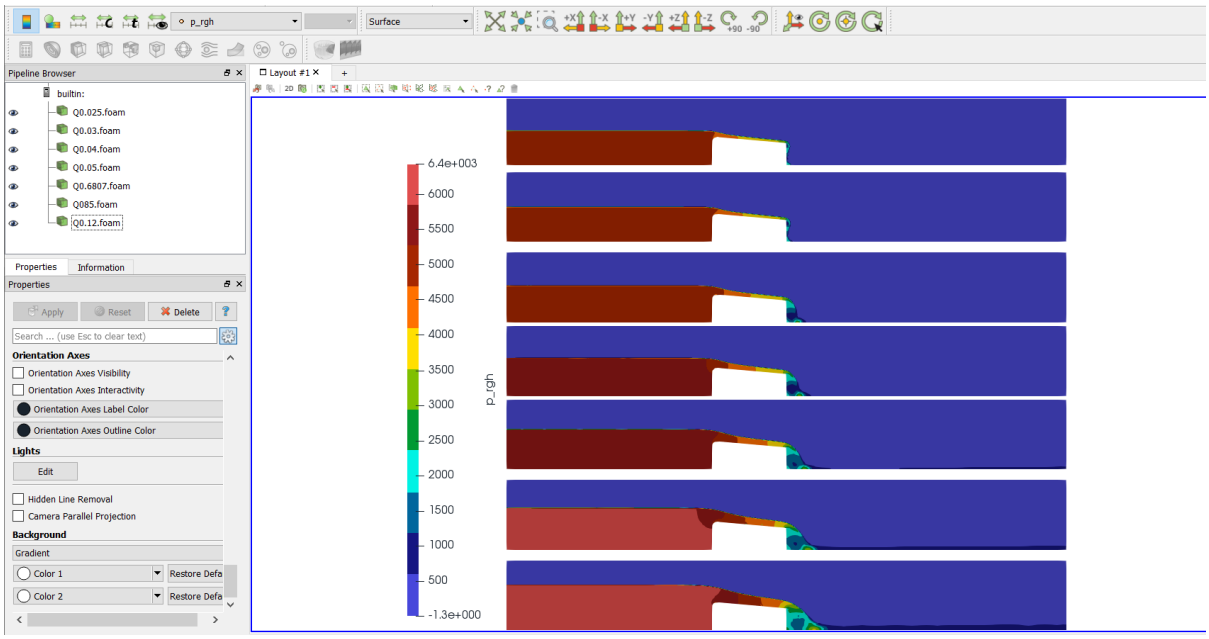

Zoomed total pressure (P_rgh) distribution for the Q of 0.12 m^3/s

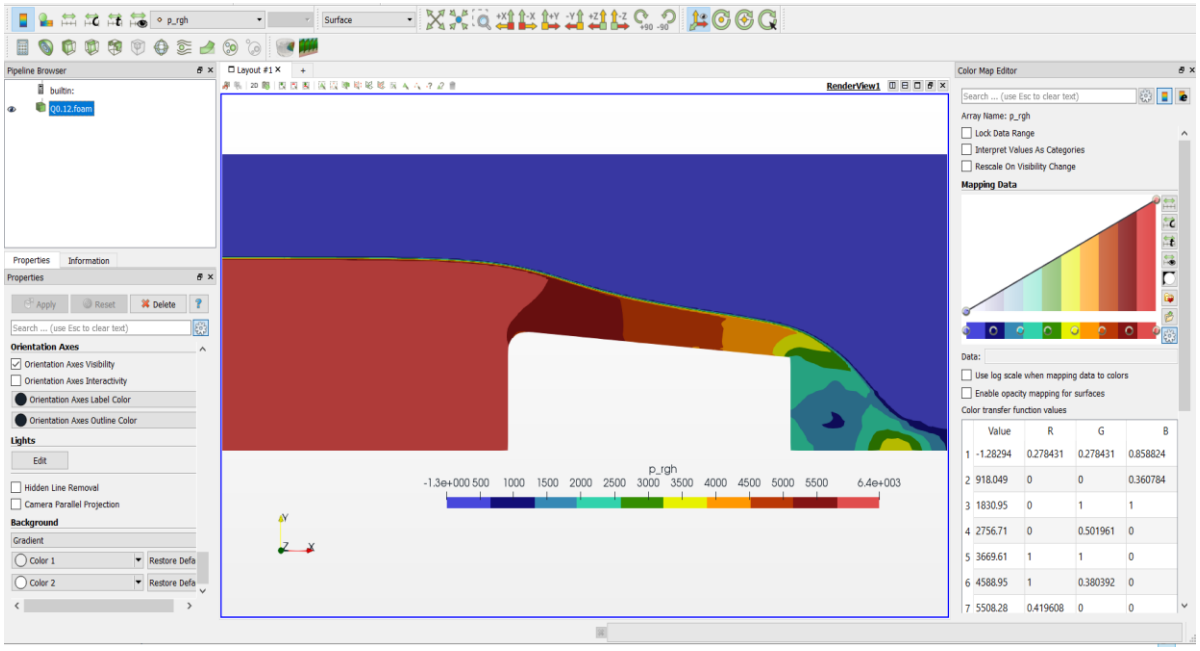

Zoomed velocity distribution for Q = 0.12 m^3/s

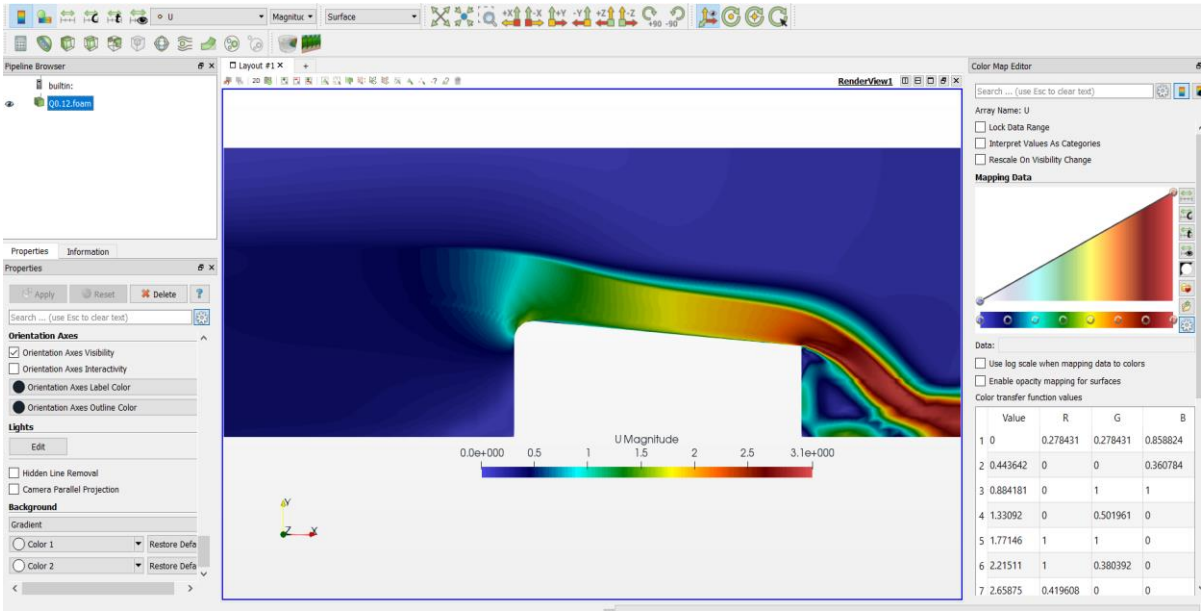

Zoomed pressure(p) for Q = 0.12 m^3/s

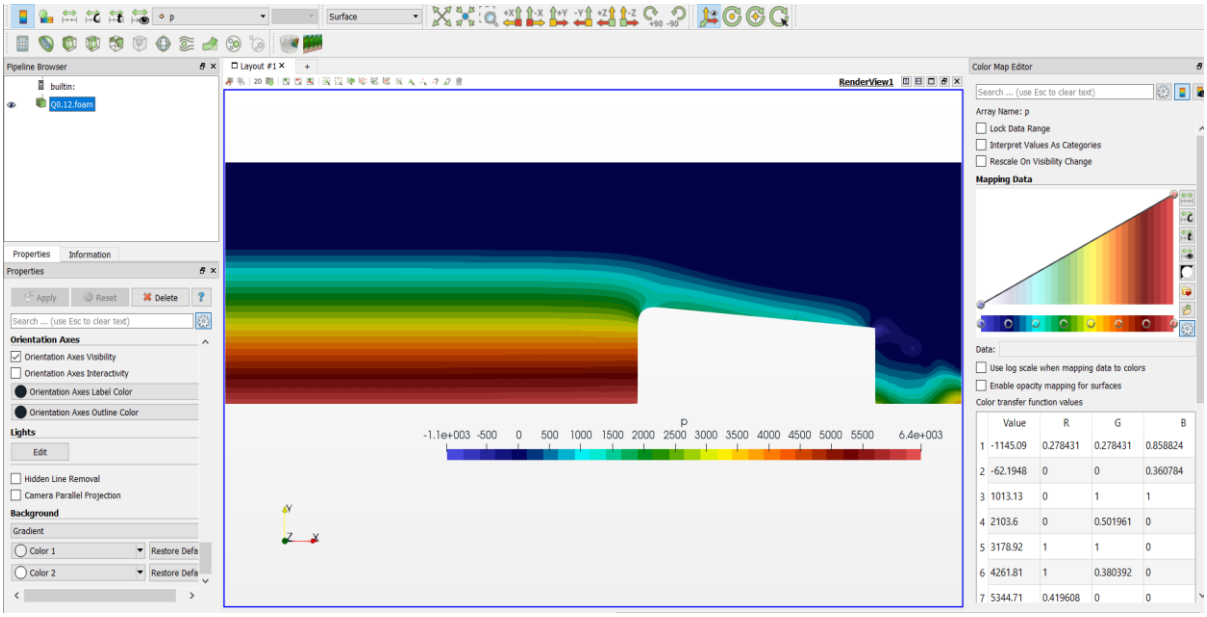

Velocity distribution Q = 0.06807 m^3/s

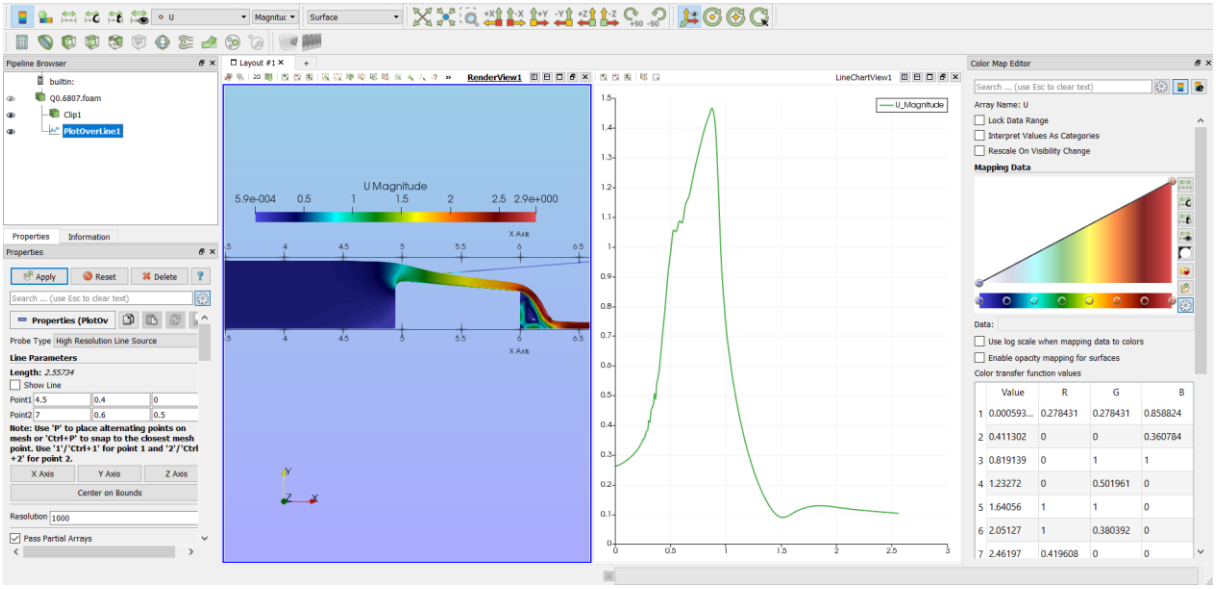

Pressure distribution Q=0.06807 m^3/s

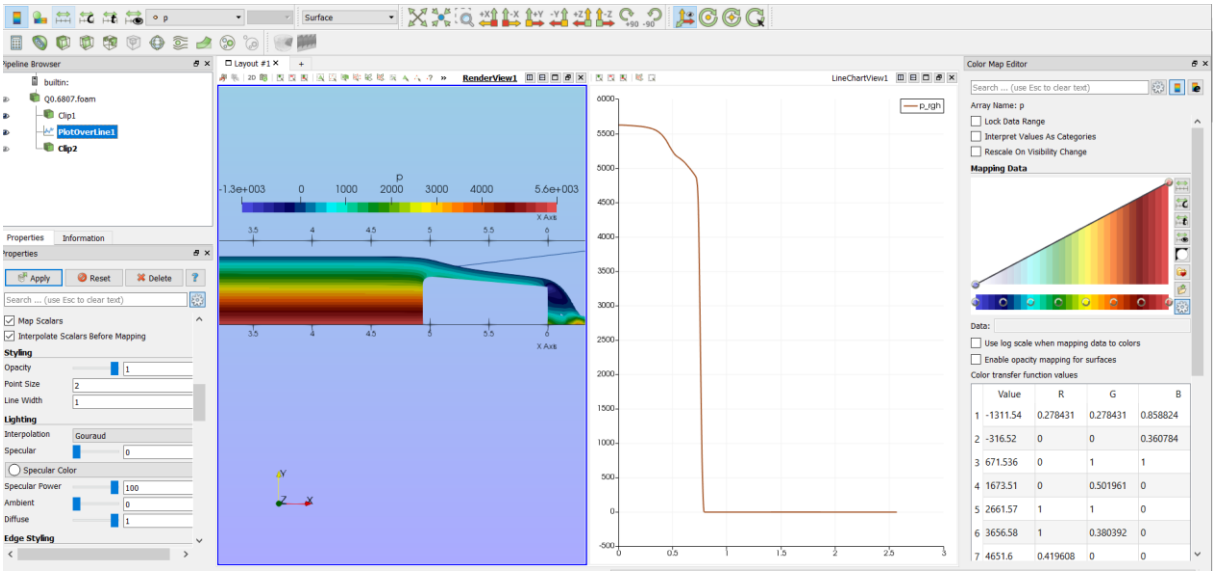

NTNU

M.Sc. THESIS IN HYDRAULIC ENGINEERING

Candidate: Mr. Beyene Feye Fulasa

Title: Investigation on different shapes of broad-crested weirs by means of CFD

1. Background

Broad-crested weir shapes are often used in spillways for the rehabilitation of old dams in Norway where restrictions on the dam structure may not allow more ideal shapes such as an ogee-crested weir. In order to increase the capacity, the upstream side of the weir is often rounded or cut, and in addition the downstream surface is also often inclined. Finding the capacity for such custom weir shapes can be challenging. At the same time, recent research into numerical modeling and Computational fluid dynamics (CFD) shows that, when properly set up, 2D width-averaged Reynolds-Averaged Navier-Stokes (RANS) model can give very accurate capacity estimates for the flow over. The aim of the master thesis will therefore be to set up a 2D width-averaged RANS model for broad crested weirs and run simulations to determine the capacity dependence on key parameters for a range of discharges. Examples of relevant parameters for testing can be the upstream cut shape, e.g. radius for a rounded shape and angles for straight cut, as well as the angle of inclination downstream, though the parameters should be determined from the literature study, and be based on identified gaps in the available studies. In addition, other relevant hydraulic variables could be identified. A relevant example is the pressure distribution along the weir.

Figure 1: Example of a broad crested weir with roundly shaped edges

2. Work description

The thesis shall cover, though not necessarily be limited to the main tasks listed below.
Based on the available documentation the following shall be carried out:

1 Literature review on physical and CFD modelling of broad crested weir flow.
2 Identification of reference cases for validation of a RANS model based on the literature study.
3 Set up a 2D width-averaged RANS model for broad crested weirs.

4 Numerical simulation including numerical parameter sensitivity (e.g. mesh, timestep) and validation against reference cases from the litereature.
5 Identify test-parameters and ranges for the parameters to test for the model based on gaps in the available literature.
6 Design a test program for simulations based on the chosen parameters and ranges. Run simulations to determine the capacity, (and possibly other variables) dependence on the chosen parameters for a range of discharges.
7 Scientific documentation of the simulation set up and results.
8 Discussion of the results
9 Conclusions
10 Proposals for future work
11 Presentation

The literature review should outline the previous contributions in a condensed manner and result in the motivation for the current study.

3. Supervision

Associate Prof. Nils Rüther will be the main supervisor and Associate Prof. Elena Pummer as well as Dr. Øyvind Pedersen from Multiconsult AS will be the co-supervisor. The supervisors shall assist the candidate and make relevant information, documents and data available.
Discussion with and input from other research or engineering staff at NTNU or other institutions are recommended. Significant inputs from others shall be referenced in a convenient manner.
The research and engineering work carried out by the candidate in connection with this thesis shall remain within an educational context. The candidate and the supervisors are free to introduce assumptions and limitations, which may be considered unrealistic or inappropriate in a contract research or a professional/commercial context.

4 Report format and submission

The report should be written with a text editing software. Figures, tables and photos shall be of high quality. The report format shall be in the style of scientific reports and must contain a summary, a table of content, and a list of references.
The report shall be submitted electronically in B5-format .pdf-file in Blackboard, and three paper copies should be handed in to the institute. Supplementary working files such as spreadsheets, numerical models, program scripts, figures and pictures shall be uploaded to Blackboard. The summary shall not exceed 450 words. The Master's thesis should be submitted within 15th of June 2019.
The candidate shall present the work at a MSc. seminar towards the end of the master period. The presentation shall be given with the use of power-point or similar presentation tools. The date and format for the MSc. seminar will be announced during the semester.

Trondheim, 14. January 2019

Nils Rüther
Associate Professor
Department of Civil and Environmental Engineering
NTNU

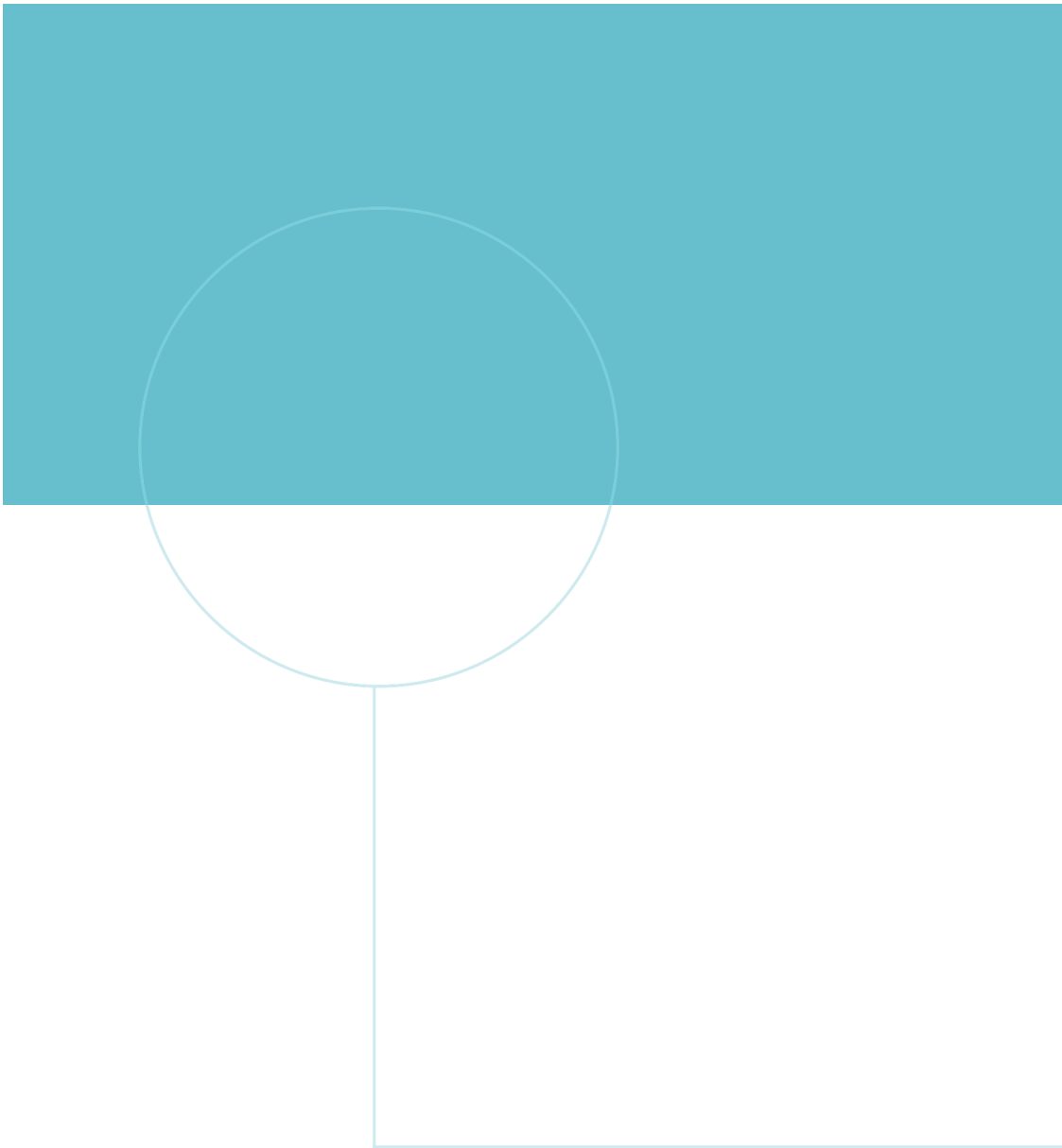

NTNU
Norwegian University of
Science and Technology